CDM Camp Dresser & McKee

Summary Report

ARCO Chemical Company
Beaver Valley Plant
Data and Analysis Review

for: Pennsylvania Department of Environmental Resources Southwest Region

June 1995

Summary Report

ARCO Chemical Company
Beaver Valley Plant
Data and Analysis Review

for: Pennsylvania Department of Environmental Resources Southwest Region

June 1995

DRESSER & McKEE INC.

Contents

List of Tables

Section 1 Introduction 1-1

1.1 Purpose 1-1
1.2 Overview and Objectives 1-1

Section 2 Discussion 2-1

2.1 Central Plant/Styrene II (CP/S2) Area 2-1

2.1.1 Contaminant Concentrations 2-1
2.1.2 CP/S2 Area -- Hydraulic Properties of the Aquifer 2-5
2.1.3 Analysis of Total Mass in the Groundwater System 2-6
2.1.4 Contaminant Mass Loadings 2-10
2.1.5 Appropriateness of CP/S2 Groundwater Models for Remediation Design 2-13
2.1.6 Feasibility of Pump-and-Treat in the CP/S2 Area 2-16

2.2 Over-The-Hill (OTH) Tank Farm Area 2-16

2.2.1 Contaminant Concentrations 2-17
2.2.2 Hydraulic Properties of the Aquifer 2-19
2.2.3 Analysis of Total Mass in the Groundwater System 2-23
2.2.4 Contaminant Mass Loadings 2-26
2.2.5 Appropriateness of OTH Groundwater Model for Remediation Design 2-28
2.2.6 Feasibility of Pump-and-Treat in the OTH Area 2-28

Section 3 Summary 3-1

3.1 Contaminant Concentrations 3-1
3.2 Hydraulic Properties of the Aquifer 3-1
3.3 Analysis of Total Mass in the Groundwater System 3-1
3.4 Contaminant Mass Loadings 3-2
3.5 Appropriateness of Groundwater Models 3-2
3.6 Feasibility of Pump and Treat 3-3

Appendix I Central Plant/Styrene II Area

Appendix II Over-The-Hill/Tank Farm Area: Water Table Fill Area

Appendix III Over-The-Hill/Tank Farm Area: Shallow Sand and Gravel

Appendix IV Over-The-Hill/Tank Farm Area: Deep Sand and Gravel

Appendix V Well Points Area Memorandum

List of Tables

Table		
1	Statistical Analysis of CP/S2 Area Groundwater Quality Data	2-2
2	CP/S2 Groundwater Concentrations (mg/L)	2-4
3	Occurrences of Concentrations Exceeding 10% Solubility Limit at CP/S2 Area	2-8
4	Comparison of Mass Estimates	2-9
5	CP/S2 Area Estimated Mass Loading (lbs/day) (from the entire contaminated area)	2-12
6	CP/S2 Area Estimated Mass Loadings (lbs/day) (from the DW-1 area)	2-14
7	Statistical Analysis of OTH Tank Farm Area Groundwater Quality Data	2-18
8	Water Balance Calculations for OTH Area	2-20
9	OTH Dissolved Contaminant Mass Estimates	2-24
10	Occurrences of Concentrations Exceeding 10% Solubility Limit at OTH Area Wells	2-25
11	Calculation of Mass Loading to Surface Water from OTH Area	2-27

Section 1.0 Introduction

1.1 Purpose

ARCO formerly operated a deep groundwater extraction well at the northern edge of their property close to the bank of the Ohio River (DW-1). In September of 1993, groundwater recovery at the well was terminated and since then groundwater concentrations at nearby wells have been reportedly increasing. ARCO does not believe that groundwater concentrations have been increasing because the extraction well was shut down; rather, they have suggested that the increase in concentrations is associated with seasonal fluctuations in groundwater flow patterns and the residual contamination associated with a previous release, not related to the existing presence of pure product. Furthermore ARCO reportedly believes that the horizontal hydraulic gradient, which is relatively flat, does not result in significant discharge of contaminated groundwater to the Ohio River.

The purpose of this report is to provide the Department with a summary of CDM's recent efforts toward evaluating the work performed by ARCO's consultants under Tasks 2 and 3 of their overall work plans. CDM has also reviewed and evaluated the modeling performed in support of the Task 2/3 reporting. In doing the reviews and evaluations, we have in some cases performed alternate analyses and modeling.

Our efforts were focused on evaluating the potential contaminant mass loading from the groundwater plumes in the Central Plant/Styrene II Area (CP/S2) and the Over the Hill Tank Farm Area (OTH). A greater emphasis was placed on the CP/S2 area because of the generally larger and higher-concentration plumes in that area.

1.2 Overview and Objectives

We evaluated the following items for both the CP/S2 and OTH Areas:

A. Contaminant concentrations in the groundwater discharging to the Ohio River and Raccoon Creek (RC), especially in relation to the MCL and freshwater aquatic life criteria that the Department has set as the concentration goals for groundwater discharging from the site.

B. Hydraulic properties of the aquifer systems.

C. Analysis of total mass in groundwater system.

D. Mass loadings of contaminants to the Ohio River and Raccoon Creek.

E. The appropriateness of the groundwater models for use in designing remediation systems.

The Department selected these items for review and evaluation because each is critical to the design and implementation of effective and efficient remediation systems.

The data used in the analysis were collected by ARCO and their consultants since the remediation and feasibility study investigations (RI/FS) in 1989. No additional data were collected or generated by CDM.

Section 2.0 Discussion

2.1 Central Plant/Styrene II Area

The objective of the analysis was to evaluate the potential contaminant mass loading that may result as contaminated groundwater from the CP/S2 area discharges to the Ohio River.

Groundwater quality data were available for the BTEXS compounds: benzene, toluene, ethylbenzene, xylenes and styrene. The analysis was performed using primarily benzene and ethylbenzene groundwater concentrations. Supporting documentation, including figures and calculations, are presented in Appendix I.

2.1.1 Contaminant Concentrations

Groundwater quality data from the RI/FS phase (1989) and from April 1993 were evaluated. Some 1994 data were available; however, the April 1993 data set was more comprehensive. A majority of the wells are installed in the upper 20 to 30 feet of the saturated zone. The saturated thickness is approximately 50 feet. The analysis presented herein did not distinguish between different vertical groundwater zones, because the saturated materials appear to be relatively homogeneous in this area of the site. The groundwater flow model developed for this area by ENSR used uniform properties with depth.

Descriptive statistical values, such as the geometric mean, the arithmetic mean and the median, were used to summarize the groundwater quality data. Table 1 presents a summary of benzene and ethylbenzene concentrations in the groundwater using the 1989 and 1993 data sets.

A comparison of 1989 and 1993 concentrations suggests that average benzene and ethylbenzene concentrations have decreased slightly, but overall there apppears to be little change in contaminant levels. Concentrations seem to have increased at those wells that were located hydraulically downgradient of the highly contaminated wells in 1989.

In 1993, several well clusters were installed. The shallow, intermediate and deep wells within each cluster were installed to average depths of 91 feet, 105 feet, and 121 feet, respectively. The water quality data indicate that higher contaminant concentrations exist in the shallow saturated zone, although contaminant levels exceeding the Maximum Concentration Limit (MCL) for benzene (5 ug/l) and ethylbenzene (700 ug/l) have also been detected in the deepest wells.

It is possible that vertical contaminant migration may have been influenced by groundwater recovery at well DW-1. Water level data from the newly installed well clusters were not listed in the Task 3 report, so that vertical gradients beneath the CP/S2 area could not be evaluated. The highest contaminant concentrations in the deep zone are located near DW-1; however, high concentrations of benzene and ethylbenzene were also noted south of DW-1 beneath the Nitrogen Plant.

Table 1
Statistical Analysis of CP/S2 Area Groundwater Quality Data

Well Category	Location		1989 Benzene ug/l	1989 Ethylbenzene ug/l	1993 Benzene ug/l	1993 Ethylbenzene ug/l
All Wells	All Areas	Average:	55,860.91	31,249.60	22,381.45	6,799.28
		Geometric Mean:	1,829.44	1,860.39	155.85	118.53
		Median:	4,863.00	13,000.00	92.00	60.00
Wells Sampled in both 1989 & 1993	Central Plant Area	Average:	77,178.12	17,027.74	55,205.88	15,688.09
		Geometric Mean:	1,256.02	768.62	1,456.20	755.10
		Median:	1,250.00	11,000.00	740.00	5,500.00
	Styrene II Area	Average:	1,667.36	1,005.54	40.71	22.50
		Geometric Mean:	38.53	29.88	15.24	9.91
		Median:	2.50	6.00	8.00	11.00
	CP + S2 Areas	Average:	55,154.15	12,354.59	39,116.04	11,118.96
		Geometric Mean:	454.61	298.10	385.18	213.36
		Median:	640.00	720.00	195.00	95.00

We also developed estimates of the contaminant concentrations in the CP/S2 groundwater, for two zones. The first zone is the interior, more widely contaminated zone, with an average width parallel to the river of about 1,850 feet. The second zone is the DW-1/wellpoint area where contaminated groundwater is currently discharging to the Ohio River. The width of this zone is about 500 feet.

The contaminant concentrations appear to be higher in the zone away from the river, in the main plant area. However, high concentrations have been measured in DW-1 and wellpoints zone along the river, especially when DW-1 is not pumping.

ARCO pumped DW-1 for several years, and then turned it off, back on again for 8 months, and then off again in 1993-94. Wellpoint data collected at different periods of DW-1 operation provided information on the movement of the dissolved BTEXS plume(s), the amount of induced infiltration from the river, and the average concentrations in the groundwater. (See Appendix for Well Point Memo.)

During pumping of DW-1, the BTEXS concentrations in wellpoints immediately downgradient of the well dropped to lower levels. After the well was turned off, concentrations started to increase significantly after about 100 days, eventually reaching relatively stable levels. This appears to be the result of the plume(s) breaking through at the wellpoints, following the loss of capture by DW-1.

We estimate that DW-1, when pumping at 200 to 300 gpm, is inducing about 85 per cent of its flow from the Ohio River. This estimate is based on modeling simulations, and use of analytical equations presented by Wilson (Water Resources Research, October, 1993). With this percentage estimate, the water quality readings taken from DW-1 pumped water samples can be used to approximate the groundwater plume concentrations. These equations apply:

$$Cgw * Qgw + Criv * Qriv = Cp * Qp$$

$$Qp = Qgw + Qriv$$

$$Qriv = 85\% * Qp \qquad Qgw = 15\% * Qp$$

where C is for concentration, Q is for flow, "gw" indicates groundwater, "riv" indicates river, and "p" is for pumped water. Assuming the river has no detectable concentrations of the BTEXS compounds:

$$Cgw = Cp * Qp / Qgw = Cp / 0.15$$

Table 2 summarizes our estimates of groundwater plume concentrations. Also presented for comparison are AHI's estimated concentrations, from their RI/FS report (4/28/89). AHI prepared their estimates by plotting the measured concentrations, in cross-sections running perpendicular to the groundwater travel direction, through the highest concentration portions of the plume.

by the Department

Table 2
CPA/S2 Groundwater Concentrations (mg/L)

Contaminant	*Interior Plume Area*			*Wellpoints Downgradient of DW-1*		*Based on Readings from DW-1*	
	AHI 1989 (Avg)	*CDM 1992 (Avg)*	*CDM 1994 (Avg)*	*(Median)*	*(Max)*	*(Med)*	*(Max)*
Benzene	216	95	22 - 56	13	21	2	3.2
Toluene	130	67	NC	2	4	0.3	0.6
Ethylbenzene	52	28	7 - 31	16	26	2.4	3.9
Xylenes	11	6	NC	0.3	2	0.1	0.3
Styrene	20	8	NC	0	0.4	<0.1	0.1
Total BTEXS	429*	204	NC	31	54	4.6	8

Notes:
* AHI presented 390 mg/L for BTEXS, whereas 429 mg/L is computed.
NC indicates that these values were not computed.

2.1.2 Hydraulic Properties of the Aquifer

CDM has evaluated all of the available information on aquifer hydraulic properties. This information includes boring logs, groundwater and river levels, pumping test results, slug testing data, and modeling performed by ARCO's consultants.

Groundwater in this area generally flows from the east/northeast to the west/northwest towards the Ohio River. The saturated thickness is approximately 50 feet.

Pumping tests conducted at the CP/S2 area have provided data describing the hydraulic properties of the sand and gravel unit in this area. The geometric mean of the hydraulic conductivity values calculated from the Task 3 pumping tests results is 548 feet/day, with values ranging from 25 to 3,972 feet/day. Some hydraulic testing was also performed during Task 2 using rising head tests. The results presented in the Task 2 report are lower than those presented for Task 3. The geometric mean of the Task 2 hydraulic testing data is 36 feet/day, with values ranging from 1 to 388 feet/day.

The CP/S2 area sits on a terrace, and higher topographic elevations are located only to the south. This high southern area is most likely an upgradient groundwater recharge area to the CP/S2 area. Water level data and topographic mapping could be used to make a further assessment of the upgradient watershed area.

Water level data from the RI are available; however, at that time deep extraction wells were operating and groundwater flow patterns differ from those of today. The contours presented in the Task 3 report are not accompanied by a data table.

In their Task 3 groundwater flow model of the CP/S2 area, ENSR used a groundwater recharge rate of 6 in/yr. At this recharge rate the upgradient watershed would have to be approximately 188 acres in size, which is much larger than the watershed area estimated from the map of regional topography.

CDM has concluded that the following are acceptable estimates for the hydraulic properties of the aquifer in the CP/S2 area. These are areal averages, and may not be accurate at each location within the CP/S2 area. However, the aquifer appears to be relatively homogeneous throughout most of the area, and so use of areal averages is appropriate for remediation planning efforts.

T = Transmisivity = 12,500 ft^2/day

b = Aquifer thickness = 50 ft

Kh = Horizontal hydraulic conductivity = 250 ft/day

Kv = Vertical hydraulic conductivity = Kh / 4 = 62.5 ft/day

Sy = Specific yield = 0.15 to 0.25

These values are close to those presented by AHI in their 1989 RI/FS report, but the transmissivity and hydraulic conductivity values are significantly lower than those derived by ENSR in the Task 2/3 efforts. ENSR's high estimates appear to have resulted from inadequate model calibration efforts, and misapplication of pumping test data.

We used the following equation to compute the total groundwater discharge rate:

$$Q = K * b * w * i = T * w * dh / L$$

where Q is the groundwater flow rate (ft3/day), k is the average horizontal hydraulic conductivity (ft/day), b is the thickness of the contaminated portion aquifer (ft), w is the width of the contaminated area discharging to the river (ft), i is the average groundwater gradient (ft/ft), T is the average transmissivity of the aquifer (ft2/day), dh is the change in water table elevation (ft), and L is the distance along the flow path that this change occurs (ft).

The width of the contaminated groundwater zone of the CP/S2 area is estimated to be approximately 1850 feet.

The size of the upgradient watershed was estimated using the calculated cross-sectional flow rate. The upgradient watershed would be approximately 113 acres and 75 acres, for groundwater recharge rates of 10 in/year and 15 in/yr, respectively. Using a regional map presented in the Task 2 report by ENSR, located in Appendix I, the upgradient watershed to the CP/S2 area was estimated to approximately 83 acres.

We estimate that the following parameter values are appropriate:

$K = 250$ ft/day $b = 50$ ft $T = 12{,}500$ ft^2/day

$w = 1{,}850$ ft $dh = 0.5$ ft $L = 1{,}000$ ft $i = 0.0005$ ft/ft

This results in an estimated groundwater discharge rate:

$Q = 11{,}560$ ft^3/day = 60 gpm (gallons per minute) = 86,400 gpd (gallons per day)

2.1.3 Analysis of Total Mass in the Groundwater System

Dissolved Contaminant Mass

In 1992, CDM performed an analysis of the amount of contaminant mass in the subsurface below the CP/S2 area. The August 1992 analysis was performed using the 1989 RI/FS data. Since groundwater concentrations have not attenuated significantly since 1989, the estimates of dissolved contaminant mass calculated by CDM in August 1992 will be used in the analysis of potential contaminant loading to the Ohio River. The estimated benzene and ethylbenzene masses in the saturated zone in the CP/S2 area, based on the August 1992 data, are 53,304 lbs (24,265 kg) and 16,324 lbs (7,403 kg), respectively.

LNAPL

A review of the 1989 product thickness data shows LNAPL in several wells beneath the CP/S2 area. However, only 11 wells in the CP/S2 had reported LNAPL present in the wells in 1993. The maximum measured thickness in 1989 was 0.61 feet. The maximum measured thickness in 1993 was 0.21 feet.

Groundwater quality data from 1993 indicate that concentrations at several wells exceed 10% of the solubility limit concentration for benzene and ethylbenzene, suggesting that there may be pure product, or LNAPL, near the wells. Table 3 lists the wells with reported concentrations exceeding 10% of the solubility limit for benzene and ethylbenzene.

Water level fluctuations may have smeared the product across the soil column, reducing the product thickness. It is also possible that the mass of LNAPL has diminished with time because of volatilization, dissolution and weathering. Product thickness measurement and data interpretation procedures, as well as water level data, need to be studied to further evaluate the potential reasons for the decrease in product thickness.

Comparison of Mass Estimates Computed by CDM and Others

As was previously mentioned, CDM performed an analysis to evaluate the amount of contaminant mass in the subsurface below CP/S2 area. Likewise, ARCO also performed an inventory of subsurface BTEXS and aromatic hydrocarbon mass. One estimate of the amount of contaminant mass present in the system was presented by the ARCO/Beazer Task Group in "Estimates of Remediation Performance and Criteria For Discontinuing Operation of Remediation System Components" dated October, 1991. More recently, Edmond Donhert of Environmental Consulting Services performed an inventory of subsurface contaminant mass for ARCO; the results of his analysis are presented in a memorandum to ARCO dated January 20, 1994.

A comparison of the mass estimates is presented in Table 4.

The contaminant mass estimates calculated by CDM are greater than those computed by Donhert. Average contaminant concentrations, derived from Donhert's and CDM's calculations, are shown in Table 4. Average groundwater concentrations from CDM's calculations are typically higher than those from Donhert's calculations. Also, CDM used a higher porosity (0.25) than Donhert (0.20), which resulted in the computation of a greater pore volume of contaminated water, and hence more contaminant mass in the saturated zone.

The contaminant mass estimates computed by CDM are also greater than those calculated earlier by ARCO. Furthermore, the estimates developed by Donhert and ARCO are not consistent, with Donhert's estimates being slightly lower than ARCO's (1991) and CDM (1992). Both CDM and ARCO used the RI/FS data. Donhert may have used more recent data; however, as an earlier comparison showed, contaminant concentrations in the highly contaminated areas have not attenuated significantly between 1989 and 1993. Donhert's estimates may be skewed by data from wells at the periphery of the plume or in locations where groundwater contamination is not present.

Table 3
Occurrences of Concentrations Exceeding 10% Solubility Limit at CP/S2 Area

	Contaminant:	BENZENE	ETHYLBENZENE
10% Solubility Limit (ug/l):		178,000	15,200
		Concentrations	
Well	Date	BENZENE	ETHYLBENZENE
		ug/l	ug/l
MW-001	Apr-93	180,000	29,000
MW-013	Apr-93		50,000
MW-017	Apr-93		23,000
MW-034	Apr-93		75,000
MW-036	Apr-93	225,000	
MW-038	Apr-93	180,000	46,000
MW-101	1989 (RI/FS)		177,500
MW-13B	1989 (RI/FS)	280,000	
MW-16	1989 (RI/FS)		37,000
MW-17	1989 (RI/FS)		52,000
MW-18	1989 (RI/FS)		78,000
MW-19	1989 (RI/FS)		32,000
MW-2	1989 (RI/FS)	240,000	
MW-21	1989 (RI/FS)		99,000
MW-211S	Apr-93		45,000
MW-25	1989 (RI/FS)		24,000
MW-25	Sep-92		30,800
MW-25	Jan-93		16,500
MW-25	Aug-93		20,941
MW-25	Jan-94		21,000
MW-25	May-94		30,000
MW-26NEW	1989 (RI/FS)		34,000
MW-27	1989 (RI/FS)		56,000
MW-29	1989 (RI/FS)		110,000
MW-30	1989 (RI/FS)		130,000
MW-31	1989 (RI/FS)		59,000
MW-32	1989 (RI/FS)		37,000
MW-33	1989 (RI/FS)		22,000
MW-34	1989 (RI/FS)		96,000
MW-35	1989 (RI/FS)		87,000
MW-36	1989 (RI/FS)		18,000
MW-38	1989 (RI/FS)	410,000	28,000
MW-39	1989 (RI/FS)		50,000
MW-40A	1989 (RI/FS)	290,000	

Table 4
Comparison of Mass Estimates

Reference	Zone	BTEXS Mass (lbs)	Soil Volume (cy)	Avg. Conc. (mg/kg)
Donhert, 1994	Unsaturated Soils	540,000	4,485,566	41
CDM, 1992	Unsaturated Soils	6,357,589	7,267,321	270
ARCO, 1991	Unsaturated Soils (beneath source areas)	400,000	296,296	416*
ARCO, 1991	Unsaturated Soils (immediately above water table)	1,700,000	222,222	2,361*
Reference	**Zone**	**BTEXS Mass (lbs)**		
Donhert, 1994	LNAPL	210,000		
CDM, 1992	LNAPL	4,544,779		
ARCO, 1991	LNAPL	1,900,000		
Reference	**Zone**	**BTEXS Mass (lbs)**	**Pore Volume (gallons)**	**Avg. Conc. (mg/l)**
Donhert, 1994	Saturated (GW)	74,000	160,591,860	55
CDM, 1992	Saturated (GW)	114,936	87,841,006	157
Reference	**Zone**	**BTEXS Mass (lbs)**		
Donhert, 1994	All	1,624,000	-1	
CDM, 1992	All	11,306,730	-2	

* CP area only

(1) Includes mass in GW, LNAPL, unsaturated zone (Subtotal: 824,000 lbs.) and in smear zone (800,000 lbs.)

(2) Includes mass in GW, LNAPL, unsaturated zone (Subtotal: 11,017,304 lbs.) and mass sorbed to soil (289,426 lbs.).

Donhert also discussed the presence of additional aromatic hydrocarbon constituents present in the LNAPL and the smear zone. He termed these constituents as "C8+HC" in his memorandum. The concluded presence of these C8+HC constituents is based on the results of LNAPL sampling and analysis which showed that the pure product consisted not only of BTEXS, but also of compounds with higher boiling points than BTEXS including 1,2-diethyl benzene (DEB); 1,3,5-triethylbenzene (TEB); and naphthalene.

The presence of these other constituents suggests that other releases of hydrocarbon contaminants, besides BTEXS, have occurred. These contaminants have not been reported in the groundwater, possibly because the laboratory analyses did not analyze for heavier hydrocarbons.

2.1.4 Contaminant Mass Loadings

We estimated CP/S2 area contaminant mass loadings to the Ohio River, for two different conditions. The first estimate presented below represents our best estimate of the loadings that would occur if the current plume area is allowed to discharge to the river, without any capture well pumping. The second estimate is for the current loadings to the river in the DW-1 area, based on our analysis of DW-1 area and river wellpoint data.

The major differences between the two analyses are the width of the contaminated areas, and the average concentrations in them. The plume area in the main plant area has higher concentrations, and is significantly wider, than the contaminated zone near DW-1.

We developed our estimates of the mass loadings by calculating average concentrations and multiplying by the estimated groundwater discharge rate. The following equation expresses this calculation:

$$M = C * Q * F$$

where M is the mass flux rate (lbs/day), C is the average concentration of a contaminant (mg/L), Q is the groundwater flow rate (ft^3/day) through the contaminated zone to the Ohio River, and F is a conversion factor 0.0000624 (lbs * L/mg * ft^3). This assumes that there is no significant pumping and that ambient groundwater flow is driven by rainfall-recharge. (Cite ICF's estimate on "N" where it is estimated they use 6"/year from ENSR 1994 +D+M 1994) This calculation also assumes that mass transport is not significantly affected by partitioning onto subsurface sediments or by biodegradation or volatilization.

The mass loading rates are based on the average groundwater concentrations. As such, they reflect only the impact of the dissolved contaminant mass. Pure product is present, so that additional soluble contaminant mass is present to supply the existing groundwater plume, and to potentially discharge directly to the Ohio River. Likewise, if there are highly contaminated groundwater zones that have not been detected by the existing monitoring well network, the average concentration of the plume and the amount of contaminant mass in the saturated zone may be greater.

Full CPA/S2 Plume Area

For the full contaminated area, we calculated loadings for the total of the five BTEXS compounds (labeled "Total BTEXS"): benzene, toluene, ethylbenzene, xylenes, and styrene. We also estimated the loadings of ethylbenzene and benzene individually, because concentrations for these contaminants are the highest of the BTEXS series, in relation to their respective concentration goals. In particular, ethylbenzene would likely be the last contaminant to drop below its concentration goal, during remediation. This conclusion was also presented by ARCO in their October 1991 report.

For the average concentrations, C, we used estimates that are presented previously in Section 2.1.1. The concentrations for Total BTEXS, benzene, and ethylbenzene represent our best estimate of the average concentrations within the contaminated CP/S2 area.

For the groundwater flow rate, we used estimates that are based on our analysis of the aquifer's hydraulic properties, presented in Section 2.1.2.

This is based on assuming that the contaminated groundwater extends through the entire vertical column of the aquifer, the thickness designated as b. Therefore, the specific discharge is constant with depth. This may overestimate the loading somewhat; however, there have been significant concentrations found in deep wells in the contaminated zone. For comparison, we also compute groundwater flow rates and mass loadings for a 10 foot thick plume.

ARCO's consultants for Tasks 2/3 (ENSR and Dohnert) did not present any estimates of CP/S2 contaminant mass loadings. However, we have used their estimates of average concentrations (Dohnert, 1994) and our estimates of groundwater flow rate to calculate a mass loading rate, for comparison purposes.

Also, ARCO's consultant for the RI/FS work, Applied Hydrology, Inc. (AHI), developed estimates of benzene and ethylbenzene average concentrations and the groundwater flow rate (AHI, 4/28/89).

Table 5 presents calculations of mass loading rates using estimates of average contaminant concentrations and groundwater flow rates from CDM, AHI, and Donhert, for comparison. These estimates are for ambient, non-pumping conditions, given the average groundwater concentrations measured in the 1988 to 1993 period.

Current Loadings from the DW-1 Area

We used the same technique for estimating the current mass loadings to the river in the DW-1 area. We performed calculations for all of the individual BTEXS compounds and for Total BTEXS.

The estimated contaminant concentrations, C, are based on measured concentrations from DW-1 samples, and on our analysis of the amount of induced river water infiltration. (Section 3.1.1) We assumed that the river water has undetectable concentrations of BTEXS. Our estimated

Table 5
CPA/S2 Area
Estimated Mass Loadings (lbs/day)
(from the entire contaminated area)

Consultant	*Contaminant*	*M Mass Loading Rate (lbs/day)*		*Q Groundwater Flow Rate (ft3/day)*		*C Concentration (mg/L)*
		b = 50 ft	*b = 10 ft*	*b = 50 ft*	*b = 10 ft*	
CDM	Total BTEXS	147	30	11,560	2,312	204
AHI	Total BTEXS	168	37	6,921	1,384	390
Donhert	Total BTEXS	40	8	11,560	2,312	55
CDM	Benzene	16 - 40	3 - 8	11,560	2,312	22 - 56
AHI	Benzene	93	19	6,921	1,384	215
CDM	Ethylbenzene	5 - 22	1 - 4	11,560	2,312	7 - 31
AHI	Ethylbenzene	22	4	6,921	1,384	50

Note: b is the plume thickness.

aquifer concentrations were confirmed by plotting the time history of contaminant concentrations at the wellpoints and sandpack wells along the river bank. See Well Point Memo in Appendix V.

These same data allowed us to estimate the width of the contaminated groundwater plume that is currently discharging in the DW-1 area. The contaminated area defined by the wellpoints is approximately 500 feet wide.

We retained the same estimates for all the other hydraulic parameters as used in the calculations presented above. This includes the assumption that the full saturated thickness is contaminated, because our DW-1 induced infiltration estimate (used for estimating the dilution of the plume by pumped river water) was based on the same assumption.

In summary, we estimate that the following hydraulic parameter values are appropriate for the DW-1 discharge area:

$K = 250$ ft/day $\quad b = 50$ ft $\quad T = 12{,}500$ ft^2/day

$w = 500$ ft $\quad dh = 0.5$ ft $\quad L = 1{,}000$ ft $\quad i = 0.0005$ ft/ft

This results in an estimated groundwater discharge rate: $Q = 3{,}125$ cfd.

Table 6 presents calculations of mass loading rates using contaminant concentrations and groundwater flow rates. The concentration ranges represent the median to the maximum values estimated based on our river-water dilution calculations.

The table presented below summarizes our estimate of the potential mass loading to the nearby surface waters.

		Mass Loading (lbs/day)	
Area	Discharge Zone	Benzene	Ethylbenzene
Entire Contaminated Area	Ohio River	16 - 40	5 - 22
DW-1 Area	Ohio River	2.5 - 4.1	3.1 - 5.1

2.1.5 Appropriateness of CP/S2 Groundwater Models for Remediation Design

The ENSR MODFLOW model of the CP/S2 area appears to be inappropriate for use in remediation design efforts. Apparent misinterpretation of the pumping test data led ENSR to include a very high hydraulic conductivity layer at the water table. This resulted in a modeled horizontal hydraulic conductivity that is approximately 10 to 15 times higher than our estimate, and a simulated transmissivity that is about 3 to 4 times higher.

Table 6
CPA/S2 Area
Estimated Mass Loadings (lbs/day)
(from the DW-1 area)

Consultant	*Contaminant*	*M* *Mass Loading Rate (lbs/day)*	*Q* *Groundwater Flow Rate (ft3/day)*	*C* *Concentration (mg/L)*
CDM	Benzene	2.5 - 4.1	3,125	13 - 21
CDM	Toluene	0.4 - 0.8	3,125	2 - 4
CDM	Ethylbenzene	3.1 - 5.1	3,125	16 - 26
CDM	Xylenes	<0.1 - 0.4	3,125	0.3 - 2
CDM	Styrene	0 - <0.1	3,125	0 - 0.4
CDM	Total BTEXS	6.0 - 10.5	3,125	31 - 54

ENSR's boundary conditions also appear to be incorrect. They implemented "fixed head" boundaries essentially along all lateral boundaries. However, a fixed head boundary may only be appropriate at the Ohio River. Along the other sides, no-flow or low-inflow boundaries would be more representative of aquifer conditions. In effect, the fixed head boundaries forced the model, under non-pumping conditions, to achieve a reasonable match to field-measured water levels no matter what transmissivity was simulated. Under pumping conditions, the fixed heads supplied enough water to suppress simulated drawdowns, thereby causing underestimation of the capture zones created by the pumping.

AHI's MODFLOW-based model appears to be a significantly better tool for use in remediation design. It incorporates hydraulic properties that are closer to the values we have estimated from an analysis of the data. The AHI model also may have a better representation of the site's geologic layering and bedrock surface, which is the estimated extent of the permeable aquifer materials.

Any future groundwater flow modeling of the CP/S2 area should include calibration to non-pumping conditions, and to pumping at the three pump tests as well as at DW-1. In fact, calibration to DW-1 pumping conditions is more important than the pumping tests because the DW-1 pumping occurred over a long time period, causing the aquifer to reach a hydraulic steady state. Therefore, the DW-1 data offer a significantly better set of information for estimation of induced infiltration from the Ohio River, as well as providing the data for accurate calibration of transmissivity and hydraulic conductivity values.

The pumping tests offer the means to estimate vertical hydraulic conductivity values and storage coefficients, which the DW-1 data cannot help estimate. However, these parameters are generally of secondary importance, and they can be estimated through pumping test analyses without running a computer groundwater flow model.

Contaminant transport analyses should be performed, and the usefulness of computer simulations should be explored. Such analyses would be particularly helpful for confirming the hydraulic property estimates, and for estimating contaminant velocities and retardation effects. The latter would be useful during the design of the remediation system, to help select pumping well locations and to predict the time needed to capture the plumes.

Of special interest are the data from the shutdown, restarting, and later shutdown of DW-1. The data from the riverside wellpoints and inland monitoring wells, as well as the readings from DW-1 itself, provide an indication of contaminant flushing by "clean" river water when DW-1 was pumping. More significantly, the data from the period when DW-1 was shutdown show how the plume(s) moved toward the river again, indicating the velocity of the contaminated aquifer water. See Appendix V.

To date, ARCO has not commissioned any contaminant transport analyses or model simulations, except for limited, simplified mixing tank analyses.

2.1.6 Feasibility of Pump-and-Treat in the CP/S2 Area

Pumping of groundwater, for protecting the Ohio River from discharges of contaminated groundwater, appears to be a feasible option. This would be in addition to any source (or residual source) remediation efforts, such as air sparging, soil vacuum extraction, bioventing, or other techniques that may be appropriate. CDM strongly recommends that source control and remediation proceed as quickly as possible, to reduce the contaminant loadings to the groundwater system and thereby achieving the groundwater discharge goals sooner.

The Department has indicated that the groundwater discharging from the site needs to meet applicable standards – MCLs or freshwater aquatic life criteria, whichever is the more stringent. These goals have been defined in other documents.

Some form of plume control and remediation is needed, because the existing plume concentrations are significantly higher than the goals. Moreover, ambient non-pumping groundwater levels indicate that there is a significant groundwater discharge to the river from the plume area.

Several containment technologies are available, but these are generally not feasible for this site because of the depth to the water table from the land surface. The density of plant structures and work areas, and the general level of activity at the plant, also dictate that extensive and intrusive structural remedies are likely to be infeasible.

Given that pump-and-treat is a proven and feasible plume capture and remediation technique, ARCO should investigate how to implement this technique most effectively and economically. The primary trade-off appears to be between the objective of completing the remediation efforts as soon as possible, versus the objective of minimizing the amount of clean river water pumped by the capture well(s) and then into the treatment plant.

Induced infiltration theory and a properly-calibrated groundwater flow model could provide the basis for designing the pumping well system. The theory and model could be used to select spacings between wells, and the distance from the wells to the river, to achieve adequate plume capture without inducing significant river infiltration. One approach would be to install many relatively low-rate pumping wells, to "skim" the most contaminated groundwater from the aquifer. Injection wells or infiltration galleries could also be helpful, to flush the saturated zone more quickly and to minimize the induced inflow of river water.

2.2 Over-The-Hill (OTH) Tank Farm Area

The objective of the analysis was to evaluate the potential contaminant mass loading that may result as contaminated groundwater from the OTH area discharges to Raccoon Creek.

The analysis focused on the saturated zone only. For the purpose of the analysis, the subsurface was divided into three groundwater zones. These zones are the water table zone, including the saturated fill materials; the shallow sand and gravel zone; and, the deep sand and gravel zone. In some locations, where the silty clay layer is absent, the shallow sand and gravel zone is phreatic.

The analysis was performed using benzene and ethylbenzene groundwater quality concentrations. Supporting documentation, including figures and calculations, are presented in Attachments II (water table zone), III (shallow sand and gravel) and IV (deep sand and gravel).

2.2.1 Contaminant Concentrations

In most cases, three sets of data were obtained during the remediation investigation and feasibility study phases. In addition, quarterly data have been collected during 1994. The geometric and arithmetic means, as well as the median were computed for each groundwater zone using the April 1994 data. In general, the arithmetic means tended to be higher, while the geometric mean and median were comparable. Because of the distribution of groundwater quality data, geometric means or medians tend to be more representative of the values within a given data set. All three values were used to compute the potential mass loading to the rivers; since the arithmetic mean was generally the highest value, the potential loading computed from the arithmetic mean represents a more conservative estimate.

Groundwater concentrations measured at wells in the OTH area exceed the concentration goals set by the Department. The water table/fill zone appears to be the most contaminated layer; however, concentrations at several wells in both the shallow and deep sand and gravel layers exhibit benzene and ethylbenzene concentrations above the goals.

Water Table/Fill Area

There are five wells in this category; the wells are MW-114, MW-115, MW-116, MW-156, MW-168. Four of the wells are located near and south of the wastewater treatment lagoon. The fill materials are confined to the eastern portion of the OTH area, generally surrounding the lagoon. The 1994 data suggest that concentrations at the wells are decreasing; however, a review of the historical data has shown that concentrations have decreased, then increased in the past, which may indicate that a continuing source is present. In several cases, historical concentration values exceeded 10% of the solubility concentration suggesting that pure product may be present. No pure product was detected in 1989 in any of these wells. In 1993, 0.1 inch of product was detected at MW-115. The screen zones of the shallow wells intercept the water table; therefore, if pure product is present near a shallow well, the well should indicate it presence.

Descriptive statistical values were calculated using the April 1994 benzene and ethylbenzene concentrations. These are presented in Table 7. The statistical values significantly exceed the Maximum Concentration Limit (MCL) for both benzene (5 ug/l) and ethylbenzene (700 ug/l).

Shallow Sand and Gravel Zone

There are 22 wells and 5 piezometers in this category. This zone is phreatic in the western portion of the site. The sand and gravel unit is partially overlain by a silty clay layer in the eastern portion of the site. As in the fill/water table zone, groundwater concentrations in the shallow sand and gravel zone show an overall decline; however, some fluctuation in

Table 7
Statistical Analysis of OTH Tank Farm Area Groundwater Quality Data

Contaminant	GW Zone	Arithmetic Mean ug/l	Geometric Mean ug/l	Median ug/l
Benzene				
(MCL=5 ug/l)	Water Table/ Fill	114,000.00	79,995.12	92,500.00
	Shallow Sand & Gravel	6,655.91	18.58	1.50
	Deep Sand & Gravel	1,429.57	32.49	4.00
Ethylbenzene				
(MCL=700 ug/	Water Table/ Fill	7,125.00	3,080.07	6,500.00
	Shallow Sand & Gravel	11,976.24	33.64	14.00
	Deep Sand & Gravel	468.64	9.91	4.00
Statistical data computed using April 1994 data				

concentrations is apparent. Concentrations in the shallow sand and gravel zone may be influenced by downward vertical migration of contaminated groundwater from the fill and by the groundwater mound caused by the infiltration from the lagoon.

At wells MW-148, MW-153 and MW-342, groundwater concentrations exceeding 10% of the solubility concentration for ethylbenzene were reported. In 1993, 0.4 inch of product was measured at well MW-342. In 1994 product was observed in the following wells: MW-148, MW-153, MW-155, MW-342, and OW-323.

Table 7 lists the descriptive statistics for the shallow sand and gravel zone. The values are generally lower than the statistical values for the water table/fill materials, except for the arithmetic mean of the ethylbenzene data.

Deep Sand and Gravel Zone

There are seven wells and one piezometer in this category. In general, it appears that concentrations have not changed significantly between sampling rounds. The descriptive statistics for the deep zone are listed in Table 7.

2.2.2 Hydraulic Properties of the Aquifer

Groundwater flow patterns in the OTH area appear to be more complex than in the CP/S2 area, because of the wastewater treatment lagoon and the presence of a low permeability clay layer. The geometry of the aquifer boundaries is also more complicated. These boundaries include the lagoon, Raccoon Creek, the Ohio River, and bedrock outcrops and subsurface topography.

The total groundwater flow through the OTH area is estimated to be about 1,000 ft3/day. This is approximately 10 percent or less than the estimated groundwater flow rate through the contaminated zone in the CP/S2 area. Most of the OTH groundwater flow reaches Raccoon Creek or the Ohio River, although a portion flows west/northwest and into the CP/S2 area.

Table 8 summarizes the calculation of the water balance components for each vertical groundwater zone. The hydraulic conductivity values used in Table 8 are based on reported hydraulic testing results in the Task 3 report for OTH (Dames and Moore, 1994), presented in Appendix II.

Water Table/Fill Area

Groundwater flows radially away from the fill area towards Raccoon Creek to the east and the OTH area to the west. Based on the groundwater quality data the width of the contaminated zone is approximately 375 feet. The thickness of the saturated fill material was estimated to be 2 feet. Using the average horizontal gradient (0.022 ft/ft, computed using water level data from MW-116, MW-156 and MW-168, and the Raccoon Creek staff gauge) towards the river and the an average hydraulic conductivity of 8 feet/day, the calculated rate of groundwater discharge from the fill to Raccoon Creek is 135 cubic feet per day (cfd).

Table 8
Water Balance Calculations For OTH Area

(A) Horizontal Through Flow

GW Zone	Width of Flow Zone ft	Saturated Thickness ft	Horizontal Gradient ft/ft	Hydraulic Conductivity ft/day	Flow cu ft/day
Water Table/ Fill	375.00	2.00	0.022	8.00	135.00
Shallow Sand & Gravel	180.00	15.00	0.0006	310.00	502.00
Deep Sand & Gravel	600.00	10.00	0.00023	310.00	428.00

(B) Recharge Flux

GW Zone	Area sq ft	Recharge Flux at 10"/year cu ft/day	Recharge Flux at 15"/year cu ft/day
Water Table/ Fill	39,375.00	90.00	135.00
Sand & Gravel	476,100.00	1087.00	1630.00

(C) Discharge to Surface Water

GW Zone	Flow Direction	Cross-Sectional Area sq ft	Horizontal Gradient ft/ft	Hydraulic Conductivity ft/day	Flow cu ft/day
Water Table/ Fill	Horizontal	1,860.00	0.022	8.00	327.36
Shallow Sand & Gravel	Vertical	27,000.00	0.033	0.00028	0.254
Deep Sand & Gravel	Horizontal	6,000.00	0.00023	310.00	428.00

Appendix II presents a figure from the Task 3 report showing that the approximate area upgradient of the contaminated zone is 39,375 square feet (sf). Assuming a groundwater recharge rate of 10 to 15 inches per year, the recharge flux to the water table here is 90 to 135 cfd, respectively. A portion of this recharge moves vertically towards deeper strata; however, vertical flow is limited by the silty clay layer. Based on the available data, it is believed that a majority of the groundwater recharge to the fill flows laterally within the fill materials. (Note: The model developed by Dames and Moore used a groundwater recharge rate of 6 inches per year. This value is smaller than that used in the calculation described above).

Shallow Sand and Gravel Zone

Groundwater in the shallow sand and gravel flows northward from the location of the bedrock outcrop (south of OTH) and southward from a piezometric high caused by infiltration from the wastewater treatment lagoon. The resulting piezometric surface is a flat gradient zone bounded by a piezometric high on either side. From the OTH area groundwater flows northwestward towards the central plant area following a very flat gradient, and eastward towards Raccoon Creek. The small hydraulic gradients are a result of the relatively high hydraulic conductivity and transmissivity of the sand and gravel unit. Groundwater discharge from the shallow sand and gravel to Raccoon Creek is influenced by the presence of the silty clay underlying the creek and surrounding area.

Appendix III presents a figure from the Task 3 report. The horizontal flow rate was computed using an estimated cross-sectional flow area 180 feet wide and 15 feet thick. A hydraulic conductivity of 310 ft/day and a horizontal gradient of 0.0006 ft/ft was used to compute a horizontal flow rate of 502 cfd.

An approximate vertical flow rate from the shallow sand and gravel to Raccoon Creek was also computed. Using a flow area of 27,000 sf (this zone corresponds to the approximate width of Raccoon Creek (150 feet) and the length of the flow zone from the OTH area (180 feet)), a vertical hydraulic conductivity of 0.00028 ft/day (obtained from groundwater flow model input), and a gradient of 0.033 ft/ft, a vertical (upward) discharge rate of 0.254 cfd was calculated (See calculations in Appendix III). A comparison of the vertical and horizontal discharge rates suggests that only a small portion of the groundwater in the shallow sand and gravel discharges to Raccoon Creek, according to ARCO's data and modeling analysis.

The hydraulic properties of the silty clay have not been well defined in the existing reports. The hydraulic conductivity used in the calculations was based on values used in the Dames and Moore model of the OTH site. If the actual vertical hydraulic conductivity of the clay is greater than that used in the model, more groundwater from the shallow sand and gravel zone will discharge to Raccoon Creek.

Deep Sand and Gravel Zone

Groundwater in the deep sand and gravel flows from the location of the bedrock outcrop northeastward towards the confluence of the Ohio River and Raccoon Creek. Based on boring log data, the silty clay layer is believed to be present near the confluence of these two surface water bodies. The presence or absence of this layer will influence groundwater discharge rates to the Ohio River and Raccoon Creek. The hydraulic influence of this silty clay layer has not been well defined in previous reports.

Vertical gradients beneath the site from the shallow sand and gravel are generally downward. The number of monitoring points in the deep sand and gravel zone is limited. Based on the data, groundwater levels in the deep sand and gravel do not seem to be significantly influenced by the wastewater treatment lagoon; however, it is possible that some localized mounding is present beneath the lagoon.

Appendix IV presents a figure from the Task 3 report. The horizontal flow rate was computed using a cross-sectional flow area of 6,000 sf (600 wide x 10 deep), a hydraulic conductivity of 310 ft/day, and a horizontal gradient of 0.00023 ft/ft. The resulting groundwater discharge rate is 428 cfd.

Recharge to Sand and Gravel

The groundwater in the sand and gravel layer receives recharge directly from precipitation infiltration, where the silty clay is absent. Where the clay is present, the sand and gravel layer is recharged by groundwater leakage through the clay. The hydraulic characteristics of the clay are not well known, but for the analysis it was assumed that groundwater leakance through the clay is small.

The recharge by direct precipitation infiltration was computed using an area of 476,100 sf (the approximate area of the OTH region where the clay is absent) and a groundwater recharge rate of 10 in/yr and 15 in/yr. The computed recharge flux is 1,087 cfd and 1,630 cfd for the two recharge conditions.

Discussion of Water Balance

The water balance was estimated using an annual groundwater recharge rate of 10 to 15 inches per year. This value is slightly greater than the value used by Dames and Moore in their modeling analysis. Dames and Moore did not document the reasons for the selection of this recharge rate. The flow components computed for this memorandum balance more closely using the greater recharge rate.

Since precipitation infiltration is assumed to be the only source of groundwater recharge, the estimated cross-sectional flow rate and recharge flux should roughly balance. For the water table/fill zone, the estimated recharge flux is 90 to 135 cfd which is comparable to the computed cross-sectional flow rate of 135 cfd. The recharge flux to the sand and gravel unit is estimated to range from 1,087 to 1,630 cfd, which is slightly larger than the estimated horizontal flow rate computed for the unit (930 cfd).

Dames & Moore performed the Task 2/3 work for ARCO in the OTH area. Their hydraulic testing and data analyses resulted in hydraulic conductivity estimates that appear to be reasonable. Their horizontal hydraulic conductivity estimates for the sand and gravel units average about 310 ft/day, and for the water table/fill area about 8 ft/day. Their sand and gravel estimated hydraulic conductivity is very close to our estimate of approximately 250 ft/day for the CP/S2 area.

2.2.3 Analysis of Total Mass in the Groundwater System

Dissolved Contaminant Mass

The amount of dissolved contaminant mass (benzene and ethylbenzene only) in the three groundwater zones was computed by multiplying the average benzene and ethylbenzene concentrations by the approximate volume of groundwater in the contaminated zones. Table 9 summarizes the results. Figures showing the areas used to compute the volume of groundwater are included in Appendices II through IV. The estimated benzene and ethylbenzene masses in the OTH Area based on the April 1994 data are 122-1,407 lbs and 6-2,083 lbs, respectively.

The amount of contaminant mass contained within the silty clay layer was not evaluated because only one well is screened in this unit, and the extent of contamination could not be defined. Total aquifer volume was multiplied by a porosity of 0.2 and 0.35 for the fill and sand and gravel units, respectively, to compute the volume of contaminated groundwater. A lower porosity was used for the fill materials because the low hydraulic conductivity suggests that the fill may be dense and compact. The pore volume was then multiplied by the contaminant concentration (arithmetic, geometric mean and median) to estimate an approximate range of contaminant mass. The estimated contaminant mass of benzene and ethylbenzene is 128-3,490 lbs.

LNAPL

During three monitoring events in 1989, there was no evidence of pure product in the OTH monitoring wells. In 1993, product was detected in wells MW-115, MW-342 and MW-147. A trace amount of LNAPL was detected in wells MW-340 and OW-323. In 1994, LNAPL was observed in wells MW-148, MW-153, MW-155, MW-342, and OW-323.

Concentrations in some wells exceed 10 percent of the solubility limit, also suggesting that LNAPL may be present near these wells. Table 10 lists the dates and locations where concentrations suggest the presence of LNAPL. In April 1994, concentrations exceeding 10 percent of the solubility concentration were detected in the following wells: MW-147, MW-156, ME-166, MW-342 and OW-323.

Since a pool of LNAPL could not be defined based on ARCO's data, the amount of contaminant mass contained within this phase was not computed. If LNAPL is indeed present, it will serve as a reservoir of contaminants to the groundwater.

Comparison of Mass Estimates Computed by CDM and Others

ARCO performed an inventory of subsurface BTEXS and aromatic hydrocarbon constituents. The results are reported in a memorandum to ARCO by Edmond Donhert of Environmental

Table 9
OTH Dissolved Contaminant Mass Estimates

Contaminant	GW Zone	Area (sq ft)	Thickness (ft)	Volume (cu ft)	Porosity	Pore Volume (cu ft)	Factor (to lb)	Mass Computed Using: Arithmetic Mean (lb)	Geometric Mean (lb)	Median (lb)	Range (lb)
Benzene											
	Water Table/ Fill	61,425	2	122,850	0.20	24,570	6.24E-08	174.91	122.74	141.92	122 to 179
	Shallow Sand & Gravel	520,200	15	7,803,000	0.35	2,731,050	6.24E-08	1,135.11	3.17	0.26	<1 to 1135
	Deep Sand & Gravel	300,000	10	3,000,000	0.35	1,050,000	6.24E-08	93.73	2.13	0.26	<1 to 93
										Total	122-1407
Ethylbenzene											
	Water Table/ Fill	61,425	2	122,850	0.20	24,570	6.24E-08	10.93	4.35	9.97	4 to 11
	Shallow Sand & Gravel	520,200	15	7,803,000	0.35	2,731,050	6.24E-08	2,042.45	5.74	2.39	2 to 2042
	Deep Sand & Gravel	300,000	10	3,000,000	0.35	1,050,000	6.24E-08	30.73	0.65	0.26	<1 to 30
										Total	6-2083

Mass estimates from April 1994 data.

Table 10
Occurrences of Concentrations Exceeding 10% Solubility Limit at the OTH Area Wells

Contaminant	10% Solubility Limit ug/l	GW Zone	Well	Date	Concentration ug/l
Benzene	178,000	Water Table/ Fill	MW-166	Apr-93	380,000
			MW-156	Jun-93	360,000
			MW-156	Apr-94	250,000
Ethylbenzene	15,200	Water Table/ Fill	MW-156	Apr-93	25,000
		Shallow Sand & Gravel	MW-323	Jun-93	51,000
			MW-323	Apr-94	54,000
			MW-342	Jun-93	150,000
			MW-342	Apr-94	140,000
		Deep Sand & Gravel	MW-147	Jun-93	75,000

Consulting Services. The results are presented in terms of total BTEXS mass. To compare Donhert's estimates to the calculations presented in this report, the amount of benzene and ethylbenzene mass was estimated from Donhert's total reported BTEXS mass.

The latest 1993 data set was used to develop a comparison, since Donhert's memorandum was written in January 1994 and his analysis most likely included 1993 data. The calculated BE/BTEXS ratio calculated using average June 1993 concentrations is 0.74.

This ratio was multiplied by Donhert's estimated amount of mass in the saturated zone (9000 lbs) to get an estimated mass of 6,660 lbs of benzene and ethylbenzene. This value is larger than the estimated mass of 128-3490 lbs presented earlier in this section. The most likely reason for this difference is that the analysis presented here does not consider the contamination or the thickness of the silty clay material, whereas Donhert incorporated the total thickness of the saturated overburden into his calculations. As such, Donhert's estimates of contaminant mass are greater, and may be more representative of the amount of mass in the saturated subsurface; however, the groundwater quality of the silty clay unit and the contaminant migration pathway from the water table zone to the sand and gravel unit have not been defined, so that it is unknown whether the entire thickness of the silty clay unit is contaminated.

The mass estimates presented in this report generally represent the dissolved mobile mass present in the system and therefore will be used to evaluate the mass loading to surface water from the different vertical groundwater zones.

2.2.4 Contaminant Mass Loadings

We estimated OTH area contaminant mass loadings using the same technique as used for the CP/S2 area, as explained under item 2.1.4. We computed mass loadings to Raccoon Creek and the area where this stream enters the Ohio River. Table 11 presents calculations of mass loading rates using contaminant concentrations and groundwater flow rates. The concentration ranges represent the median to the maximum values estimated based on our river-water dilution calculations.

The mass loading rates presented there are based on the April 1994 groundwater concentrations. As such, they reflect only the impact of the dissolved contaminant mass. If pure product is present (there are data that suggest that this may be a possibility) additional soluble contaminant mass is present to supply the existing groundwater plume. Likewise, if there are highly contaminated groundwater zones that have not been detected by the existing monitoring well network, the average concentration of the plume and the amount of contaminant mass in the saturated zone may be greater. The table presented below summarizes our estimate of the potential mass loading to the nearby surface waters.

Table 11
Calculation of Mass Loading to Surface Water from OTH Area

Contaminant	GW Zone	Discharge to Surface Water cu ft/day	Concentrations: Arithmetic Mean ug/l	Concentrations: Geometric Mean ug/l	Concentrations: Median ug/l	Factor to lb/day	Mass Loading Computed Using: Arithmetic Mean lb/day	Mass Loading Computed Using: Geometric Mean lb/day	Mass Loading Computed Using: Median lb/day
Benzene									
	Water Table/ Fill	327.36	114,000.00	79,995.12	92,500.00	6.24E-08	2.33E+00	1.63E+00	1.89E+00
	Shallow Sand & Gravel	0.25	6,655.91	18.58	1.50	6.24E-08	1.06E-04	2.95E-07	2.38E-08
	Deep Sand & Gravel	428.00	1,429.57	32.49	4.00	6.24E-08	3.82E-02	8.68E-04	1.07E-04
						Total	2.37E+00	1.64E+00	1.89E+00
Ethylbenzene									
	Water Table/ Fill	327.36	7,125.00	3,080.07	6,500.00	6.24E-08	1.46E-01	6.29E-02	1.33E-01
	Shallow Sand & Gravel	0.25	11,976.24	33.64	14.00	6.24E-08	1.90E-04	5.33E-07	2.22E-07
	Deep Sand & Gravel	428.00	468.64	9.91	4.00	6.24E-08	1.25E-02	2.65E-04	1.07E-04
						Total	1.58E-01	6.32E-02	1.33E-01

From April 1994 data.

GW Zone	Discharge Zone	Mass Loading (lbs/day) Benzene	Ethylbenzene
Water Table/Fill	Raccoon Creek	1.6 - 2.3	0.06 - 0.15
Shallow Sand & Gravel	Raccoon Creek	<0.01	<0.01
Deep Sand and Gravel	Confluence Ohio River & Raccoon Creek	<0.01 - 0.04	≤0.01

2.2.5 Appropriateness of OTH Groundwater Model for Remediation Design

Dames & Moore developed a MODFLOW-based groundwater flow model of the OTH area. They used hydraulic properties that appear to be reasonable. Their calibration efforts and documentation could be improved somewhat, but our overall conclusion is that the model can be used for remediation design purposes. We recommend, however, that the Department ask for additional documentation on the model's calibration, to ensure that it adequately matches the measured data.

Contaminant migration modeling could prove useful in the OTH area, but we recommend that modeling resources be allocated preferentially to the CP/S2 area where contaminant concentrations and off-site discharges are significantly higher.

2.2.6 Feasibility of Pump-and-Treat in the OTH Area

Groundwater pumping appears to be a feasible option for controlling contaminant migration in the OTH area. As discussed above with respect to the CP/S2 remediation efforts, pump-and-treat could be used at OTH primarily for halting the discharge of contaminated groundwater to the rivers. This technique can also be used, with recharge or injection of treated groundwater, in ways that could enhance the hydraulic control of the plume(s) and the removal of contaminant mass from the aquifer. For example, the infiltration of "clean" lagoon water could help to flush the aquifer layers.

Groundwater flow modeling could be used to optimize the design of the groundwater pumping and reinfiltration system, by identifying optimal well spacings, locations, and pumping rates. This would be done so that induced river water infiltration and overall pumping rates are minimized, and the pumping wells are spaced properly to ensure adequate plume capture.

In any remediation design for the OTH area, other techniques in addition to pump-and-treat should be evaluated and implemented, if possible, so that the primary and residual source materials are remediated. Remediating the source should be a high priority, in general. This is because removal of contaminants from the unsaturated zone and from LNAPL is likely to be more cost-effective than only pumping and treating groundwater.

Section 3.0
Summary

3.1 Contaminant Concentrations

Groundwater data collected by ARCO and its consultants since the RI/FS in 1989 indicate that contaminant concentrations are in general significantly higher than the goals set by the Department.

Benzene and ethylbenzene concentrations in the CP/S2 area have decreased slightly but overall there appears to be little change.

At the OTH area, the concentrations in the fill/water table and the shallow sand and gravel zones show an overall decline, however, some fluctuations are apparent. In the deep sand and gravel zone, the concentrations have not changed significantly. The sand and gravel concentrations are in general lower than those in the water table/fill area.

3.2 Hydraulic Properties of the Aquifer

Evaluation of available data for the CP/S2 area aquifer resulted in estimates close to those presented by AHI in the 1989 RI/FS report. However, they are significantly different than those derived by ENSR in their Task 2/3 reports for the CP/S2 area. For the OTH area, our estimates match reasonably well with those derived by Dames and Moore.

Contaminated groundwater beneath the CP/S2 area discharges to the Ohio river at an approximate discharge rate of 11,560 ft^3/day. The total groundwater flow through the OTH area is estimated to be about 1,000 ft^3/day. This is approximately 10 percent or lower than the estimated rate through the contaminated zone in the CP/S2 area.

Groundwater flow patterns in the OTH area appear to be more complex than in the CP/S2 area because of the more complex geometry, the presence of a wastewater treatment lagoon, and the low permeability clay layer.

3.3 Analysis of Total Mass in the Groundwater System

Estimates of contaminated mass were performed by ARCO (for the CP/S2 are only), by Donhert, a private consultant for ARCO, and by CDM. The contaminant mass estimated by CDM was in general higher than that computed by the others for the CP/S2 area. In the OTH area, Donhert's estimate is greater because he included the silty clay material. However, it is unknown whether the entire thickness of the silty clay is contaminated.

The estimated benzene and ethylbenzene masses in the saturated zone in the CP/S2 area, based on the August 1992 data, are 53,304 lbs and 16,324 lbs, respectively. The estimated benzene and ethylbenzene masses in the OTH Area based on the April 1994 data are 122 to 1,407 lbs and 6 to 2,083 lbs, respectively.

LNAPL has been detected in several CP/S2 wells; also, contaminant concentrations exceeding 10 percent of the solubility concentration for benzene and ethylbenzene have been detected, suggesting the presence of pure product near wells that have not had pure product reportedly detected in them. Water level data and product thickness measurement techniques need to be reviewed to confirm the reported thickness, to evaluate product thickness measurement and data interpretation procedures, and to identify whether water levels have fluctuated and smeared the product across the soil column.

LNAPL has been detected in only a few OTH wells; however, contaminant concentrations exceeding 10 percent of the solubility concentration for benzene and ethylbenzene have been detected suggesting the potential presence of pure product near these wells. In 1989, no wells had LNAPL detected at them; whereas in 1994 LNAPL was observed in 5 wells. Water level data and product thickness measurement techniques need to be reviewed to identify whether water levels have fluctuated and smeared the product across the soil column and whether a pool of pure product is present.

3.4 Contaminant Mass Loadings

The total mass loading in the CP/S2 area for ambient, non pumping conditions are 16-40 lbs/day and 5-22 lbs/day for benzene and ethylbenzene respectively. The total mass loadings in the OTH area are 1.6-2.3 lbs/day and 0.06-0.15 lbs/day for benzene and ethylbenzene respectively, about 10-100 times lower than the CP/S2 area.

The mass loading estimates to the surface water presented in this report represent the contribution of contaminants from the saturated zone only. If a benzene or ethylbenzene source exists, the magnitude and duration of mass loading will change. The estimate presented in this memorandum reflects a "snap-shot" in time of the potential mass loading rate.

3.5 Appropriateness of Groundwater Models

The groundwater modeling performed by ARCO's consultants was reviewed. In general, this review concluded that the assumptions for the models of the CP/S2 and OTH areas were not always consistent. For instance, the hydraulic conductivities used in the separate models differ for the same unit. Furthermore, the calibrated hydraulic conductivity values are not always consistent with field data. In terms of previous estimates of the contaminant mass reservoir in the subsurface, analysis results compiled by ARCO at different times are not similar or consistent.

The groundwater flow models that have been developed do not seem to have been tested or documented enough for use in design of remediation systems. Specifically, simulated water balances should be evaluated to demonstrate that the models realistically simulate the hydraulics and water balance of the system, and that the calibrated parameters are consistent with field data. This is particularly important because the models may be used to evaluate different remedial pumping rates and zones of capture. The boundary conditions for the models should be evaluated closely. A more appropriate modeling approach may be to simulate the groundwater flow system beneath the entire plant with one model instead of dividing the area into discrete models that may not represent the system's boundaries accurately.

3.6 Feasibility of Pump and Treat

Pump and treat methods can be used effectively at this site; however, other remediation techniques may provide more cost-effective results, such as air sparging, soil vacuum extraction, bioremediation, or some combination. Groundwater pumping can be used to complement these systems, and to control the plumes during the implementation of other techniques.

Modeling of groundwater pumping systems should be performed to help design the optimum arrangement of pumping wells, and to select an optimum pumping rate for the objectives of the system. Optimization tools should be explored and used, if appropriate.

APPENDIX I

Central Plant/Styrene II Area

ESTIMATED CONTAMINANT MASSES

Media ("compartment")	Contaminant Mass (LBS)*				
	Central Plant Area		Styrene II Area		PRP 10/91 Report
	All Data	Hits Only	All Data	Hits Only	
Vadose Zone	6,292,167	6,165,362	65,422	57,388	2,100,000
LNAPL	4,544,779 **	4,544,779 **	0	0	1,900,000
Dissolved in Groundwater	113,782	107,305	1,154	1,071	28,307
Sorbed on Soil in Groundwater ≠	286,520	270,210 ≠	2,906 ≠	2,697 ≠	See Text
TOTAL	11,237,248	11,087,656	69,482	61,156	4,028,307
Percent of CPA's Mass ("All Data")	100%	99%	1%	1%	36%

* Digits are retained for reference to computation tables, not for accuracy.

** One data point accounts for 50% of Mass.

≠ Assumes same water-soil ratio as in CPA "All Data" column.

From memo to PADER from CDM, 8/92

Comparison of Wells Tested During Task 2 and Task 3
Hydraulic Conductivity Estimates (ft/d)

Well	*Task 2 (Rising Head)*	*Task 3 (Pump)*	
204D	11	323,422	$\bar{x} = 372.5$
207M	168	231	
211S	188	300,480	$\bar{x} = 390$
211D	1	270,210	$\bar{x} = 240$
212D	9 2 $\bar{x} = 5.5$	540 810 $\bar{x} = 675$	
17	28 118 $\bar{x} = 73$	2,210 3,252 $\bar{x} = 2,731$	
141	388	1,903	

Geometric Mean:	34 ft/d	601 ft/d
# Results:	7	

TABLE 3-1

Results of Pressure Packer Rising Head Tests
Central Plant/Styrene II Plant
ACC Beaver Valley Plant
Monaca, Pennsylvania

WELL	SCREENED INTERVAL (ft)	K (cm/sec)	K (ft/day)
201S	60-90	6.15E-02	174
204M	85-105	4.49E-02	127
* 204D	112-122	3.97E-03	11
* 207M	82-102	5.94E-02	168
207D	110-125	3.25E-03	9
209S	63-93	8.05E-02	228
209M	99-109	6.20E-03	18
209D	118-128	1.61E-02 TEST #1	46
		9.03E-03 TEST #2	26
* 211S	59-89	6.63E-02	188
* 211D	90-110	3.10E-04	1
* 212D	102-117	3.20E-03 TEST #1	9
		8.63E-04 TEST #2	2
218S	65.5-95.5	5.28E-02	150
222D	113-128	1.07E-02 TEST #1	30
		6.40E-03 TEST #2	18
223D	113-128	8.72E-03	25
* MW17	62-82	9.84E-03 TEST #1	28
		4.16E-02 TEST #2	118
* MW141	67-82	1.37E-01	388

* Analyzed in Task 3

Geometric Mean:		
	Shallow	146 ft/d
	Medium	73 ft/day
	Deep	11 ft/day
	Total	36 ft/day

From Task 2 Report (ENSR, 12/93)

TABLE 4

NITROGEN PLANT – AQUIFER PUMP TEST ANALYSIS
CENTRAL PLANT/STYRENE II PLANT
ACC BEAVER VALLEY PLANT
MONACA, PENNSYLVANIA

PUMP TEST WELL 227P

Parameters	Shallow				Deep	
	NIT–P2	* 211S	213S	MW–38	* 211D	* 212D
Discharge rate, ft^3/min	26.74	26.74	26.74	26.74	26.74	26.74
Radial distance from pumping well, ft	20	38	191	100	34	120
Time, min (early data)	3	4	70	13	1.4	2.2
Drawdown, ft (early data)	0.2	0.22	0.06	0.05	0.25	0.12
Time, min (late data)	18	10	130	58	90	22
Drawdown, ft (late data)	0.17	0.13	0.09	0.067	0.3	0.078
Dimensionless time match point (early data)	1	1	1	1	1	1
Dimensionless drawdown match point (early data)	1	1	1	1	1	1
Dimensionless time match point (late data)	1	1	1	1	1	1
Dimensionless drawdown match point (late data)	1	1	1	1	1	1
K_v/K_h	0.25	0.25	Theis	Theis	0.25	0.1
Average saturated thickness, ft	48	48	48	48	48	48

Calculated parameters	NIT–P2	211S	213S	MW–38	211D	212D
Transmissivity, ft^2/min (early data) K=	330 11	300 10	1050 35	1290 43	270 9	540 18
Transmissivity, ft^2/min (late data) K=	390 13	480 16	720 24	960 32	210 7	810 27
Storage coefficient (dimensionless)	7.98E–02	2.68E–02	6.80E–02	5.53E–02	1.03E–02	2.71E–03
Specific yield (dimensionless)	5.63E–01	1.13E–01	8.42E–02	1.84E–01	5.52E–01	4.17E–02

Geometric mean for the transmissivity, ft^2/min	17

K=510 ft/d

Note: Field data are presented in Appendix I–3.

* Wells tested in Task 2

Number of Results: 34
Geometric Mean of all values: 548 ft/day

From Task 3 Report (EN[illegible]

TABLE 5
DYLARK PLANT – AQUIFER PUMP TEST ANALYSIS
CENTRAL PLANT/STYRENE II PLANT
ACC BEAVER VALLEY PLANT
MONACA, PENNSYLVANIA

PUMP TEST WELL 224P

Parameters	Shallow				Deep
	DYL–P2	* MW–17	MW–18	203S	* 204D
Discharge rate, ft^3/min	28.07	28.07	28.07	28.07	28.07
Radial distance from pumping well, ft	20	47	155	198	27
Time, min (early data)	0.6	10	9	22	5.5
Drawdown, ft (early data)	0.024	0.025	0.014	1.7	0.17
Time, min (late data)	0.6	5	9	1400	55
Drawdown, ft (late data)	0.024	0.017	0.014	1.75	0.13
Dimensionless time match point (early data)	1	1	1	1	1
Dimensionless drawdown match point (early data)	1	1	1	1	1
Dimensionless time match point (late data)	1	1	1	1	1
Dimensionless drawdown match point (late data)	1	1	1	1	1
K_v/K_h	Theis	Theis	Theis	0.25	0.5
Average saturated thickness, ft	58	58	58	58	58

Calculated parameters	DYL–P2	MW–17	MW–18	203S	204D
Transmissivity, ft^2/min (early data) K=	2309 93	2210 89	3972 160	25 1	323 13
Transmissivity, ft^2/min (late data) K=	2309 93	3252 131	3972 160	25 1	422 17
Storage coefficient (dimensionless)	1.40E–01	4.05E–01	5.98E–02	7.37E–04	9.92E–02
Specific yield (dimensionless)	1.40E–01	2.97E–01	5.98E–02	4.56E–02	1.30E+00

Geometric mean for the transmissivity, ft^2/min	32

K=794 ft/d

Note: Field data are presented in Appendix I–6.

* Wells tested in Task 2

From Task 3 Report (ENSR, 4/94)

TABLE 6

STYRENE II PLANT – AQUIFER PUMP TEST ANALYSIS
CENTRAL PLANT/STYRENE II PLANT
ACC BEAVER VALLEY PLANT
MONACA, PENNSYLVANIA

PUMP TEST WELL 225P

Parameters	Shallow		*		Intermediate	Deep
	STY–P2	STY–P5	MW–141	MW–142	* 207M	206D
Discharge rate, ft^3/min	28.07	28.07	28.07	28.07	28.07	28.07
Radial distance from pumping well, ft	20	49	96	87	64	46
Time, min (early data)	0.48	1.1	3	4.5	1.2	1.8
Drawdown, ft (early data)	0.21	0.27	0.03	0.035	0.25	0.28
Time, min (late data)	15	68	3	4.5	85	140
Drawdown, ft (late data)	0.2	0.27	0.03	0.038	0.25	0.3
Dimensionless time match point (early data)	1	1	1	1	1	1
Dimensionless drawdown match point (early data)	1	1	1	1	1	1
Dimensionless time match point (late data)	1	1	1	1	1	1
Dimensionless drawdown match point (late data)	1	1	1	1	1	1
K_v/K_h	0.25	0.25	Theis	Theis	0.25	0.5
Average saturated thickness, ft	56	56	56	56	56	56

Calculated parameters	STY–P2	STY–P5	MW–141	MW–142	207M	206D
Transmissivity, ft^2/min (early data) k=	283 11	206 8	1903 74	1646 64	231 9	206 8
Transmissivity, ft^2/min (late data) k=	283 11	206 8	1903 74	1517 59	231 9	180 7
Storage coefficient (dimensionless)	1.28E–02	3.79E–03	2.42E–02	3.80E–02	2.62E–03	6.79E–03
Specific yield (dimensionless)	4.19E–01	2.34E–01	2.42E–02	3.50E–02	1.85E–01	4.93E–01

Geometric mean for the transmissivity, ft^2/min	17

k = 510 ft/d

Note: Field data are presented in Appendix I–10.

* Wells tested in Task 2

From Task 3 Report (ENSR, 4/94)

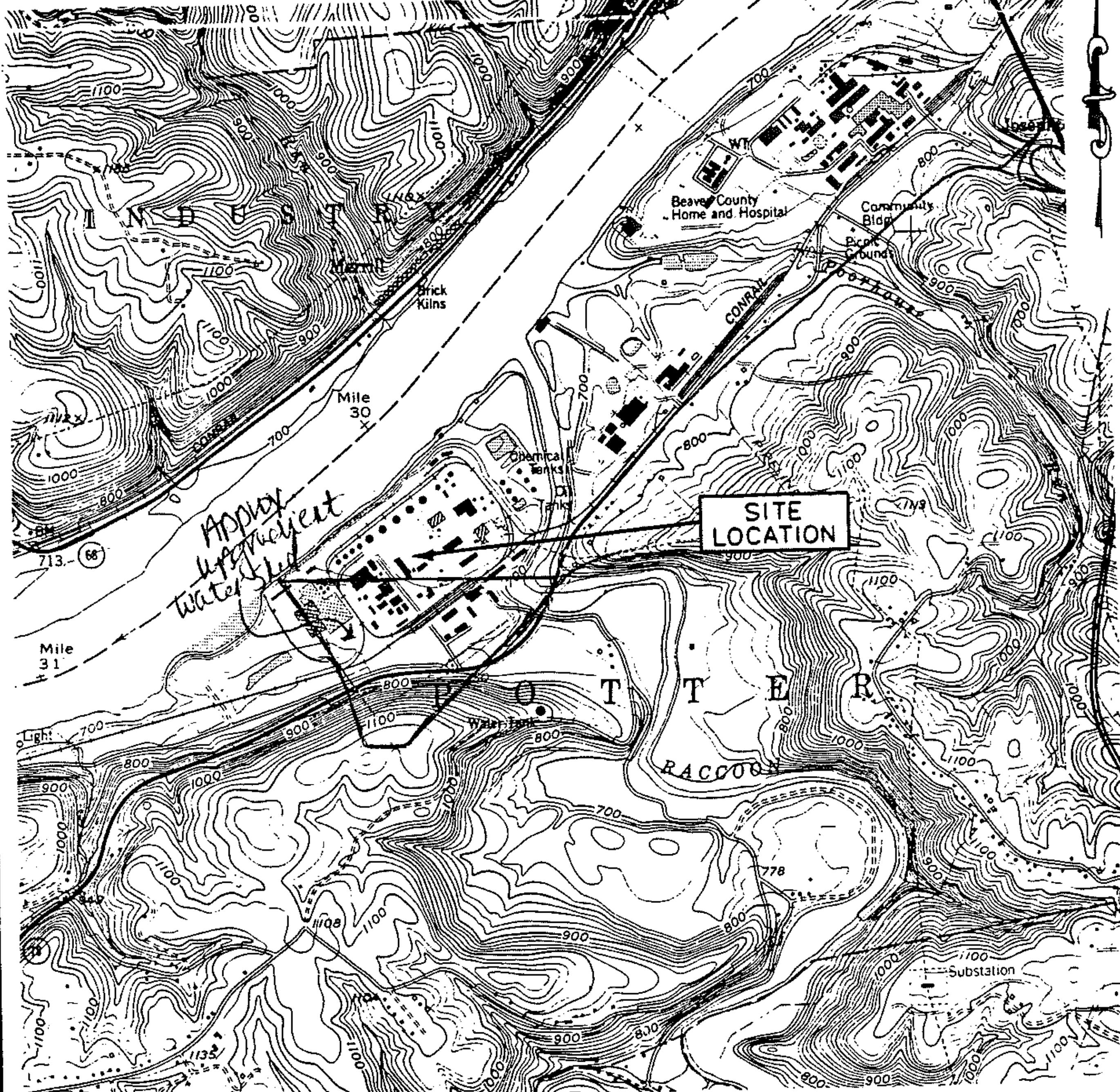

Scale: 1:24,000

Scale 0 2000 4000 6000 8000 10000 Feet

Scale 0 0.5 1 2 Miles

REFERENCE:
Beaver, Pennsylvania, USGS 7.5 Minute Quadrangle

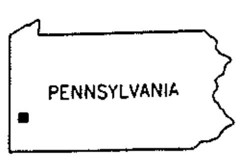

QUADRANGLE LOCATION

ENSR™
ENSR CONSULTING AND ENGINEERING

FIGURE 1-1
SITE LOCATION MAP
ARCO BEAVER VALLEY PLANT
MONACA, PENNSYLVANIA

Drawn:	MSH	Date: 10/26/93	Project Number:	Rev:
Appr'd:	MEF	Revised: 11/4/93	0480-223	0

From CP/S2 Task 2 Report (ENSR, 1993)

Geometric mean of K values from pumptests: 548 ft/day

B ≈ 50 ft ⇒ A = 1850 × 50 = 92500 ft²

i = 0.5/2307.5 = 0.00022 ft/ft

$Q = KAi = (548)(92500)(0.00022)$

= 11,152 cfd

≈ 58 gpm

≈ 83,421 gpd

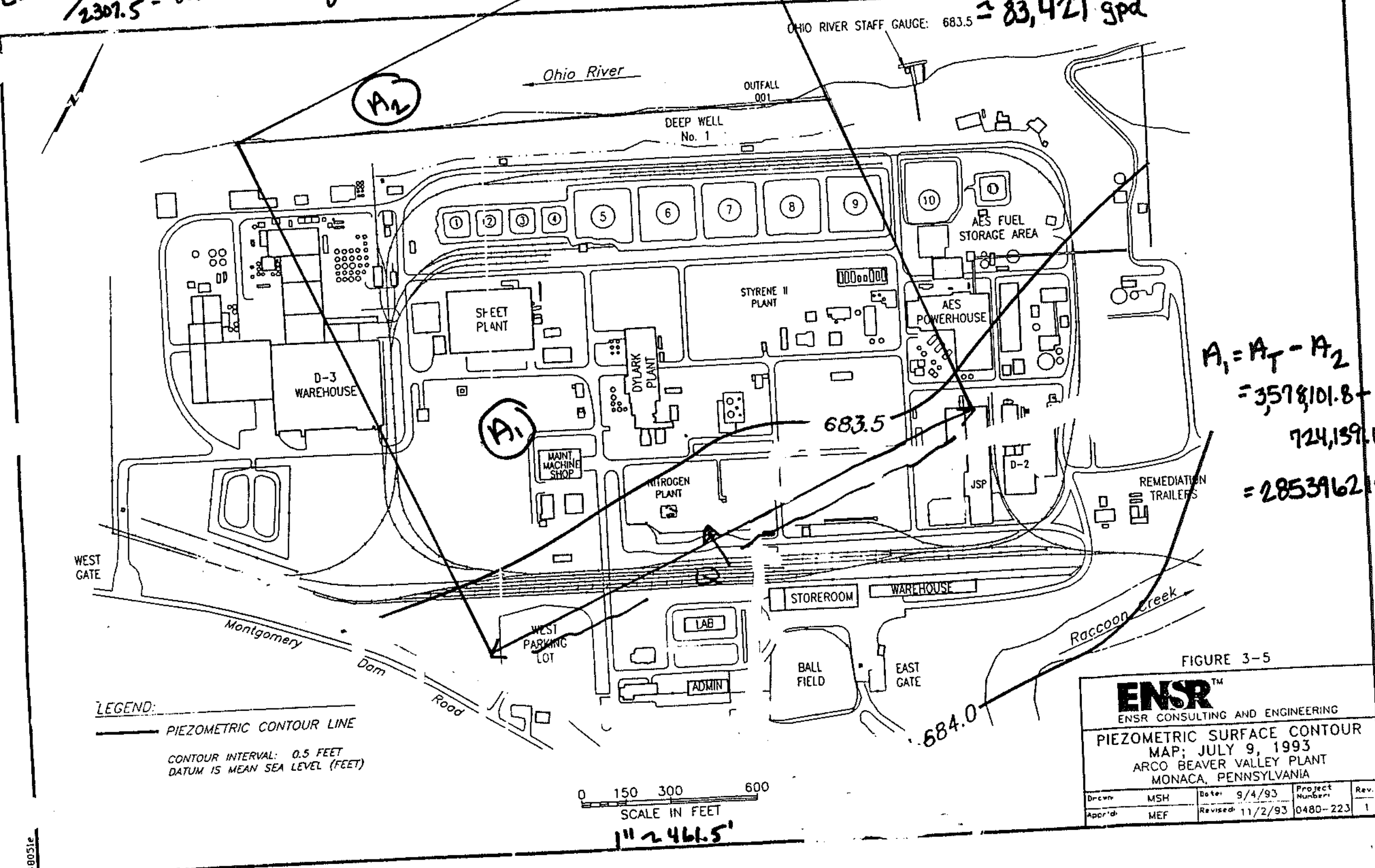

$A_1 = A_T - A_2$

= 3,578,101.8 − 724,139.65

= 2853962.15 ft²

0480S1e

TASK 2 CP/SII (1993)

:Increase from 1989
:Decrease from 1989
:No Change

Ethylbenzene 1993 MCL: 700 ug/L

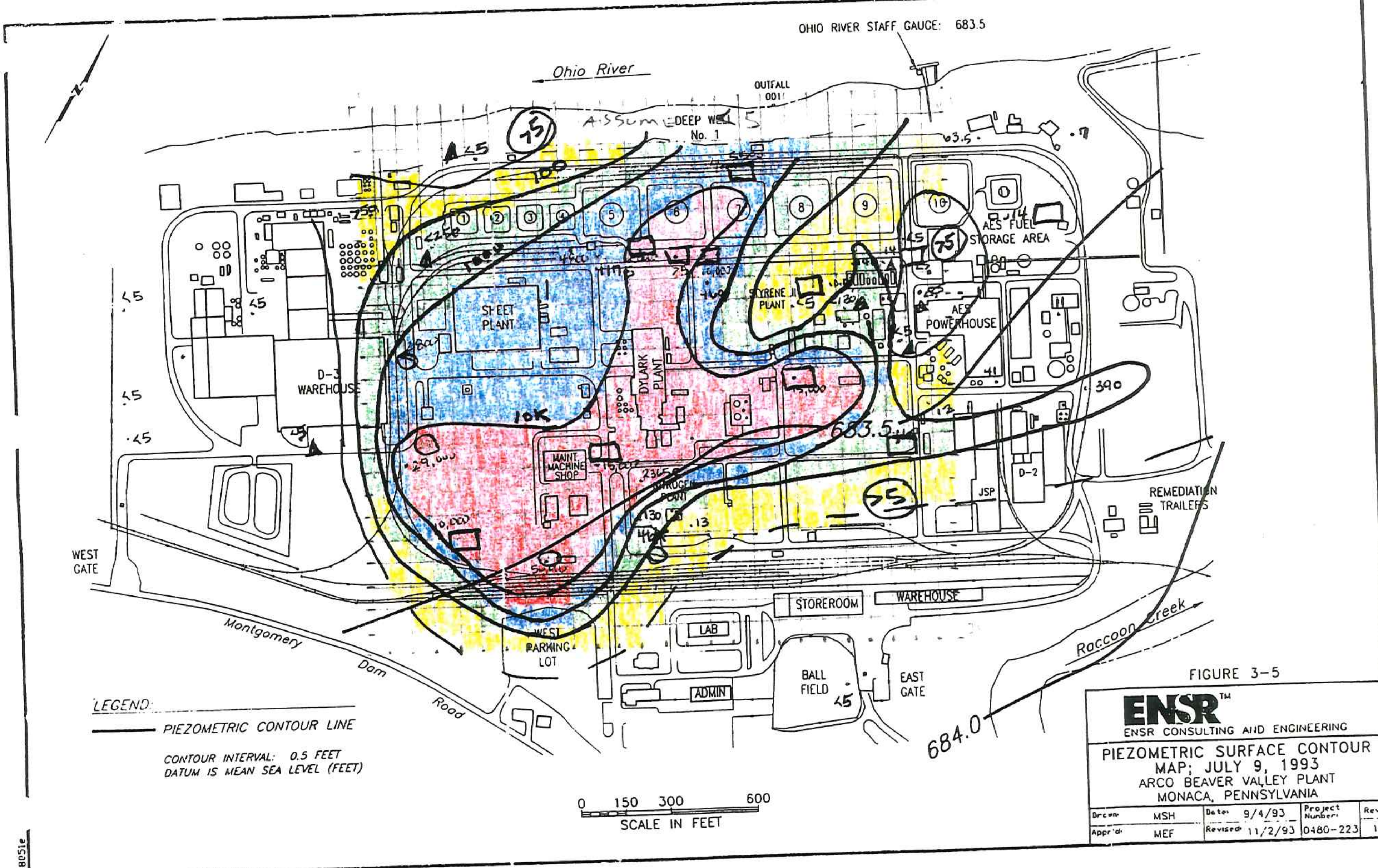

FIGURE 3-5

ENSR™
ENSR CONSULTING AND ENGINEERING

PIEZOMETRIC SURFACE CONTOUR MAP; JULY 9, 1993
ARCO BEAVER VALLEY PLANT
MONACA, PENNSYLVANIA

Drawn	MSH	Date: 9/4/93	Project Number:	Rev
Appr'd	MEF	Revised: 11/2/93	0480-223	1

LEGEND:
PIEZOMETRIC CONTOUR LINE

CONTOUR INTERVAL: 0.5 FEET
DATUM IS MEAN SEA LEVEL (FEET)

0 150 300 600
SCALE IN FEET

TASK 2 CP/SII (1993)

048051e

O :Increase from 1989
□ :Decrease from 1989
▲ :No Change

Benzene 1993 MCL: 5 ug/L

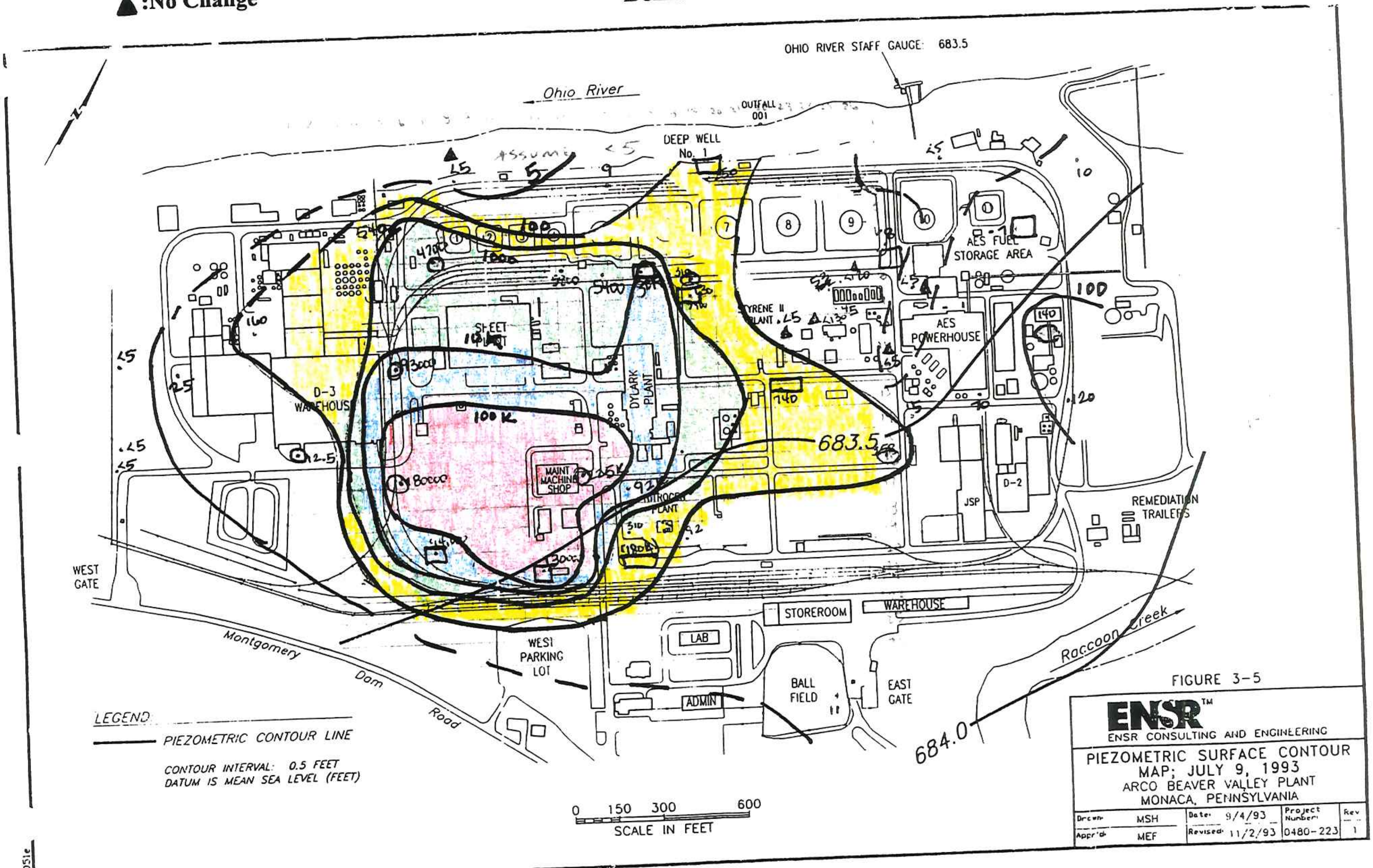

048051e

TASK 2 CP/SII (1993)

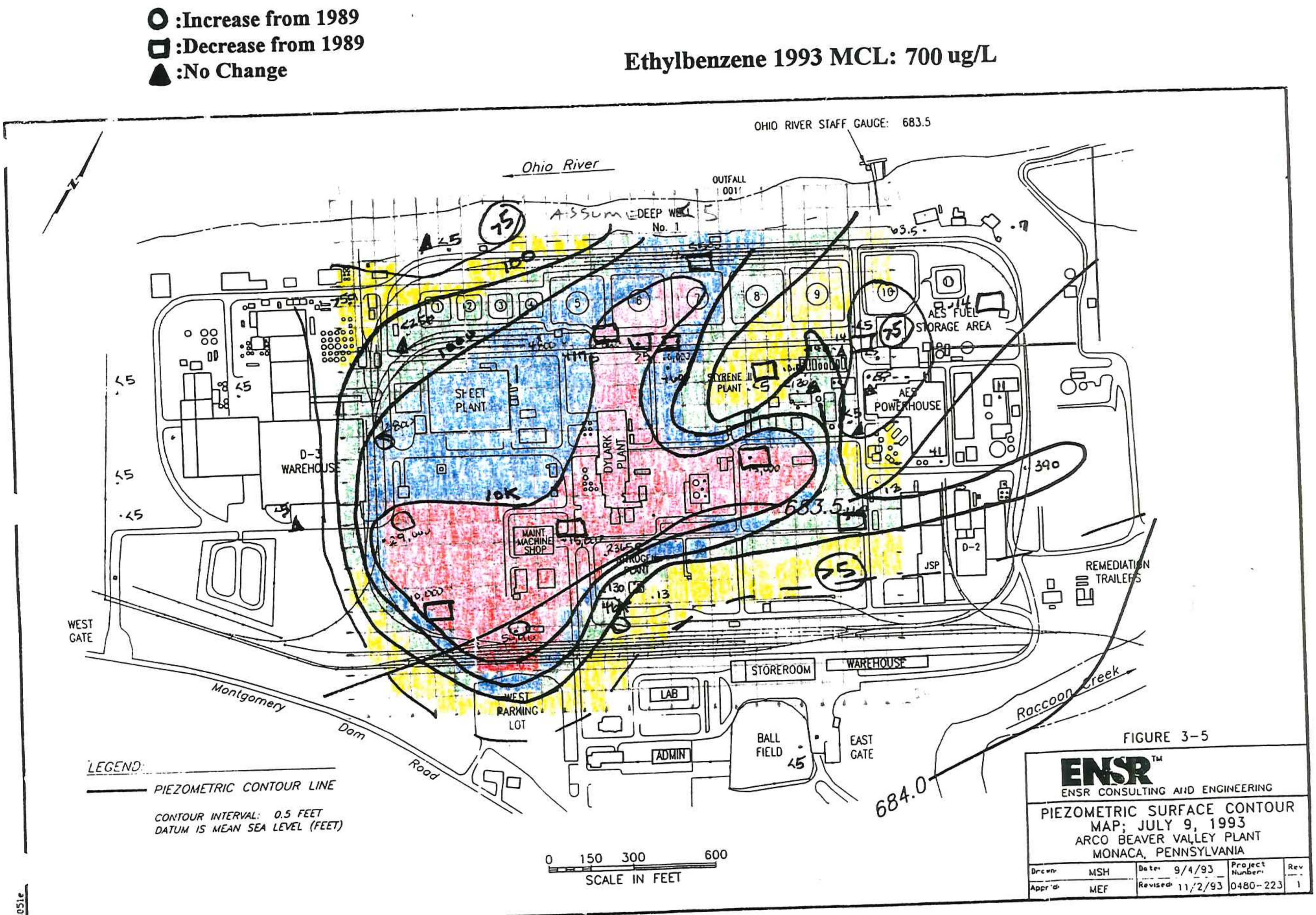

TASK 2 CP/SII (1993)

0 :Increase from 1989
□ :Decrease from 1989
▲ :No Change

Benzene 1993 MCL: 5 ug/L

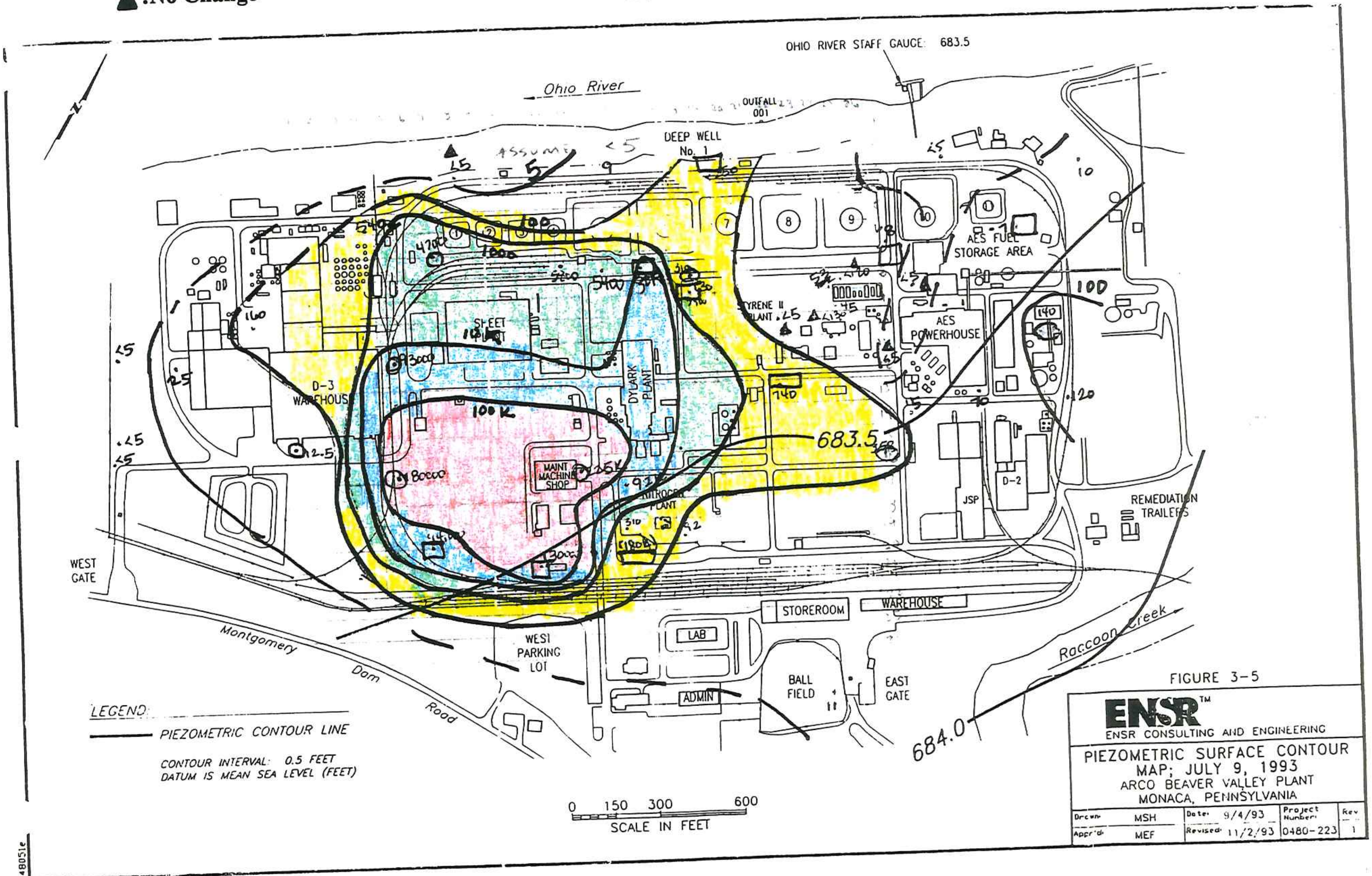

04805le

TASK 2 CP/SII (1993)

APPENDIX II

Over-The-Hill/Tank Farm Area: Water Table Fill Area

TABLE 6 (Page 1 of 2)
HYDROGEOLOGIC UNIT PARAMETERS
OVER-THE-HILL TANK FARM AREA
ARCO CHEMICAL COMPANY - BEAVER VALLEY PLANT
MONACA, PENNSYLVANIA

WELL NAME/NO.	DATA RELIABILITY	HYDROGEOLOGIC UNIT CLASSIFICATION	ANALYTICAL METHOD	APPARENT TRANSMISSIVITY (T)		APPARENT STORATIVITY (S) dimensionless	APPARENT HYDRAULIC CONDUCTIVITY (K) ft/day
				ft^2/day	gal/day/ft		
Wells Used in the Sand & Gravel Unit							
*PW-302	3	Leaky Confined	Theis/Hantush	2,211	16,540	9.9×10^{-3}	39
OW-323	1	Unconfined	Theis/Neuman	31,952	239,000	2.1×10^{-2}	819
MW-342	1	Unconfined	Theis/Neuman	31,952	239,000	1.5×10^{-2}	571
MW-343	1	Unconfined to Leaky Confined	Theis	31,952	239,000	8.0×10^{-3}	571
MW-344	1	Unconfined	Theis/Neuman	31,952	239,000	1.2×10^{-2}	673
MW-345	1	Unconfined to Leaky Confined	Theis	31,952	239,000	1.3×10^{-4}	673
MW-348	1	Unconfined	Theis/Neuman	31,952	239,000	2.2×10^{-2}	7,905
P-306S	1	Unconfined	Theis/Neuman	31,952	239,000	$8.0\ 10^{-2}$	571
P-306D	1	Leaky Confined	Theis	31,952	239,000	2.4×10^{-3}	571
OW-303	2	Leaky Confined	Theis/Hantush	6,833	51,110	5.1×10^{-4}	120
MW-149	2	Confined	Theis	31,952	239,000	1.2×10^{-1}	560
MW-151	2	Leaky Confined	Theis/Hantush	5,949	44,500	1.8×10^{-3}	104
MW-167	2	Leaky Confined	Theis/Hantush	3,668	27,440	7.2×10^{-5}	64
MW-169	2	Confined	Theis	15,294	114,400	2.5×10^{-6}	268
MW-349	2	Leaky Confined	Theis/Hantush	1,332	99,630	7.1×10^{-4}	23

From Task 3 Report (Dames & Moore, 4/94)

TABLE 6 (Page 2 of 2)
HYDROGEOLOGICAL UNIT PARAMETERS
OVER-THE-HILL TANK FARM AREA
ARCO CHEMICAL COMPANY - BEAVER VALLEY PLANT
MONACA, PENNSYLVANIA

WELL NAME/NO.	DATA RELIABILITY	HYDROGEOLOGIC UNIT CLASSIFICATION	ANALYTICAL METHOD	APPARENT TRANSMISSIVITY (T)		APPARENT STORATIVITY (S) dimensionless	APPARENT HYDRAULIC CONDUCTIVITY (K) ft/day
				ft^2/day	gal/day/ft		
Wells Used in the Sand & Gravel Unit (Continued)							
MW-170①	3	Confined/Silty Clay Aquitard	Theis	11,079	82,870	23.09	1,108
MW-108	3	Unconfined	Theis	13,017	97,370	1.03×10^{-1}	228
MW-157	3	Unconfined	Theis	16,765	125,400	6.6×10^{-1}	294
Wells Used in the Fill Unit							
*MW-156②	3	Unconfined	Theis, Neuman	35	263	139.5③	7.0
MW-116	1	Unconfined	Theis, Neuman	37	276	1.2×10^{-2}	7.4
MW-168	1	Unconfined	Theis, Neuman	47	355	1.4×10^{-2}	9.5
OW-302	1	Unconfined	Theis, Neuman	43	324	5.3×10^{-2}	8.6
OW-301	2	Unconfined	Theis, Neuman	34	257	2.4×10^{-1}	6.9

Notes:
① Well set in silty clay lithologic unit.
③ Specific yield from early-time data equals 1.8×10^{-1}
② Dewatering of test well violates Theis assumptions. Storativity calculated is too great.
* Pumping Well

RELIABILITY:
1 = Most Representative of Hydrogeologic Properties
2 = Representative of Hydrogeologic Properties
3 = Least Representative of Hydrogeologic Properties

1 Sand and Gravel Unit
Numer of Results:17
Geometric Mean: 310 ft/day
2 Reliability = 1 (except MW348)
Numer of Results:7
Geometric Mean:630 ft/day
3 Fill
Numer of Results:5
Geometric Mean: ~8 ft/day

From Task 3 Report (Dames & Moore, 4/94)

Fill/Water Table Zone

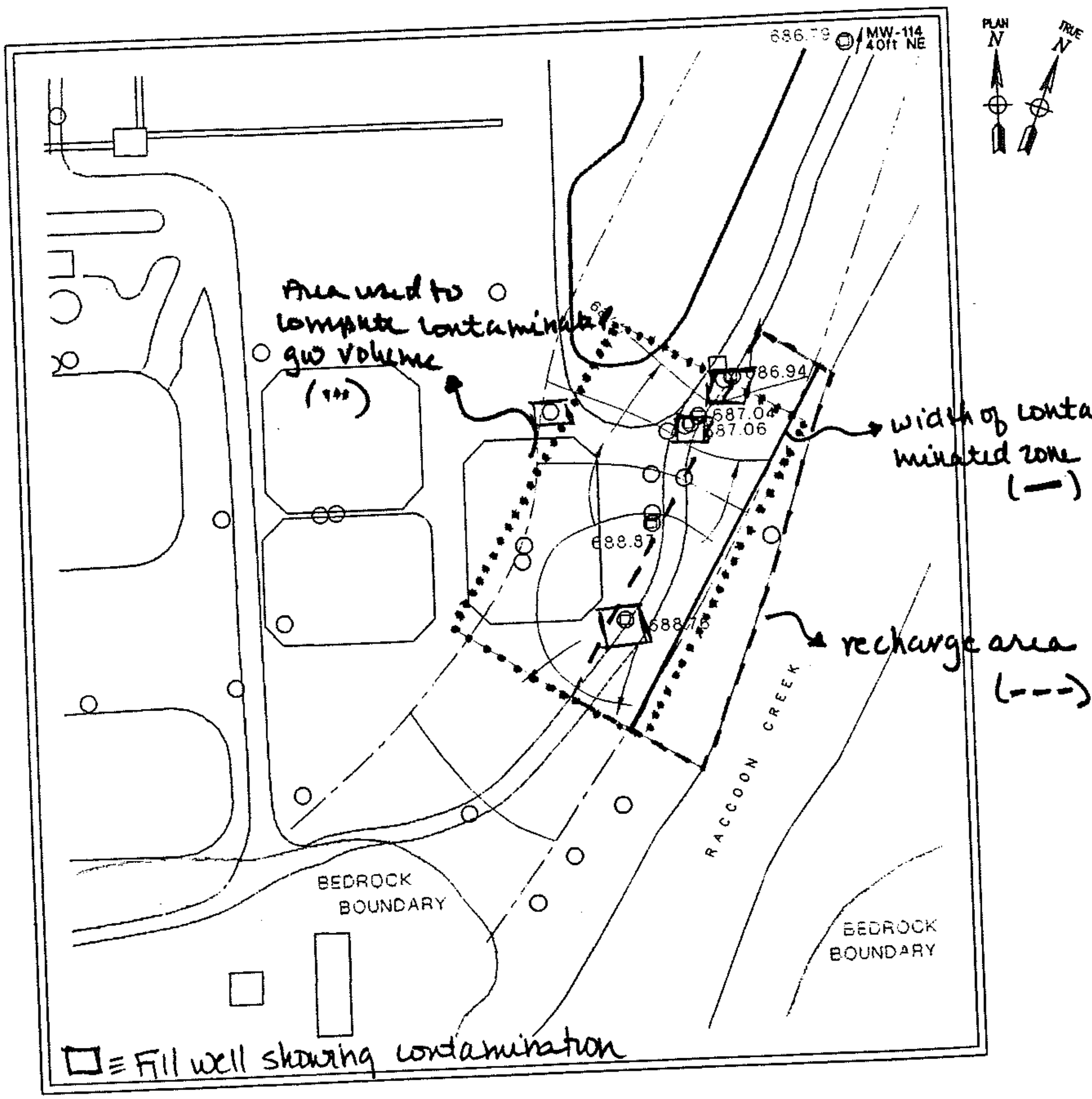

SCALE 1 inch = 150 Feet

LEGEND

○ - EXISTING MONITORING WELLS (Over-The-Hill Tank Farm Area)

688.76 ☐ - WELLS USED IN FILL UNIT HYDROGEOLOGIC TESTING (ft.)

——687.0 - GROUNDWATER ELEVATION CONTOURS (ft)

— - — - APPROXIMATE LIMIT OF SATURATED FILL MATERIAL

TITLE	GROUNDWATER POTENTIOMETRIC SURFACE MAP FILL UNIT
PROJECT	ARCO CHEMICAL – BEAVER VALLEY PLANT OVER-THE-HILL TANK FARM AREA
	DAMES & MOORE INC. PITTSBURGH, PENNSYLVANIA & TORONTO, ONTARIO

SCALE: AS NOTED	DRAWN BY: RL	JOB NO.: 05931-577	
DATE: FEB. 1994	APPR. BY:	FIG. NO.: 7	

Source: Task 3 Hydrogeological Studies Report - OTH (Dames & Moore, 1994)

CALC of $\Delta h/\Delta l$, K, b

Based on conceptual model, discharge to RC occurs

- laterally through shallow fill/silty clay
- vertically, from S&G through silty clay

Lateral flow through shallow fill

- Computer average $\Delta h/\Delta l$ from MW116, MW156, MW168 to River
- Assume thickness for saturated fill = 5'
- Length of contaminated zone in fill = 414.5'
- K for fill = 7.9 ft/d (average from date listed in Table 6 of Task 3)

Date:	MW116	MW156	MW168	RC
4/27/93	687.56	NA	686.73	682.94
Δh	4.62	-	3.79	
5/28/93	656.67	687.51	684.69	683.64
Δh	3.03	3.87	1.05	
6/15/93	688.06	686.82	686.77	683.49
Δh	4.57	3.33	3.28	
7/7/93	684.56	686.61	683.3	683.34
Δh	1.22	3.27	-0.04	
11/15/93	688.76	687.06	686.94	683.84
Δh	4.96	3.26	3.14	

Geometric of Δh: 3.07
Arth Mean of Δh: 3.34 (both excluding Δh = -0.04)

Δl 116/RC - 114'
156/RC - 176'
168/RC - 155'
Δl = 148

Compute flow through shallow fill:
$Q = KAi = (7.9)(415x5)\ 3.34/1.48 = 369.9 = 370$ cfd (1.92 gpm or 2,767 gpd)

APPENDIX III

Over-The-Hill/Tank Farm Area: Shallow Sand and Gravel

Shallow Sand and Gravel Zone

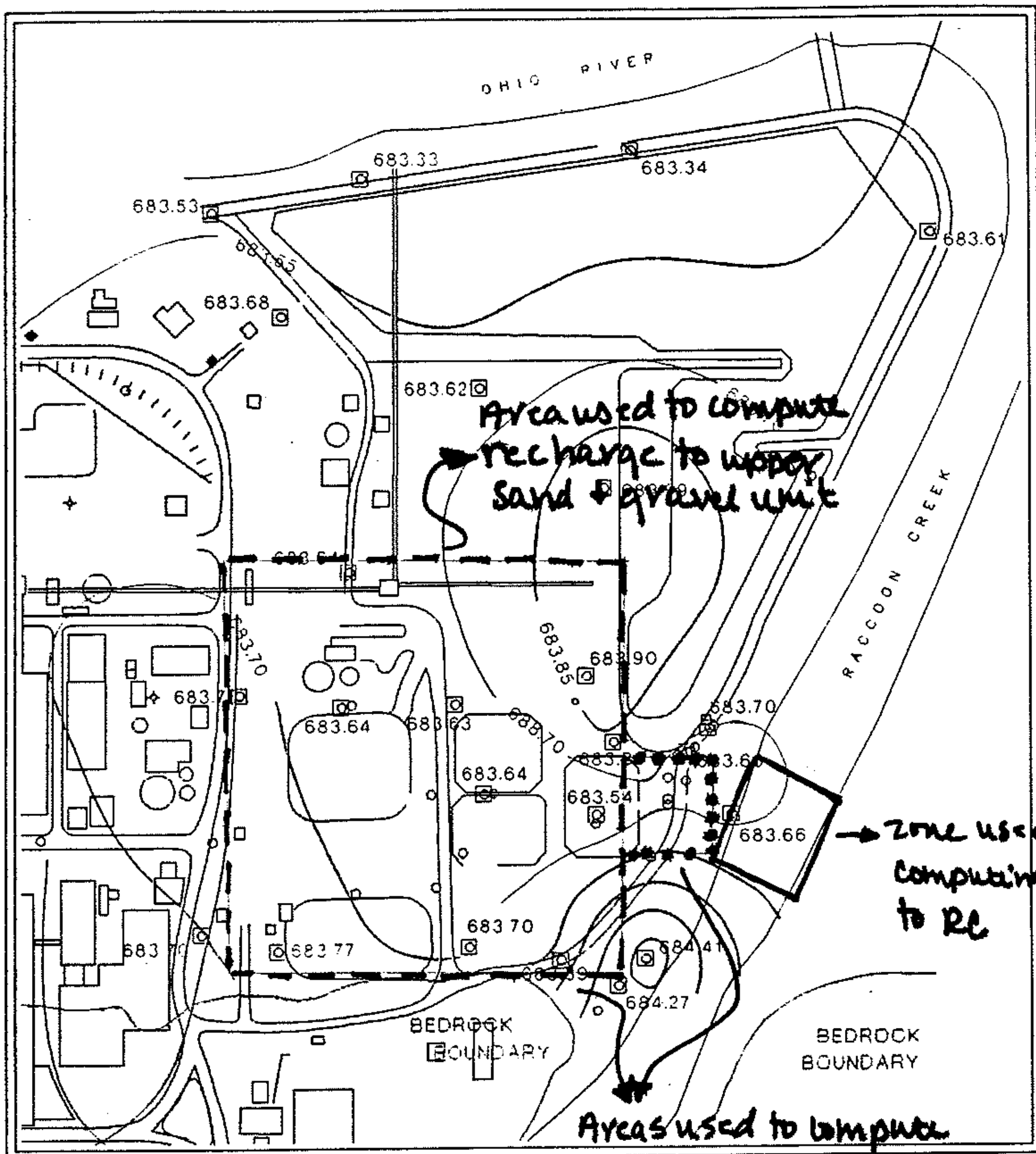

SCALE 1 Inch = 300 Feet

LEGEND

○ - EXISTING MONITORING WELLS (Over-The-Hill Tank Farm Area)

683.77 □ - WELLS USED IN SAND & GRAVEL UNIT HYDROGEOLOGIC TESTING (ft.)

——687.0 - GROUNDWATER ELEVATION CONTOURS (contour Interval 0.15 ft)

TITLE	GROUNDWATER POTENTIOMETRIC SURFACE MAP SHALLOW SAND & GRAVEL UNIT
PROJECT	ARCO CHEMICAL – BEAVER VALLEY PLANT OVER-THE-HILL TANK FARM AREA
	DAMES & MOORE INC. PITTSBURGH, PENNSYLVANIA & TORONTO, ONTARIO

SCALE: AS NOTED	DRAWN BY: RL	JOB NO.: 05931-577	
DATE: FEB. 1994	APPR. BY:	FIG. NO.: 6	

Source: Task 3 Hydrogeological Studies Report - OTH (Dames & Moore, 1994)

Flow in Shallow Sand & Gravel (S&G) Unit

- Groundwater flows northward from the location of the bedrock outcrop and southward from a high caused by the Wastewater Treatment Lagoon. The piezometric low is observed beneath the OTH area.

  From the OTH area, groundwater flows eastward to RC or northward to CP.

- The gradient between OTH and RC is relatively flat and the potential groundwater pathway to RC is restricted by the piezometric highs on either side.

- Vertical groundwater flow is generally downward toward the deeper portion of the sand and gravel zone, except one cluster (342,343) consistently shows an upward vertical gradient.

- Discharge from the shallow sand and gravel to the RC occurs across the silty clay layer.

- The thickness of the clay layer beneath RC is not known. Data from cross-sections was used to approximate the thickness.

- The depth of RC is not known.

- Some shallow sand and gravel groundwater may flow under RC. During the pump test, drawdowns were noted in wells on the eastern side of RC.

- Conclusion - There's probably limited flow from the shallow sand and gravel based on the information presented in the reports.

- Highest benzene concentrations observed at wells MW342 and MW115. Concentrations increasing at MW110, MW344, 115 and possibly MW342. This would be consistent with the hypothesis of vertical migration occurring where the silty clay layer is thin or more permeable.

  Also, concentrations seem to be increasing at wells on the south (downgradient) side of the high caused by the Wastewater Treatment Lagoon.

Vertical Flow from S&G through Silty Clay

- Use Well MW 151 and pod elevation in RC to calculate flow direction between S&G unit and RC.

Date	MW151	RC	Δh
4/27	683.35	682.94	0.41
5/28	683.7	683.64	0.06
6/15	683.71	683.49	0.22
7/7	683.59	683.34	0.25
11/15	683.66	683.84	-0.14

$\Delta h = 0.235$

- Approximate thickness of silty clay below RC = 7 feet
- K_v of clay (from model input) = 2.8×10^{-4} ft/day
- Area of upward flow (east of OTH) = 27,000 sf

Compute Q to RC

$$Q = KAi = (2.8\text{x}10^{-4}\ \text{f/d})(27{,}000\ \text{sf})\ 0.235\ \text{ft}/7\ \text{ft}$$
$$= 0.2538\ \text{cfd}$$

APPENDIX IV

Over-The-Hill/Tank Farm Area: Deep Sand and Gravel

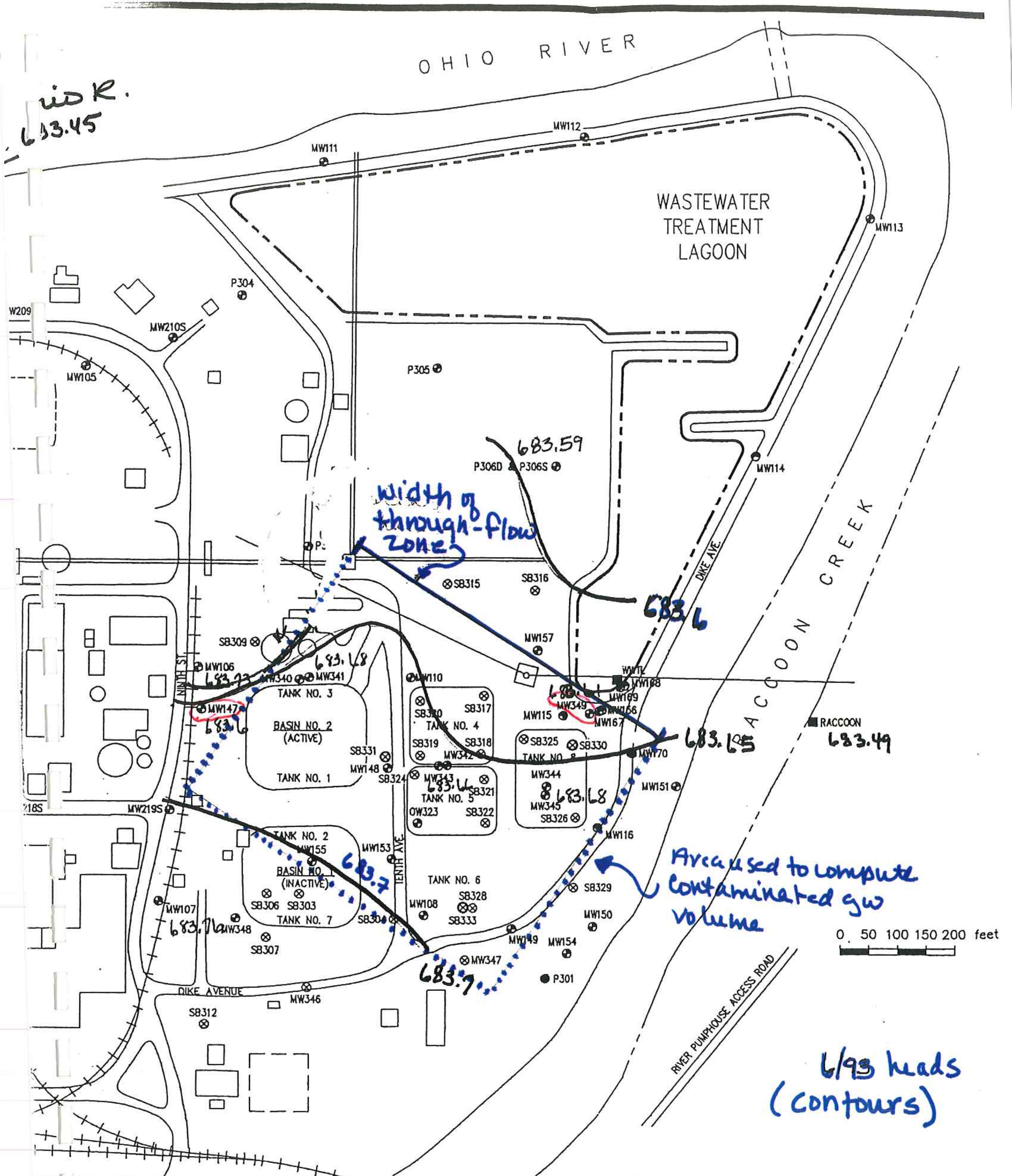

Deep Sand and Gravel Zone

Flow in Deep Sand and Gravel

- Groundwater in the deep S&G flows from the outcropping bedrock northeastward towards the confluence of Raccoon Creek and the Ohio River.

- Benzene and Ethylbenzene concentrations use generally decreasing, except at MW147 where Ethylbenzene seems to have increased.

- Based on boring logs from wells MW112 and MW113, it appears that the silty clay layer is present in these locations. As such, discharge from the S&G zone to the Ohio River maybe limited by the presence of the clay.

- Compute horizontal flow rate in deep S&G.

  K = 310 f/d (from pumping test)
  A = 600 x 10 = 6,000 sf
  i = 0.23/1,000 = 0.00023
  Q = KAi = 427.8 cfd

APPENDIX V

Well Points Area Memorandum

Memorandum

To: *Fred Baldassare*

From: *Karen Lebiedzinski, Bob Schreiber and Kris Masterson*

Date: *January 6, 1995*

Subject: *Evaluation of Contaminant Concentrations at the Well Points*

Groundwater quality data collected at well points located near the banks of the Ohio River north of the Central Plant/Styrene II (CP/S2) area were analyzed to evaluate groundwater concentration trends and to determine whether a contaminant plume from the site is discharging to the Ohio River. The analysis primarily focused on data collected after groundwater recovery at well DW-01 was terminated. The analysis included reviewing data collected during monthly monitoring of the well points, and comparing observed concentrations to those observed in the CP/S2 area. Data from DW-1 pumping samples were also analyzed. The general approach to evaluating the well point data was outlined in a memorandum to PADER dated 6/2/94.

This memorandum is organized into the following sections.

Section 1.0	Overview
Section 2.0	Summary of Well Point Data
Section 3.0	Analysis of Groundwater Hydraulics and Contaminant Dilution and Breakthrough
Section 4.0	Summary and Conclusions

Section 1.0 - Overview

Operation of Deep Well 1

As part of remediation efforts to reduce contaminated groundwater discharge to the Ohio River, ARCO installed a groundwater extraction well (Deep Well 1 or DW-01) on the North end of the site near the Ohio River. Groundwater recovery at Deep Well 1 was restarted on January 19, 1993 at a rate of 200 GPM or 38,500 cfd. The pumping was terminated on August 13, 1993.

Approach to Problem

The groundwater quality in the area was evaluated by installing 10 monitoring well points, from which groundwater samples were collected and analyzed monthly and bi-weekly from September 1993 to the present. These well points are situated along the river, running about 500 feet west and east of DW-01.

The data were examined to identify trends in the groundwater concentrations during and after the most recent shut-down of DW-01. From these data, inferences about the presence of pure product or the existence of contaminant plumes could be made. Also, hydraulic calculations were made to compare the amount of contaminant recovered by DW-01 to the amount present in the surrounding groundwater. Observed breakthrough of the plume was also compared to predicted groundwater velocity, to confirm hydraulic parameter estimates and the hypothesis of plume migration. Also evaluated was whether samples from the "sandpack" wells showed significant differences from the wellpoint samples.

Section 2.0 - Summary of Well Point Data

Time history graphs of measured benzene and ethylbenzene concentrations taken at 10 locations following the termination of groundwater recovery at DW-01 were used to study the groundwater concentration trends. Data were compiled using monthly reports from September 1988 to November 1994. The well locations are grouped as follows, noting that the wells are numbered from east to west:

Group A: Wells 5, 6, & 7 (Locations near and to the east of the Deep Well)

Group B: Wells 8, 9, & 10 (Locations near and to the west of the Deep Well)

Group C: Wells 4, 11, 12 & 13 (Locations more distant from the Deep Well)

Figures 1 to 6 show time histories of the contaminant concentrations at the well points. The plots of each well group of each contaminant are scaled alike for easy comparison. In some cases, duplicate test data were provided. The duplicate values were then averaged for use in the calculation of the statistical values. For sampling events in which the result was non-detect, half the value of the detection limit was used in the calculation of the average.

The general trend appears to be an increase in all concentrations following the shut down of DW-01. The data from September 13, 1993 indicated that all levels of benzene and ethylbenzene were below their maximum concentration limits (MCL) of 0.005 and 0.7 mg/l respectively. During the following months, benzene concentrations increased significantly in well groups A and B. Ethylbenzene concentrations also increase in groups A and B. Well Group C had values consistently below the MCL.

Benzene Results

Time histories of benzene concentration values were compiled to identify trends. Because the wells were grouped by geographic proximity, it was possible to correlate increased concentrations with the presence of contaminated plumes and/or the potential of pure product in a specific area.

Group A (Figure 1): This group of well points exhibited steadily increasing values from below the MCL of 0.005 mg/l to near 2.7 mg/l on the November 1994 sample. These values, however, are low compared to those reported at Group B.

Group B (Figure 2): These well points exhibited the highest concentrations, with maximum values near 45 mg/l. The values began to increase in November 1993, rose steadily to a maximum in March 1993 and leveled off to about 18 mg/l by September 1994. The exception was Well 9, at which concentrations decreased to 0.674 mg/l, then increased significantly to a maximum value of 44.9 mg/l in October 1994.

Group C (Figure 3): Concentrations at these well points were near or below the MCL. The exception is Well 13, which showed a sharp increase in concentrations after a period in March in which no data were available (the well point was not sampled because the well contained no water). However, the values decreased steadily to below the MCL in the following months.

Ethylbenzene Results

Ethylbenzene concentrations were evaluated in the same manner as for benzene concentrations.

Group A (Figure 4): This group showed very high concentrations of ethylbenzene after the shut down of DW-01, except Well 7. Well 6 exhibited a concentration of 132 mg/l in March with decreased to 54 mg/l by September 1994 then increased again, reaching a value of 104 in November 1994. Well 5 reached a maximum concentration of 59 mg/l in May. Concentrations decreased only slightly from July to November 1994, leveling off near 20 mg/l.

Group B (Figure 5): These well points exhibited a significant and steady rise in concentrations from December 1993 through June 1994, with maximum well point concentrations ranging from 11 to 21 mg/l. There was a steady decline in these concentrations to below 5 mg/l in July. From August-November 1994, however, levels in wells 9 and 10 increased to a maximum concentration of 64 mg/l and 40 mg/l respectively.

Group C (Figure 6): The concentrations at this group were below the MCL and stayed constant throughout the testing period.

Sand Pack Data

In order to test the hypothesis that high concentration levels were the result of the contaminated soil and not of a migrating plume of groundwater, ARCO installed wells outfitted with sand packs adjacent to Wells 5, 6, 8 and 10. Samples were then withdrawn from these wells on the same monthly schedule as the original well points and analyzed for contaminant concentrations.

Figures 7 to 14 show time histories of contaminant concentrations at each well point. The wells installed with sand packs had significantly lower concentration values of each contaminant. Wells 6 and 10, however, showed increased concentrations of both benzene and ethylbenzene during the final months of the analysis at levels which were comparable to the increasing values of the well points without the sand pack.

In June, the ethylbenzene concentration in Well 8 was above that in the well point without the sand pack. During August and September, the concentrations were also almost twice as large. For instance, in September the concentration was 11 mg/l, compared to 4.7 mg/l at the original well point.

Statistical Analysis

Statistical values, including arithmetic average, geometric mean and median, were used to summarize the concentration data over the sampling period. Table 1 presents the statistical analysis for the benzene and ethylbenzene concentrations at the September 1993 and July 1994 sampling events. The data show increased concentrations of both contaminants. The data for the Central Plant Area are also presented for comparison. The concentration averages are comparable for the two areas. When DW-01 was operating, concentrations at well points, located near DW-01, were lower, a direct result of the recovery efforts and the induced infiltration of river water.

Table 2 compares the maximum concentrations with the November 1994 data for each well. Some of the recent concentrations are lower than the maximum recorded data, but several November 1994 readings were the highest. Because of this, a long-term trend cannot be identified yet.

Evidence of LNAPL

A contaminant concentration level above 10% of the solubility limit may be an indication that LNAPL or pure product may be present near the well. Table 3 lists the values where measured levels exceeded 10% of the solubility limit. For data evaluated, none of the wells had levels of benzene which exceeded 10% of the solubility limit (178,000 ug/l). However, there were many instances of ethylbenzene levels exceeding 10% solubility concentration (15,200 ug/l). From December 1993 to July 1994, Wells 5 and 6 consistently reported concentrations which were two to nine times higher than 10% of the solubility limit. Comparably high concentrations of ethylbenzene were also reported in the Central Plant and Styrene II areas in April 1989 and April 1993 and LNAPL has been reported there. The correlation indicates the potential presence of pure product in the wellpoint and DW-01 areas.

Section 3.0
Analysis of Groundwater Hydraulics, Contaminant Dilution and Breakthrough

In order to assess the effectiveness of the DW-01 recovery efforts, several methods were used to estimate the amount of river water versus groundwater that the well was pumping. From this value and measured concentrations in DW-01, the amount of contamination in the aquifer could be estimated.

The first method used was an induced infiltration analysis, that produced the ratio of river water to the total water pumped in the well. Following Wilson (see Appendix A), the value was computed as a function of a dimensionless pumping rate and the ambient discharge to the stream. This analysis predicted that 85% of DW-01's pumping was from the river.

An alternate method used Modflow to simulate both pumping and non pumping conditions at the site. The input parameters and results are shown in Appendix B. The model yielded an estimate of 83.4% ± 5.5% for the ratio of river water to total flow into DW-01.

Using these results, Table 4 shows the estimated concentrations in the aquifer for each contaminant, as well as for the total BTEXS. This is based on a simple dilution calculation.

Water table data taken during September 1994 indicate the groundwater flow patterns under non-pumping conditions. Figure 16 shows the water table contours. From these contours, hydraulic gradients were estimated to be between 0.000375 and 0.0006 ft/ft. These values are slightly greater than the value used in the CP/SII memo, and slightly above the predicted maximum natural gradient of 0.0004 ft/ft, made by Applied Hydrology in the April 1989 RI/FS. The water flows generally northwest towards the Ohio River with a very flat gradient.

As expected, the groundwater flow pattern is dramatically different when DW-01 is pumping. A comparison of Figures 15 and 16 show an increase in hydraulic gradients from 0.000375-0.0006 to 0.000417-0.00091 while the well is pumping. The contours to the west are diverted away from the river towards the pumping well.

Plume Breakthrough

Using the estimated hydraulic gradient of 0.0006 ft/ft, the time of travel of a contaminant plume was computed. The well points are located about 150 ft from the pumping well. For an effective porosity of 0.25 and a hydraulic conductivity of 250 ft/day, the groundwater velocity using Darcy's Law is 0.6 ft/day. Using this as the rate of travel of the plume, contaminant breakthrough at the well points (150 feet away) should occur around 250 days. Examination of the time histories shows breakthrough occurring on average 230 days after DW-01 was shut off. Table 5 lists the time for each well point. These results show reasonable agreement and indicate that a plume is traveling toward the river.

Section 4.0
Summary and Conclusion

This analysis of the monthly well point data indicates that there are concentrations of contaminations entering the river which are above the goals set for the remediation at this site.

Comparison of pumping and non-pumping conditions shows a steady increase of concentrations, as evidenced by sustained rising values at the well points directly down gradient of DW-01 (Well Groups A and B). This trend shows that the pumping at DW-01 was recovering product, which is now being discharged to the river.

The high levels of ethylbenzene indicate the possible presence of pure product, which has also been confirmed by ARCO's report of a sheen on the river in November 1994.

A breakthrough analysis shows that the time of travel of the observed contaminant plumes is reasonable with the expected groundwater velocities at this site.

Dilution analysis results enabled comparison of the well point concentrations with the estimated amount of dissolved product in the aquifer. Taking into account the spatial distribution of product, and that product may be floating on the water table, the concentrations at the well points would be expected to be slightly greater than the concentrations deeper in the aquifer. Comparison of the two shows a strong indication that a plume exists in the aquifer and is flowing with the groundwater and discharging to the river.

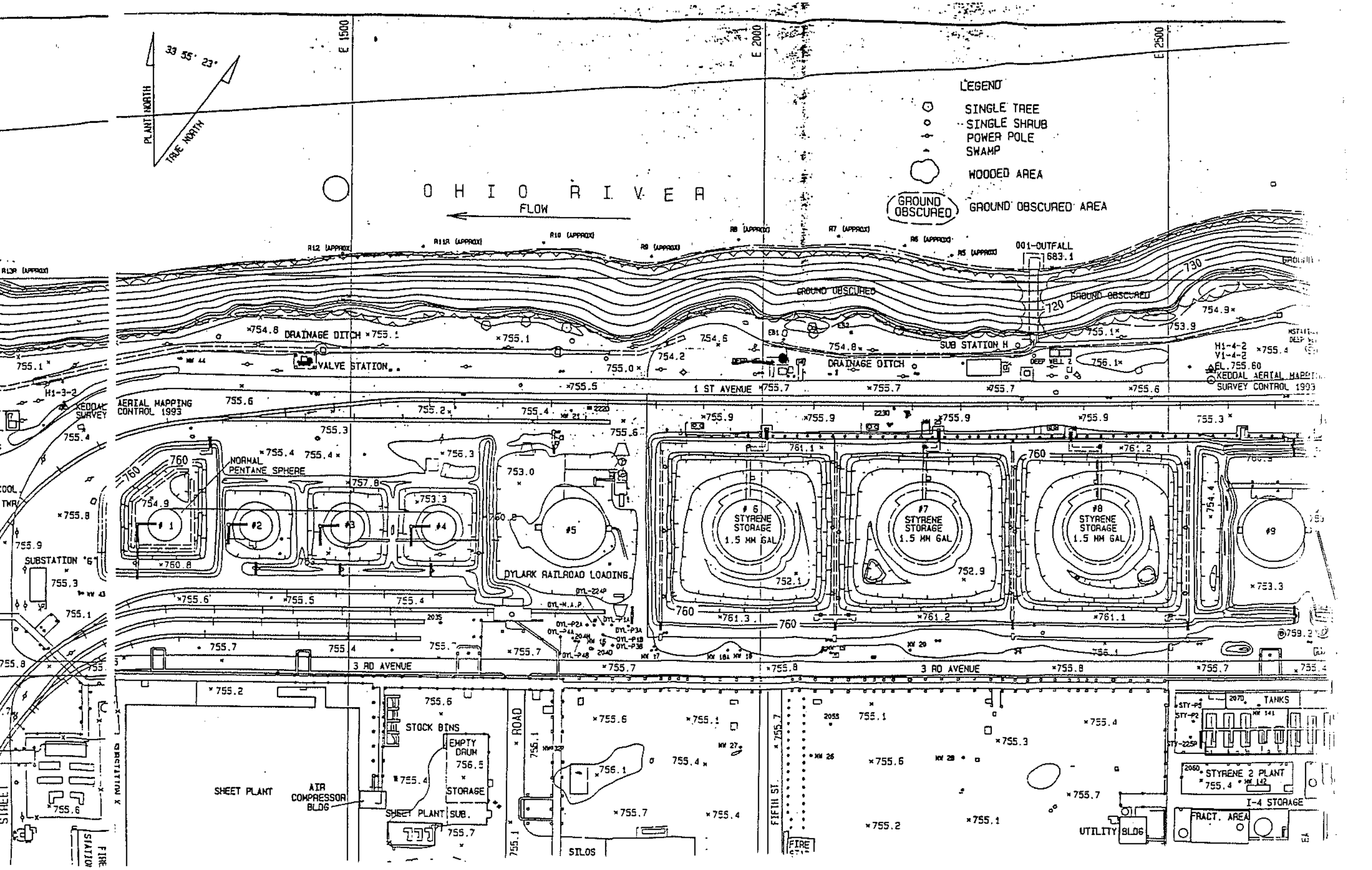

LEGEND
SINGLE TREE
SINGLE SHRUB
POWER POLE
SWAMP
WOODED AREA
GROUND OBSCURED
GROUND OBSCURED AREA
OHIO RIVER
FLOW
PLANT NORTH
TRUE NORTH
33 55' 23"
E 1500
E 2000
E 2500
001-OUTFALL
DRAINAGE DITCH
VALVE STATION
SUB STATION H
DEEP WELL 2
KEDDAL AERIAL MAPPING
SURVEY CONTROL 1993
AERIAL MAPPING CONTROL 1993
1 ST AVENUE
3 RD AVENUE
NORMAL PENTANE SPHERE
#1
#2
#3
#4
#5
#6 STYRENE STORAGE 1.5 MM GAL
#7 STYRENE STORAGE 1.5 MM GAL
#8 STYRENE STORAGE 1.5 MM GAL
#9
DYLARK RAILROAD LOADING
SUBSTATION "6"
SUBSTATION X
SHEET PLANT
AIR COMPRESSOR BLDG
STOCK BINS
EMPTY DRUM STORAGE
SHEET PLANT SUB.
ROAD
SILOS
FIFTH ST
FIRE STATION
TANKS
STYRENE 2 PLANT
I-4 STORAGE
FRACT. AREA
UTILITY BLDG
STREET

Table 1
Statistical Analysis of Groundwater Quality Data

Area	Date	Contaminant	Arithmetic Mean mg/l	Geometric Mean mg/l	Median mg/l
CP/S2	Apr 1993	Benzene	22.38	0.16	0.09
		Ethylbenzene	6.79	0.12	0.06
Well Points	Sep 1993	Benzene	0.0025	0.0025	0.0025
		Ethylbenzene	0.0059	0.0033	0.0025
Well Points	July 1994	Benzene	4.36	0.13	0.63
		Ethylbenzene	13.50	0.20	1.04

Table 2
Maximum Concentration Data at the Well Points

Contaminant	Well Group	Well	Maximum mg/l	Date	November 23, 1994 mg/l	Difference mg/l
Benzene	Group A	R-5R	1.67	May 25, 1994	1.20	0.47
		R-6	1.48	June 23, 1994	2.70	-1.22
		R-7	2.01	March 25, 1994	1.15	0.87
	Group B	R-8	40.55	March 25, 1994	17.85	22.70
		R-9	44.90	October 13, 1994	36.40	8.50
		R-10	22.35	June 9, 1994	20.05	2.30
	Group C	R-4R	0.01	February 21, 1994	undetect	0.01
		R-11R	0.05	February 21, 1994	undetect	0.05
		R-12	0.54	April 30, 1992	undetect	0.54
		R-13R	0.41	April 22, 1994	undetect	0.41
Ethylbenzene	Group A	R-5R	58.50	May 25, 1994	20.95	37.55
		R-6	131.50	March 25, 1994	77.55	53.95
		R-7	2.97	November 23, 1994	2.97	0.00
	Group B	R-8	100.00	February 21, 1992	13.60	86.40
		R-9	64.10	November 23, 1994	64.10	0.00
		R-10	40.65	November 23, 1994	40.65	0.00
	Group C	R-4R	undetect	December 7, 1993	undetect	
		R-11R	0.01	September 20, 1994	undetect	0.01
		R-12	0.04	April 30, 1992	undetect	0.04
		R-13R	undetect	September 15, 1993	undetect	

Table 3
Occurences of Concentrations Exceeding 10% Solubility Limit At Well Points

Contaminant	Solubility Limit	10% Solubility Limit	Date	Well			
				R-5R	R-6	R-8	R-9
	mg/l	mg/l		mg/l	mg/l	mg/l	mg/l
Benzene	1780.0	178.0	NONE				
Ethylbenzene	152.0	15.2	December 7, 1993	17.20	41.30		
			February 21, 1994	30.50	78.70		
			March 25, 1994	32.95	131.50	20.60	
			April 22, 1994	28.25	80.85	17.45	23.05
			May 11, 1994	28.10	60.90	11.65	
			May 25, 1994	58.50	not sampled	18.85	23.65
			June 9, 1994	43.40	102.00		33.55
			June 23, 1994	45.10	87.30		
			July 7, 1994	33.60	101.00		
			July 20, 1994	25.25	101.00		
			August 4, 1994	17.65	67.80		
			August 18, 1994	26.75	67.50		
			September 20, 1994	12.00	54.00		32.00
			October 13, 1994	19.35	63.80		51.30
			October 27, 1994	26.20	66.85		63.40
			November 14, 1994	23.50	104.45		44.35
			November 23, 1994	20.95	77.55		64.10

Table 4
Concentration Data

	DW-1 Concentrations			
		(mg/l)		
		Minimum	Median	Maximum
Benzene		0.140	1.960	3.170
Toluene		0.015	0.262	0.611
Ethylbenzene		0.150	2.370	3.930
Xylenes		0.003	0.050	0.322
Styrene		0.003	0.005	0.065
Total		0.310	4.612	8.046
	Aquifer Concentrations			
		(mg/l)		
		Minimum	Median	Maximum
Benzene		1	13	21
Toluene		0.10	2.00	4.00
Ethylbenzene		1	16	26
Xylenes		0.02	0.33	2.00
Styrene		0.02	0.03	0.43
Total		2	31	54

Table 5
Breakthrough Times for Well Points

Well #	Benzene (days)	Ethylbenzene (days)
R-5R	180	200
R-6	345	210
R-7	210	
R-8	210	240
R-9	230	210
R-10	250	330

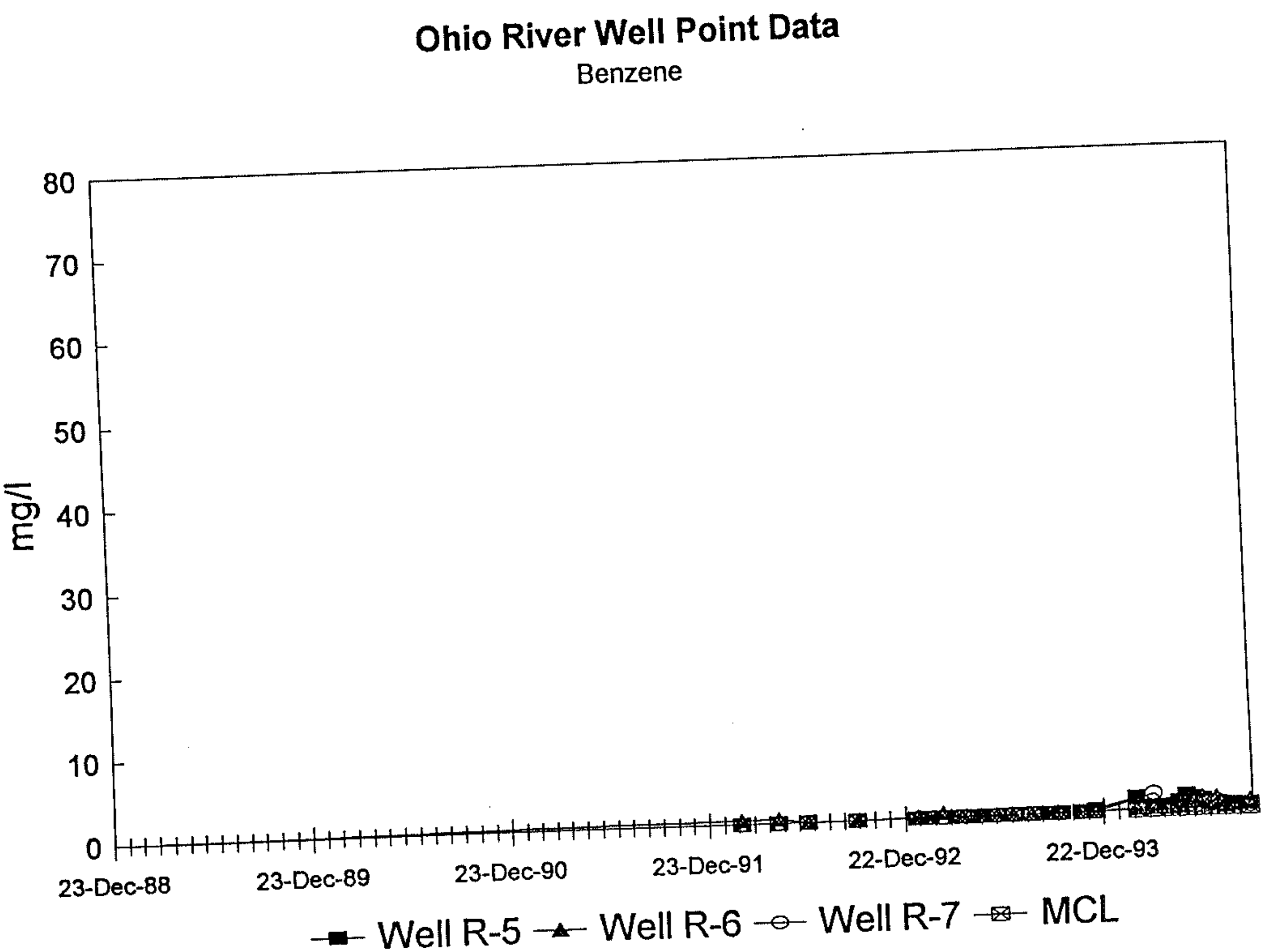

Well Group A
Figure 1

wpdata.wb1

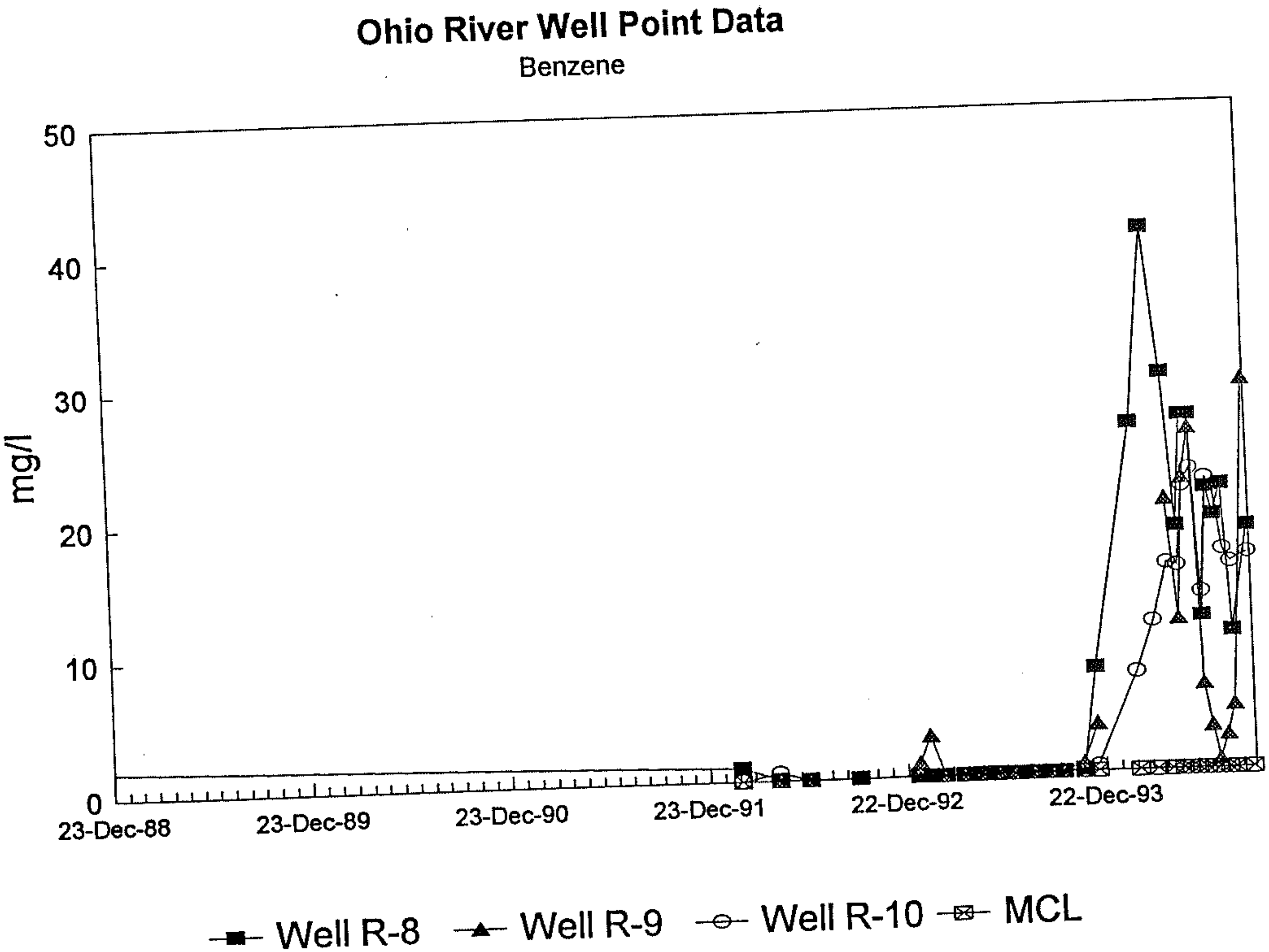

Well Group B
Figure 2

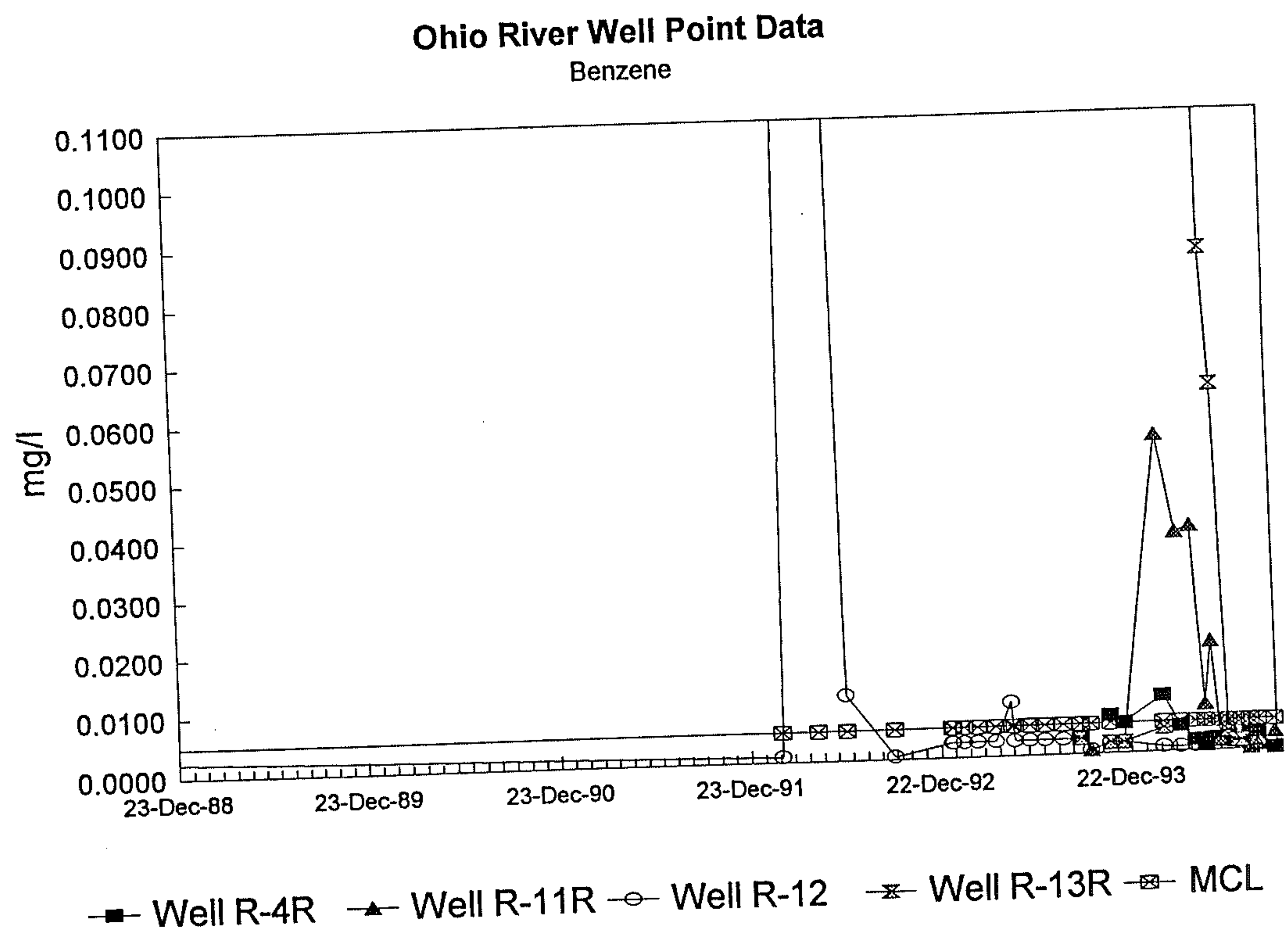

Well Group C
Figure 3

Ohio River Well Point Data

Ethylbenzene

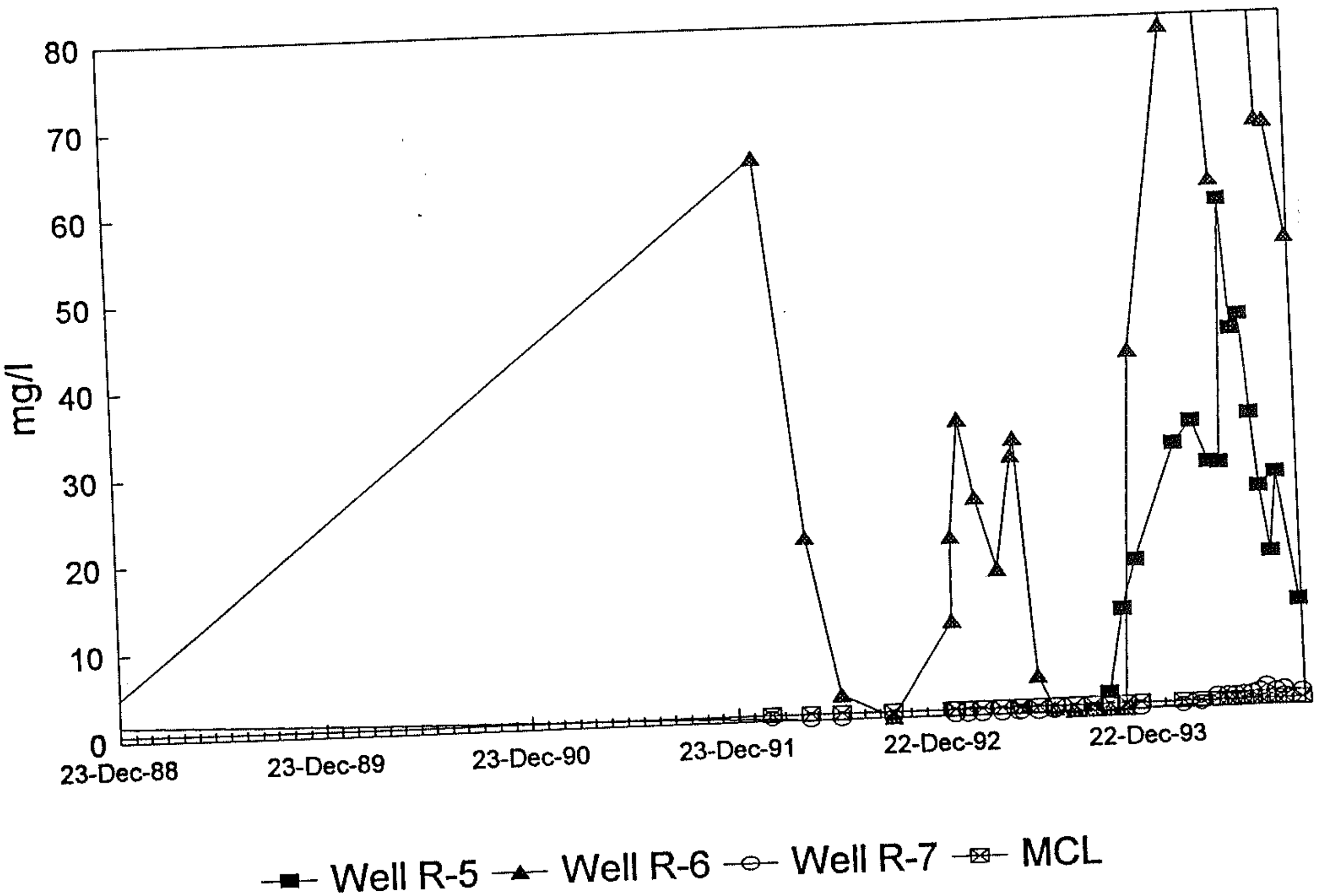

Well Group A

Figure 4

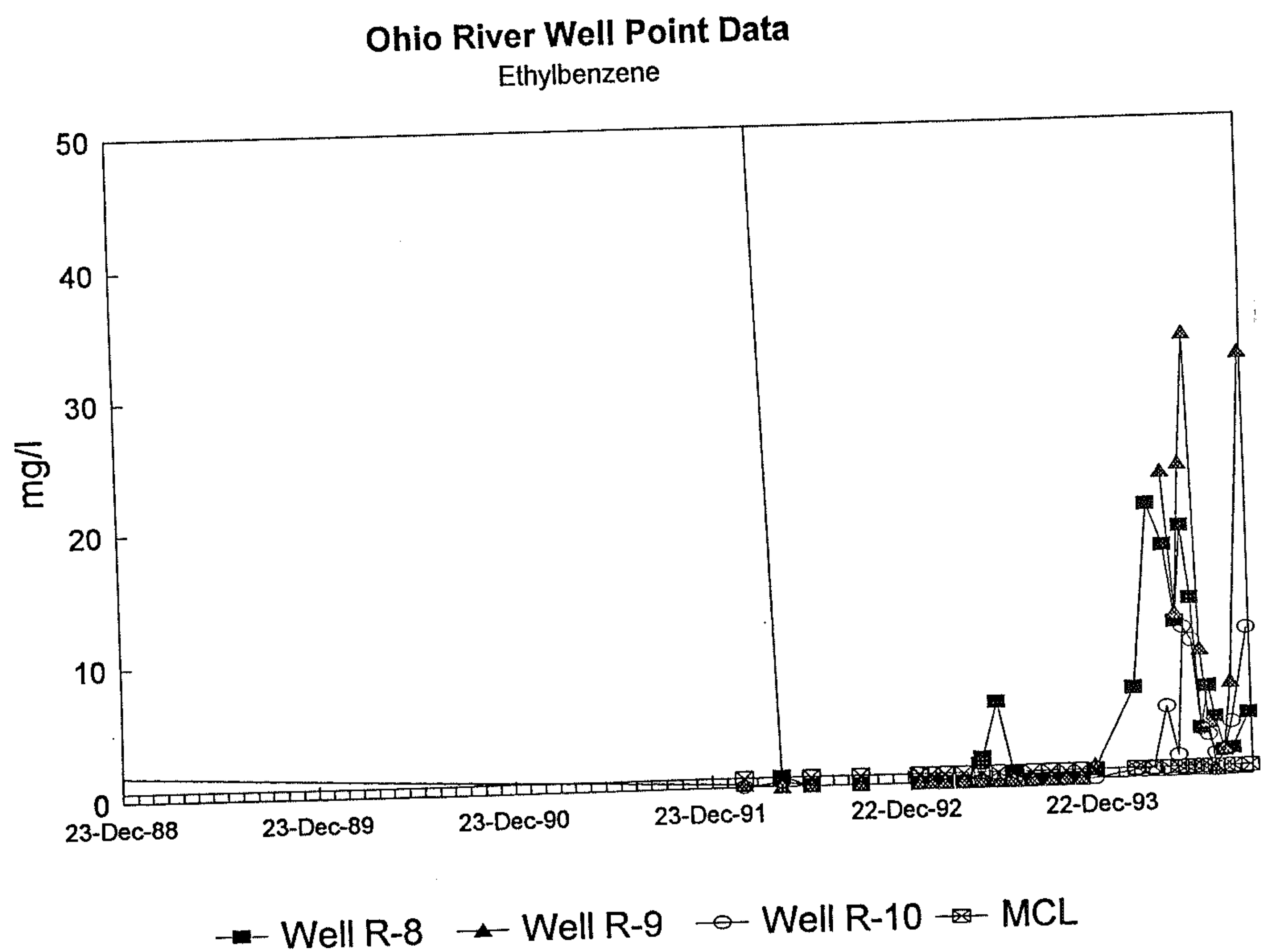

Well Group B
Figure 5

wpdata.wb1

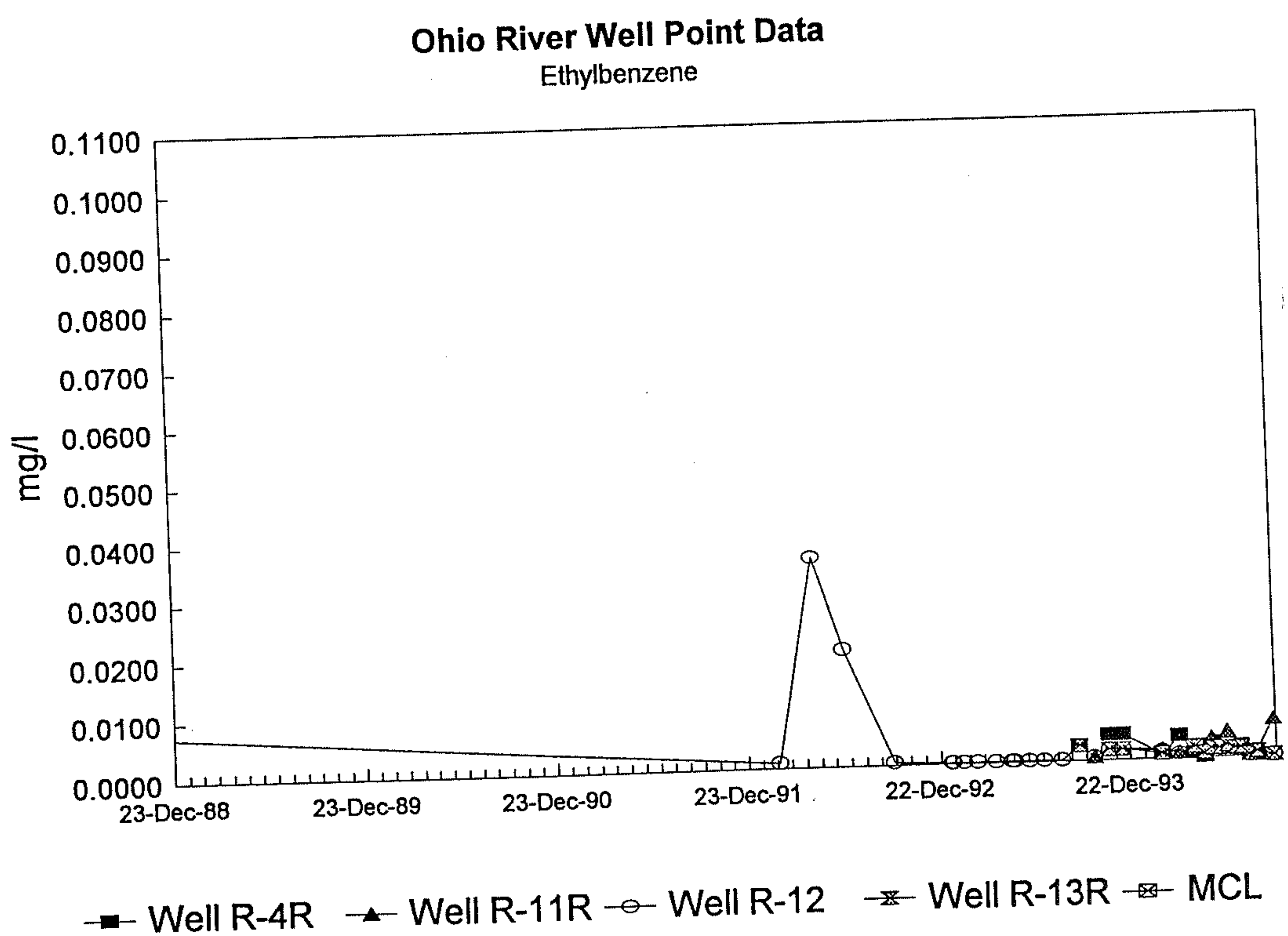

Well Group C
Figure 6

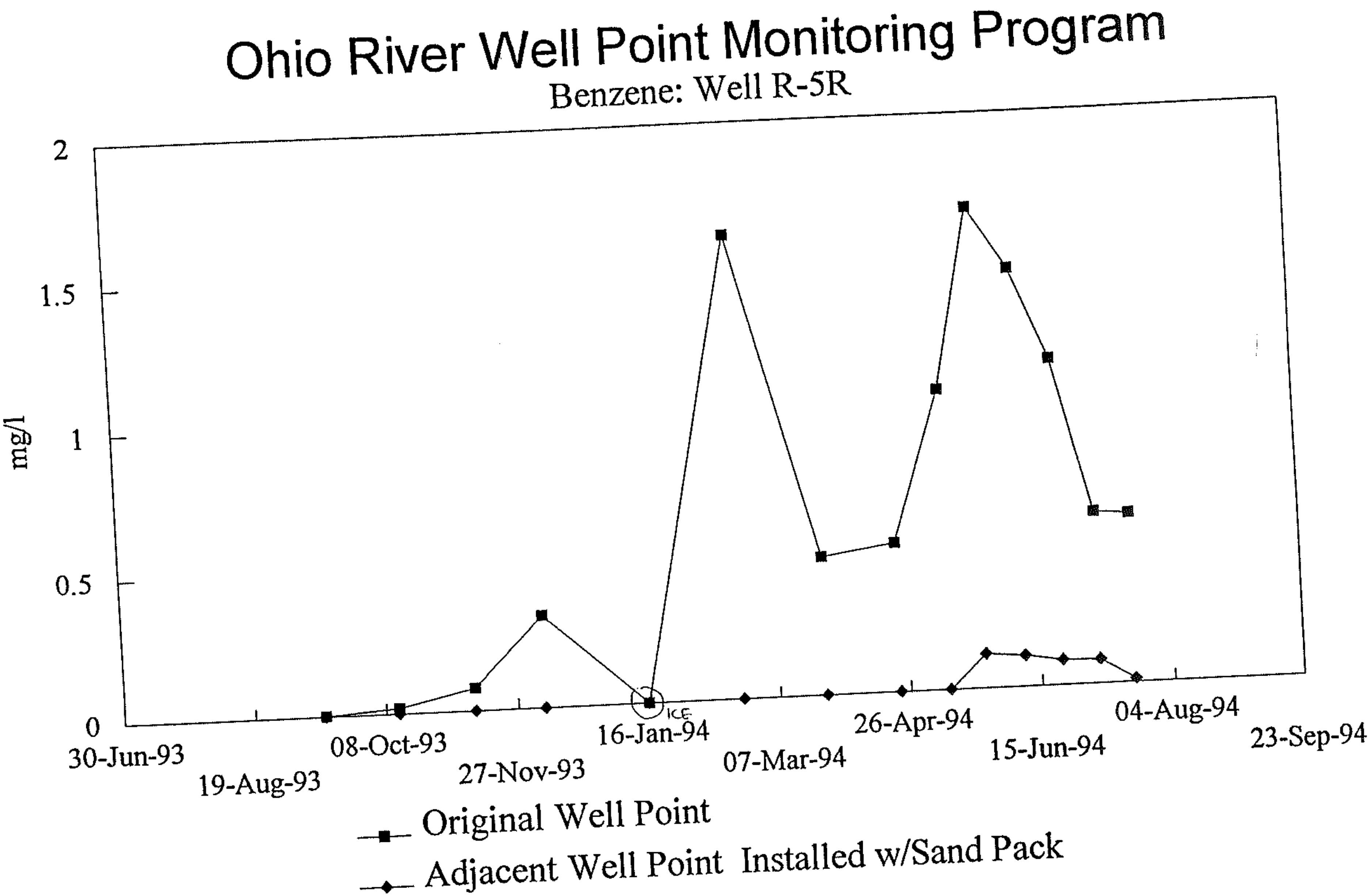

Ohio River Well Point Monitoring Program
Benzene: Well R-5R
mg/l
2
1.5
1
0.5
0
ICE
30-Jun-93
19-Aug-93
08-Oct-93
27-Nov-93
16-Jan-94
07-Mar-94
26-Apr-94
15-Jun-94
04-Aug-94
23-Sep-94
Original Well Point
Adjacent Well Point Installed w/Sand Pack

Figure 7

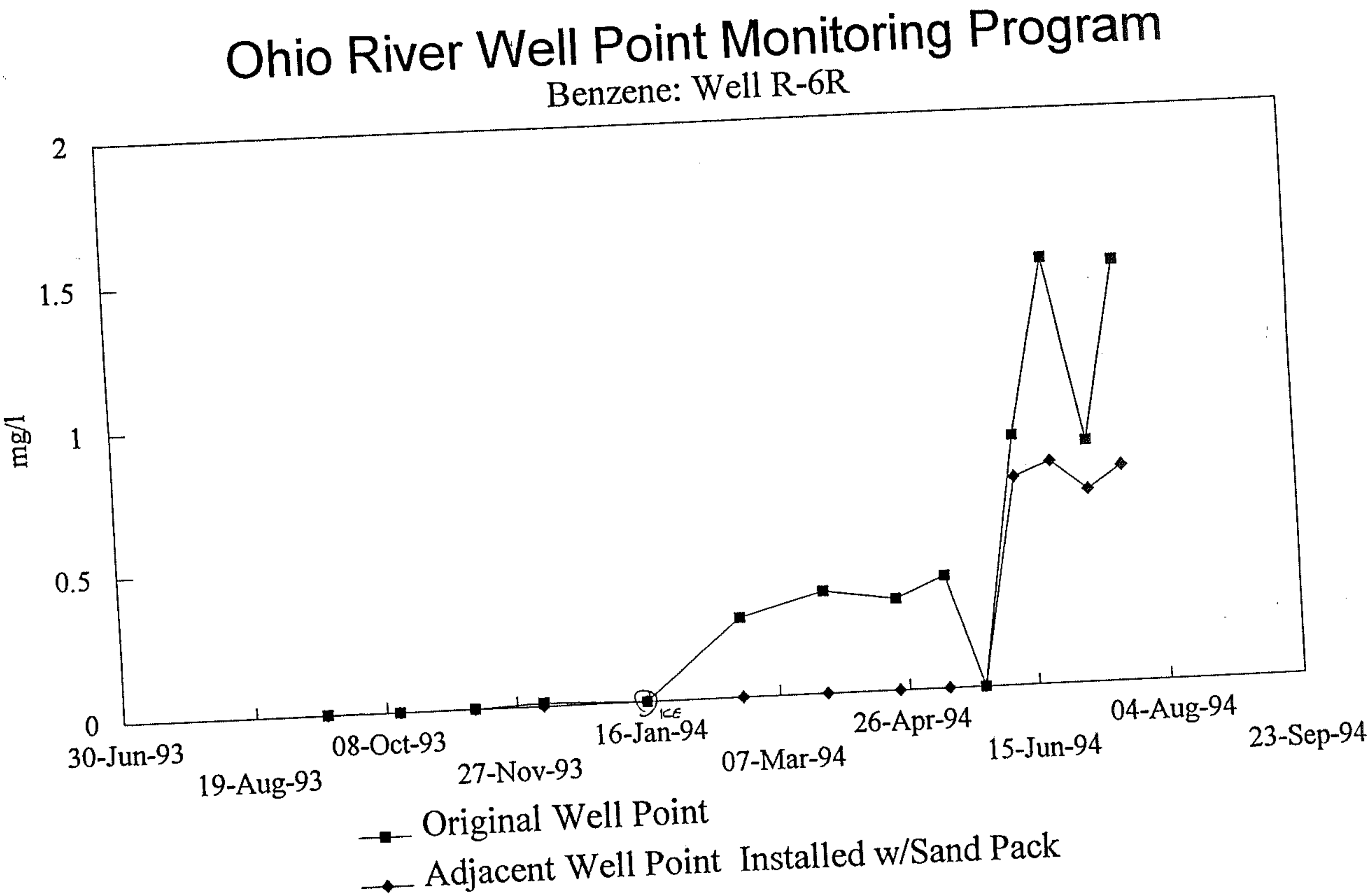
Ohio River Well Point Monitoring Program
Benzene: Well R-6R
mg/l
2
1.5
1
0.5
0
ICE
30-Jun-93
19-Aug-93
08-Oct-93
27-Nov-93
16-Jan-94
07-Mar-94
26-Apr-94
15-Jun-94
04-Aug-94
23-Sep-94
Original Well Point
Adjacent Well Point Installed w/Sand Pack

Figure 8

Ohio River Well Point Monitoring Program

Benzene: Well R-8R

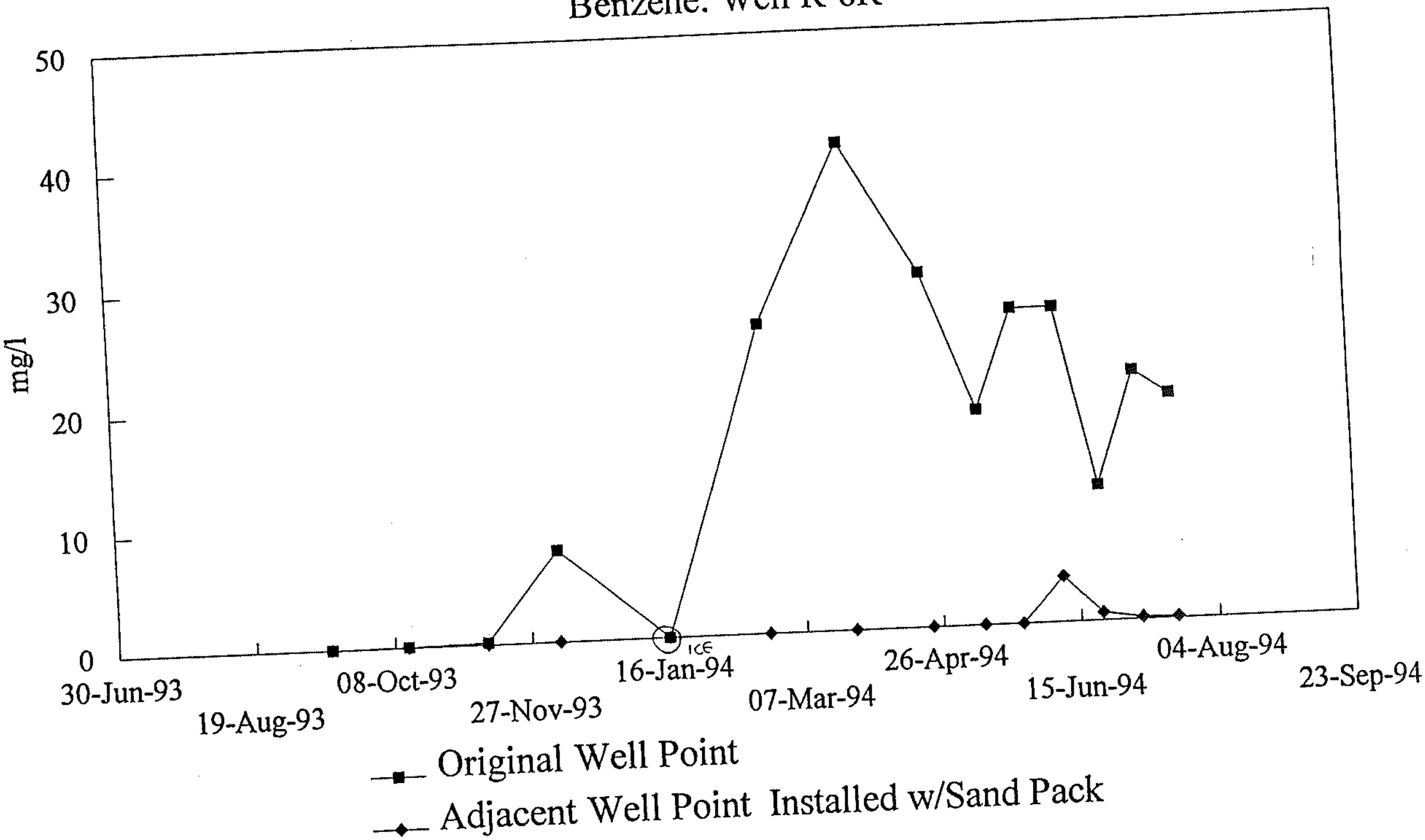

Figure 9

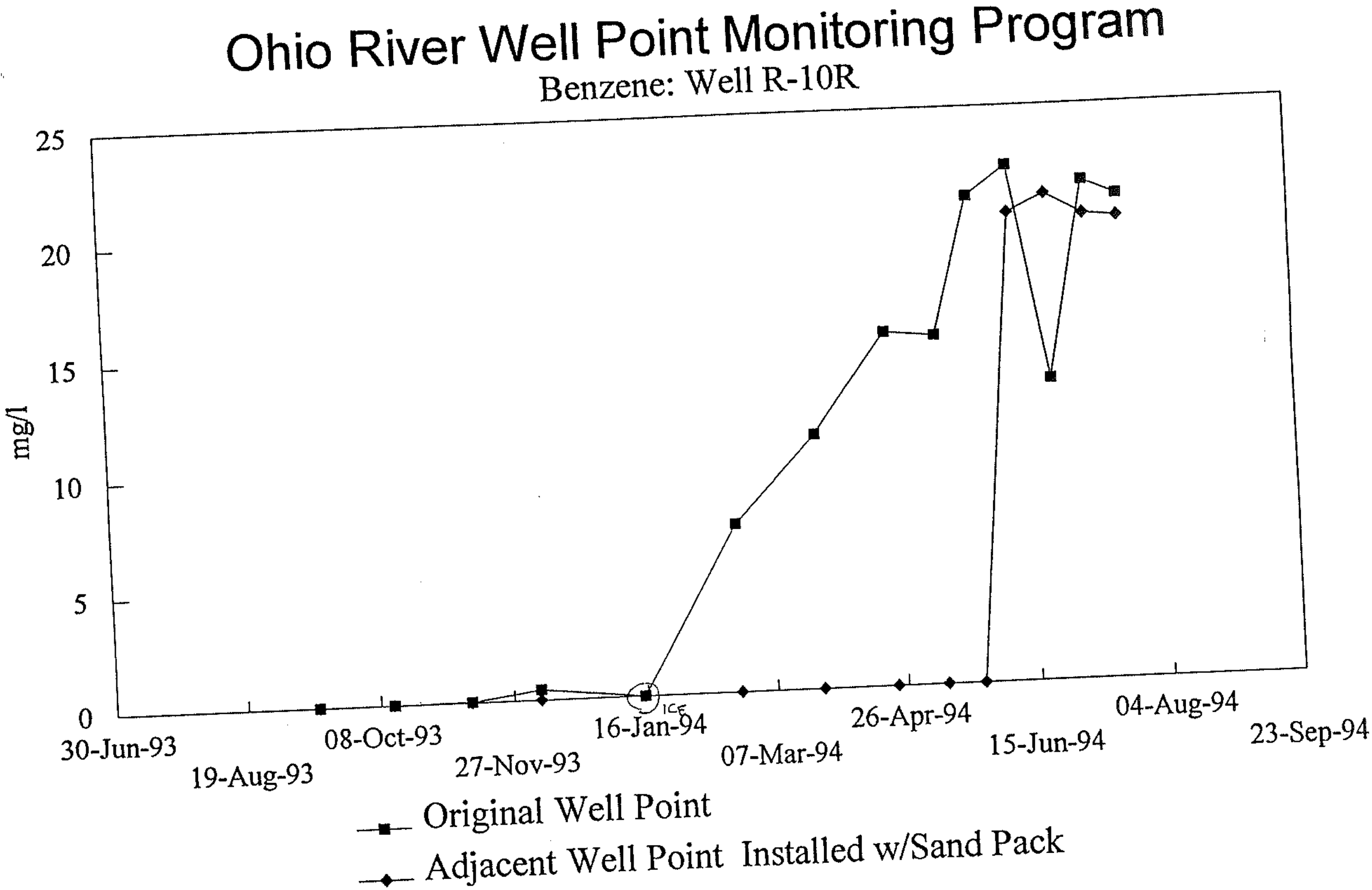
Ohio River Well Point Monitoring Program
Benzene: Well R-10R
mg/l
0
5
10
15
20
25
30-Jun-93
19-Aug-93
08-Oct-93
27-Nov-93
16-Jan-94
07-Mar-94
26-Apr-94
15-Jun-94
04-Aug-94
23-Sep-94
ICE
Original Well Point
Adjacent Well Point Installed w/Sand Pack

Figure 10

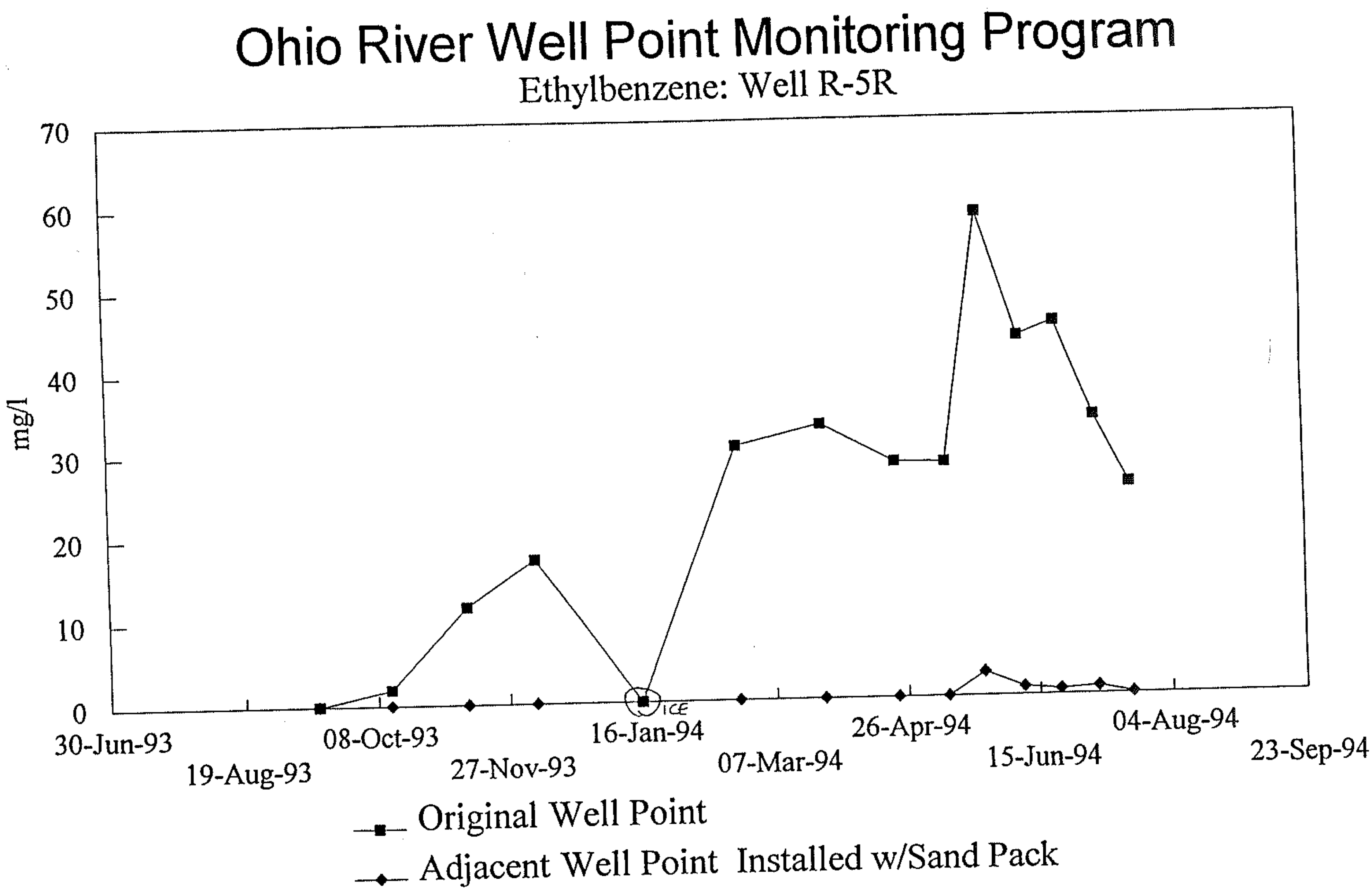
Ohio River Well Point Monitoring Program
Ethylbenzene: Well R-5R
70
60
50
40
30
20
10
0
mg/l
30-Jun-93
19-Aug-93
08-Oct-93
27-Nov-93
16-Jan-94
07-Mar-94
26-Apr-94
15-Jun-94
04-Aug-94
23-Sep-94
ICE
Original Well Point
Adjacent Well Point Installed w/Sand Pack

Figure 11

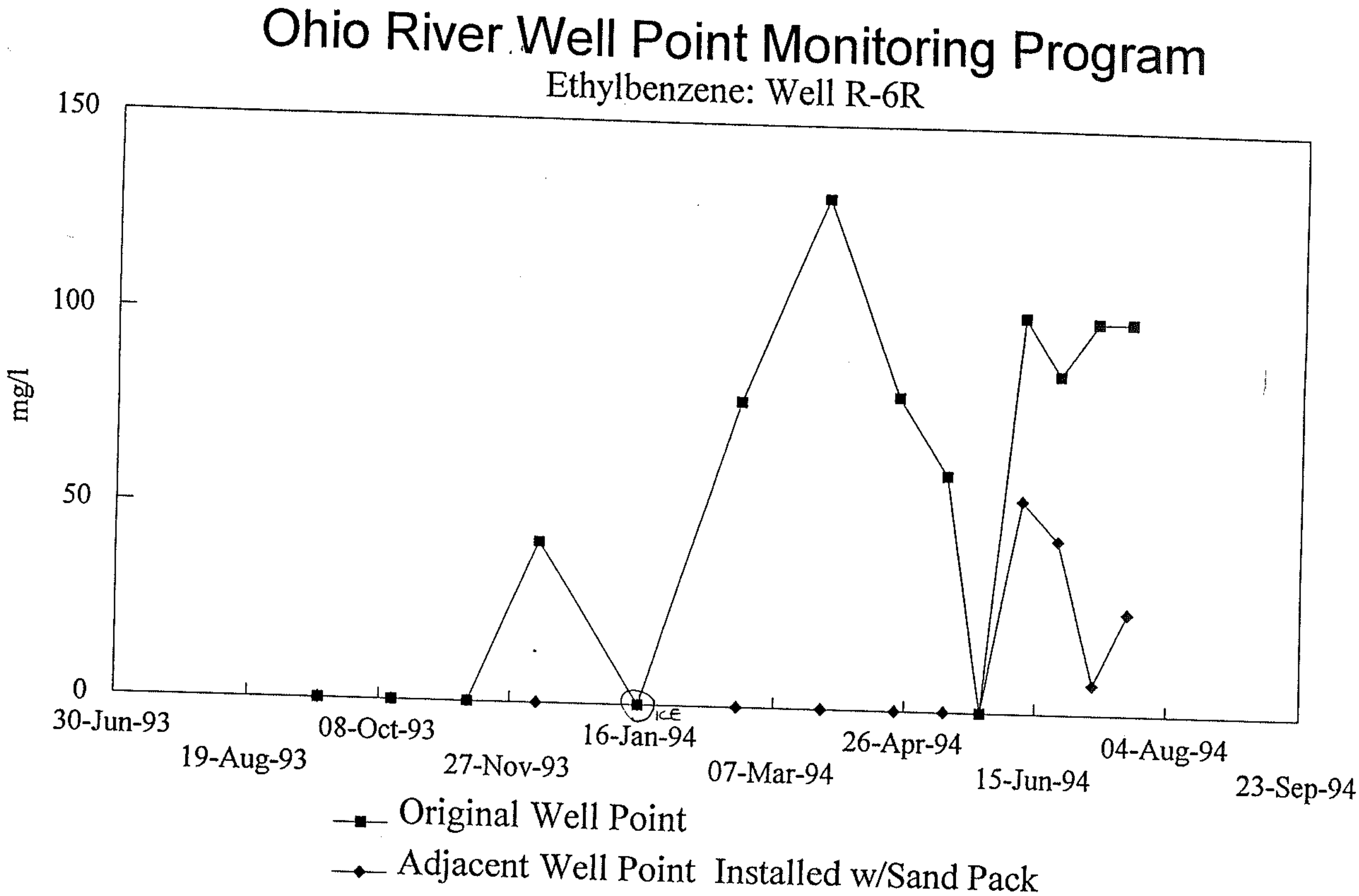

Ohio River Well Point Monitoring Program
Ethylbenzene: Well R-6R
mg/l
150
100
50
0
30-Jun-93
19-Aug-93
08-Oct-93
27-Nov-93
16-Jan-94
07-Mar-94
26-Apr-94
15-Jun-94
04-Aug-94
23-Sep-94
ICE
Original Well Point
Adjacent Well Point Installed w/Sand Pack

Figure 12

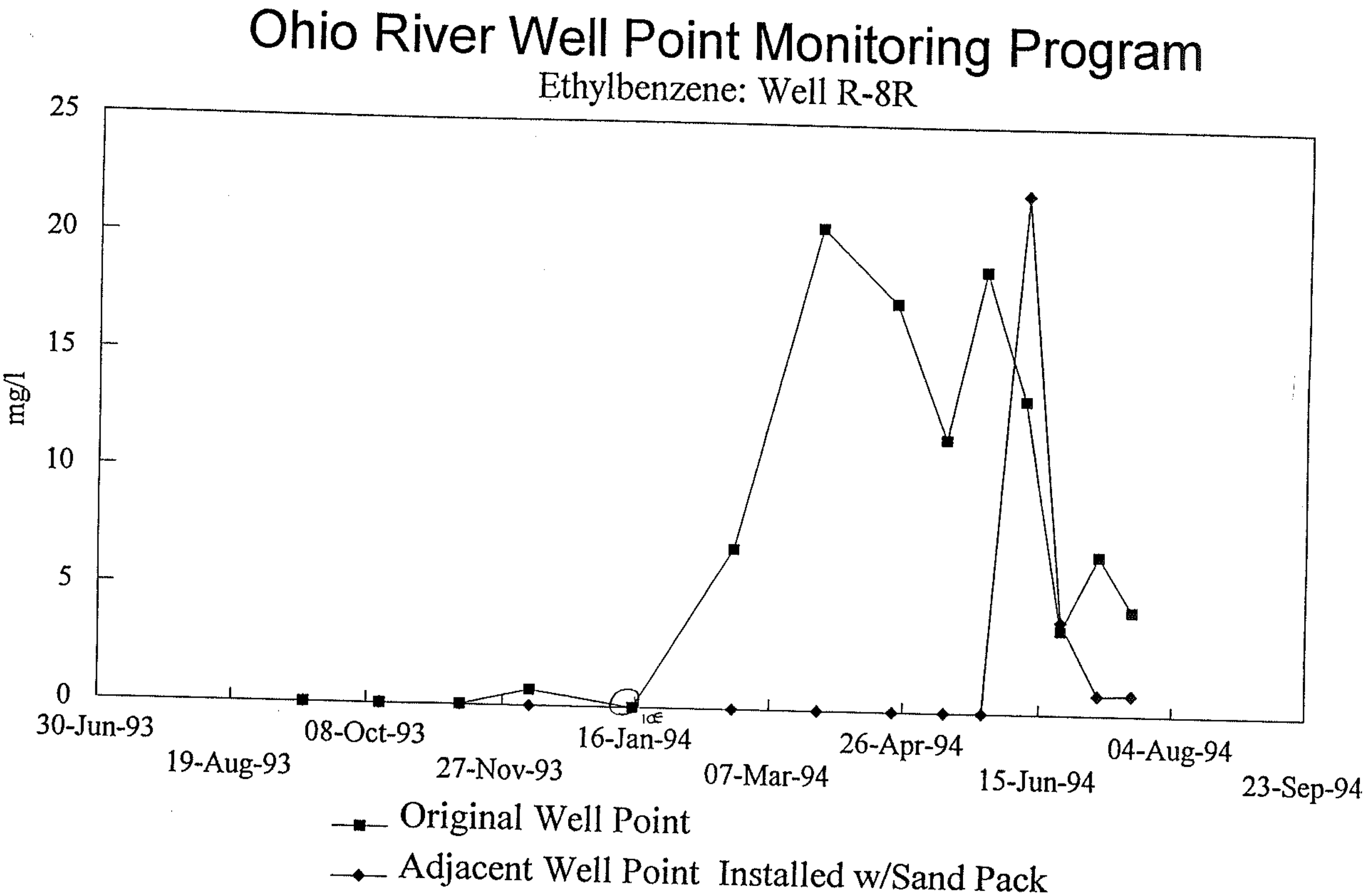

Ohio River Well Point Monitoring Program
Ethylbenzene: Well R-8R
mg/l
25
20
15
10
5
0
30-Jun-93
19-Aug-93
08-Oct-93
27-Nov-93
16-Jan-94
07-Mar-94
26-Apr-94
15-Jun-94
04-Aug-94
23-Sep-94
Original Well Point
Adjacent Well Point Installed w/Sand Pack

Figure 13

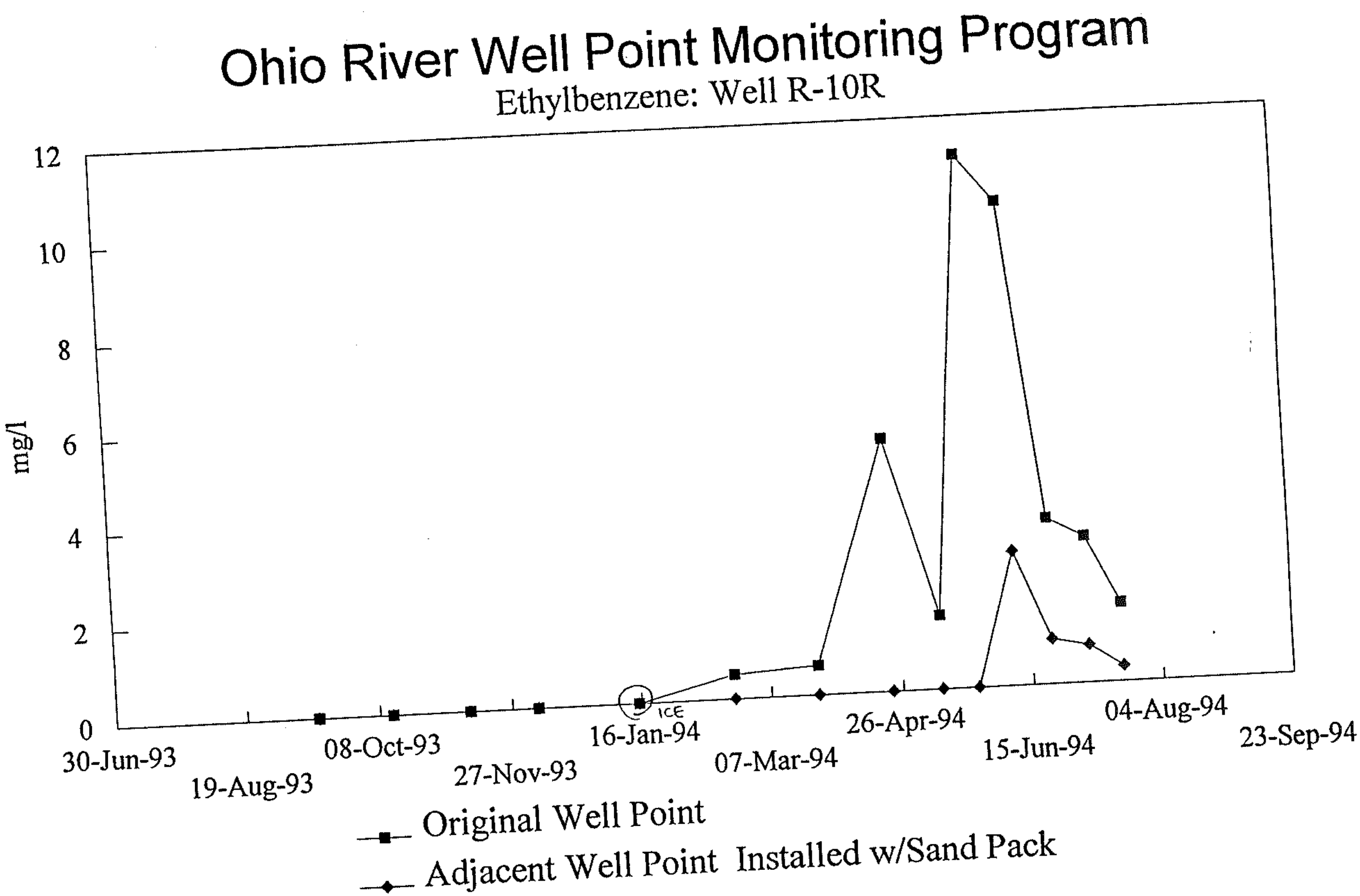

Ohio River Well Point Monitoring Program
Ethylbenzene: Well R-10R
mg/l
12
10
8
6
4
2
0
30-Jun-93
19-Aug-93
08-Oct-93
27-Nov-93
16-Jan-94
07-Mar-94
26-Apr-94
15-Jun-94
04-Aug-94
23-Sep-94
ICE
Original Well Point
Adjacent Well Point Installed w/Sand Pack

Figure 14

Figure 15

Data for Analysis of
Groundwater Hydraulics
Feb 1989 - DW01 Pumping

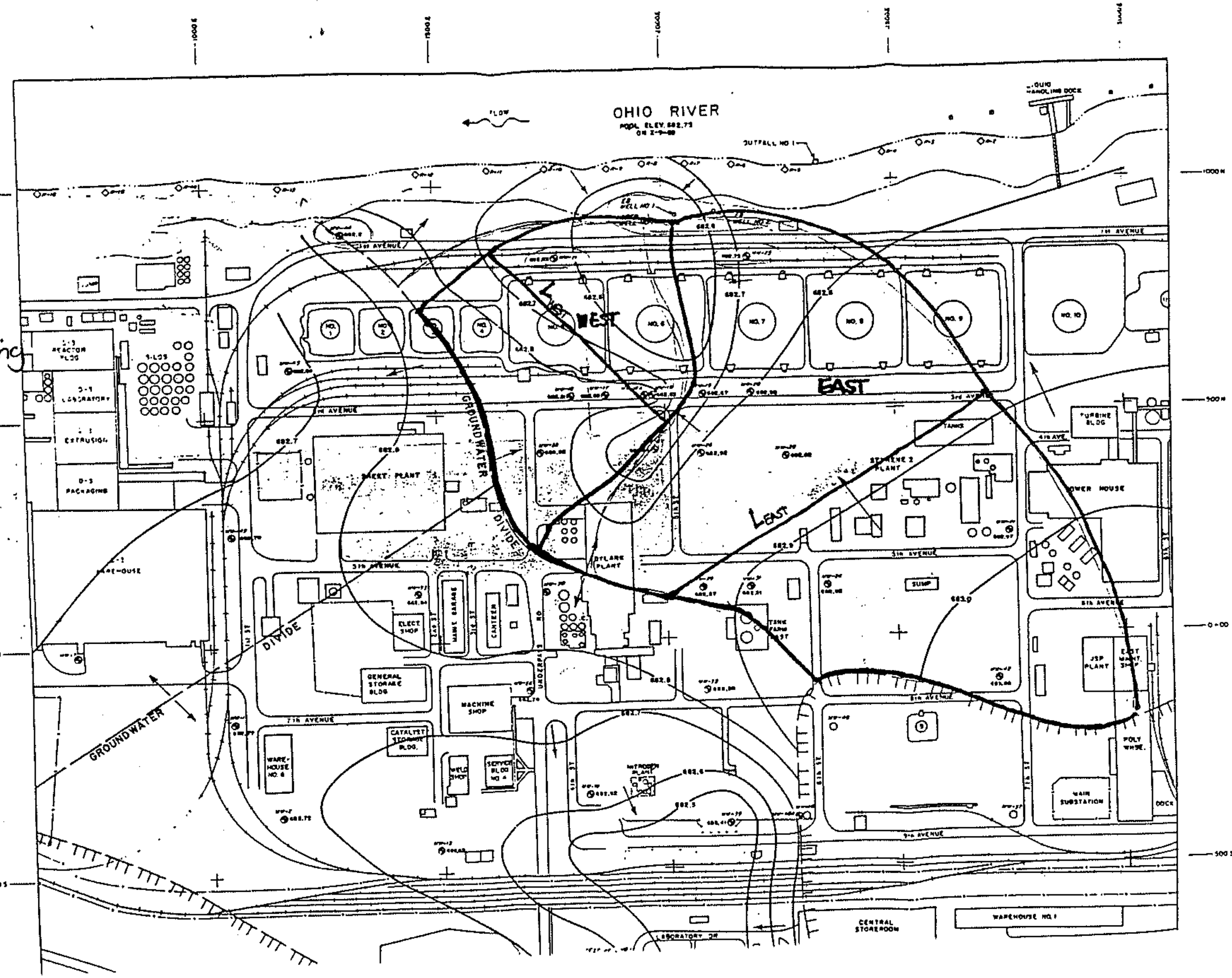

A_{WEST} = 273,799.9 ft^2

A_{EAST} = 800,995.6 ft^2

A_{TOTAL} = 1,074,795.56 ft^2

L_{WEST} = 542.44 ft

L_{EAST} = 827.36 ft

i_{WEST} = .00091 $\frac{ft}{ft}$

i_{EAST} = .004651 $\frac{ft}{ft}$

Figure 16

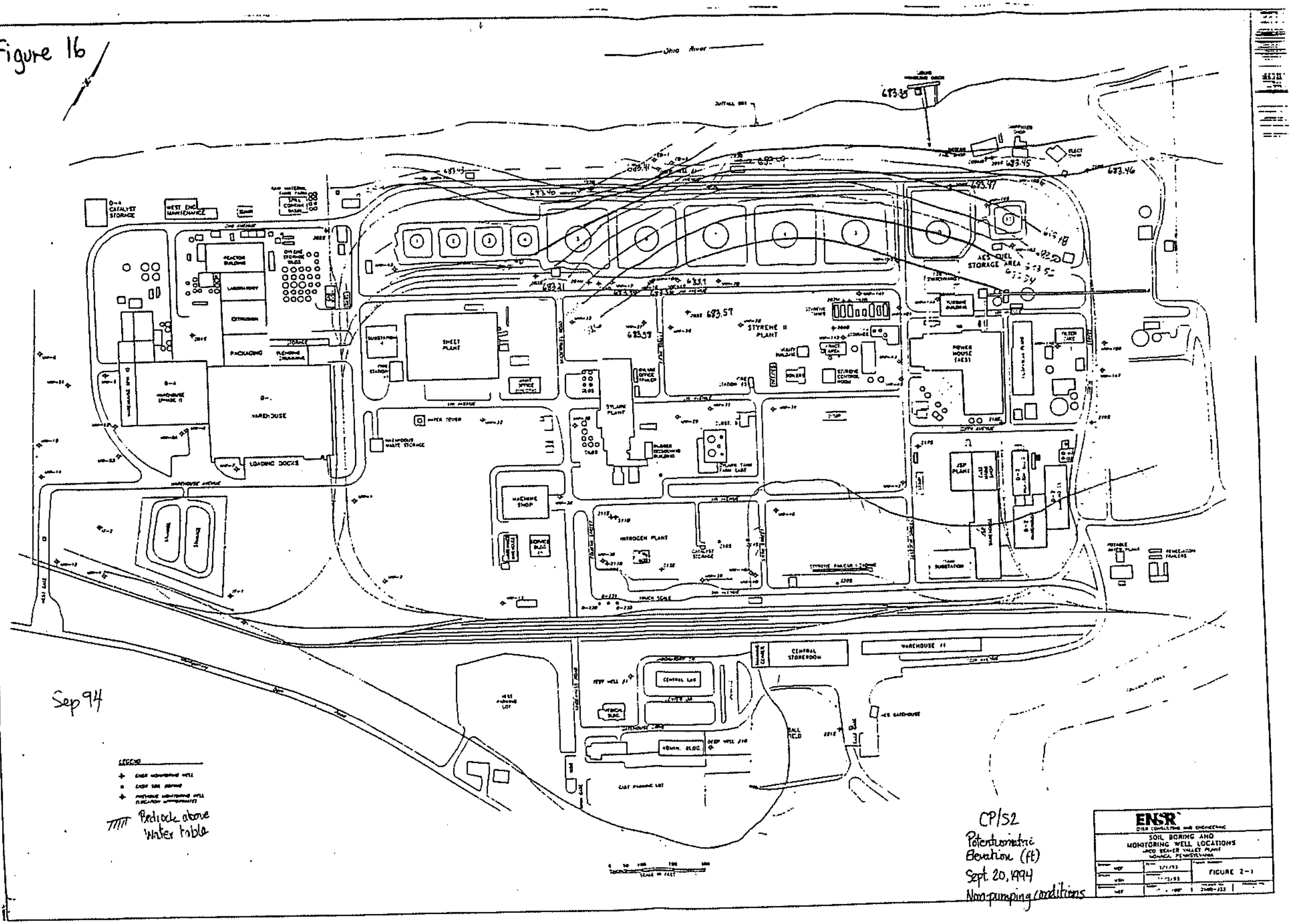
Ohio River
683.35
683.45
683.46
683.47
AES FUEL STORAGE AREA
683.57
683.59
683.21
683.40
STYRENE II PLANT
POWER HOUSE (AES)
SHEET PLANT
WAREHOUSE
LOADING DOCKS
MACHINE SHOP
HYDROGEN PLANT
CENTRAL STOREROOM
WAREHOUSE #1
CENTRAL LAB
CATALYST STORAGE
WEST ENG MAINTENANCE
REACTOR BUILDING
LABORATORY
EXTRUSION
PACKAGING
SUBSTATION
STYRENE CONTROL ROOM
BOILERS
Sep 94
LEGEND
Bedrock above water table
CP/52
Potentiometric Elevation (ft)
Sept. 20, 1994
Non-pumping conditions
ENSR
SOIL BORING AND MONITORING WELL LOCATIONS
FIGURE 2-1

Appendix A
Induced Infiltration Analysis

From J.L. Wilson. <u>WRR</u> Vol. 29 No. 10. October 1993. p. 3503-3512.

Flow in Aquifer Between an Impermeable Boundary and a Stream (see Figure 8 p. 3508).

$L = 1{,}500$ ft.
$d = 150$ ft.
$d/L = 0.1$

$N = 6$ in/year $= 1.37 \times 10^{-3}$ ft/day
$q_L = 0$
$q_a = NL = q_L = 2.05$ ft^2/day

For $Q_W = 300$ gpm $= 57{,}754$ ft^3/day

$$\beta = \frac{Q_w}{\pi d q_a} = \frac{57{,}754}{\pi(150)(2.05)} = 60$$

$$\lambda = \frac{Q_W}{2Lq_a} = \frac{57{,}754}{2(1{,}500)(2.05)} = 9.4$$

From Figure 8a $\frac{Q_S}{Q_W} = 85\text{-}90\%$

From Figure 8b $\frac{Q_S}{Q_W} = 85\%$

For $Q_W = 200$ gpm $= 38{,}503$ ft^3/day

$$\beta = \frac{Q_w}{\pi d q_a} = \frac{38{,}503}{\pi(150)(2.05)} = 40$$

$$\lambda = \frac{Q_W}{2Lq_a} = \frac{38{,}503}{2(1{,}500)(2.05)} = 6.2$$

From Figure 8a $\frac{Q_S}{Q_W} = 80\text{-}85\%$

From Figure 8b $\frac{Q_S}{Q_W} = 80\%$

WATER RESOURCES RESEARCH, VOL. 29, NO. 10, PAGES 3503–3512, OCTOBER 1993

Induced Infiltration in Aquifers With Ambient Flow

JOHN L. WILSON

Department of Geoscience, New Mexico Institute of Mining and Technology, Socorro

Well water quality depends on the relative amounts of water drawn from the pumped aquifer and nearby surface water bodies, such as streams, lakes, and wetlands. Although a surface water body may normally gain water from the aquifer, pumping can reverse gradients, causing it to lose water near the well. Surface water then enters the well by induced infiltration. Two-dimensional vertically integrated models of induced infiltration are developed for various combinations of aquifer geometry and sources of recharge. The models, which have applications in wellhead protection, aquifer pollution characterization, and aquifer remediation, are presented graphically. They show that the propensity for and rate of induced infiltration are enhanced by higher pumping rates, proximity of the well to the stream, and the presence of nearby barrier boundaries. The propensity and rate are reduced by the presence of other surface water bodies. Ambient groundwater discharge rate to the surface water body also plays a role, but not its source, whether it is from local vertical recharge, lateral inflow, or both. The results are also largely indifferent to whether the aquifer transmissivity is assumed to be a constant, or a function of water table elevation. Finally, if the well is close enough to the surface water body, say, less than 5% of the aquifer width, then the aquifer acts as if it were semi-infinite.

INTRODUCTION

Throughout the United States it is common to find high-capacity shallow wells pumping from phreatic aquifers in alluvial or glacial valleys. These wells are commonly located in low-lying areas near streams, wetlands, or ponds. One can only guess at the rationale that led early well designers to examine and eventually select a particular well site, but such factors as the shallow depth to groundwater, the large thickness of saturated pervious deposits near the center and/or lowest portion of the valley, and the proximity to a nearby surface water body seem to have played a dominant role. A simple groundwater balance shows that there is insufficient natural recharge from rainfall infiltration to supply many of these wells at their historic pumping rates, and that a portion of the pumpage must come from the nearby surface water body, such as a stream, lake, or wetland. The decline of groundwater levels around pumping wells located near a surface water body creates gradients which capture some of the ambient groundwater flow that would have, without pumping, discharged as base flow to the surface water, and at sufficiently large pumping rates induces flow out of the body of surface water into the aquifer. The sum of these two effects leads to streamflow depletion. In this paper the latter effect is referred to as induced infiltration and is due to a reversal of gradients caused by the pumping. With induced infiltration, a stream that is normally gaining becomes a losing stream in the vicinity of the well. The potential for induced infiltration is clearly documented in the theory of well hydraulics [*Theis*, 1941; *Kazman*, 1946, 1948; *Ferris et al.*, 1962; *Hantush*, 1965; *Walton*, 1970; *Bear*, 1979] and has been studied in the field [*Rorabaugh*, 1956; *Norris*, 1983].

The amount of induced infiltration is a function of many factors, including aquifer transmissivity, aquifer geometry, well pumping rate, the strength of the hydraulic connection between the aquifer and surface water body due to stream penetration and clogging layer, and the presence of other sources of water supplying the well. Quantifying the amount of induced infiltration in terms of these parameters is an important factor in conjunctive water use as water demand increases and the reliability of surface supplies is threatened by streamflow depletion. The streamflow depletion problem has been well-studied, particularly in the western and mid-western states [e.g., *Theis*, 1941; *Kazman*, 1948; *Glover and Balmer*, 1954; *Rorabaugh*, 1956; *Hantush*, 1959, 1965; *Jenkins*, 1968; *Walton*, 1970]. In the east, streamflow depletion is usually not the critical issue, but water quality is. Because of the potential for pollution of both ground and surface waters from varied sources and by varied pollutant species, quantification of the amount of induced infiltration becomes an important factor in evaluating the reliability of well water quality. Below we use the term "stream" to describe the surface water body, but the issues, approach, and results also apply to rivers, ponds, lakes, and wetlands.

The two induced infiltration problems, streamflow depletion and water quality, are different. The depletion problem is inherently time dependent. When pumping starts, the well initially obtains its supply of water from aquifer storage. Eventually, the cone of depression of the well intercepts the stream and the drawdown comes to an equilibrium, with the streamflow reduced by the rate at which the well is pumping. If under ambient conditions the stream is gaining, it is not necessary for the well to actually reverse gradients and induce infiltration. It depletes streamflow simply by capturing some of the ambient aquifer discharge before it reaches the stream as base flow. In fact, as long as the stream and aquifer are in hydraulic connection, the rate of streamflow depletion is relatively independent of whether or not the stream is actually gaining or losing, and the actual sources of the water being pumped.

However, in a water quality analysis whether a stream is originally gaining or losing is paramount. A polluted stream that is gaining even under pumping conditions cannot generally pollute an aquifer. If the pumping rate is increased and the polluted gaining stream becomes a losing stream over a short distance, due to induced infiltration toward the well, it pollutes only the aquifer between the well and the stream. As the pollution enters the well it is diluted by the other sources

Paper number 93WR01393.
0043-1397/93/93WR-01393$05.00

of well water, such as ambient aquifer flow. If, on the other hand, it is the aquifer that is polluted, then the well pumping rate can be increased until it induces infiltration of sufficient good quality stream water to dilute the pollution. Over the long term, these water quality issues can often be viewed from a steady state perspective, for wells that pump more or less continuously to supply water for industrial or domestic use. Pumping for irrigation usually is too intermittent to be amenable to steady state analysis.

Although the streamflow depletion problem has been studied for many years, the water quality induced infiltration problem has not. I have encountered the water quality problem in numerous practical situations and developed the simple models presented here to aid in its study. The models help with understanding induced infiltration phenomena and provide a "first cut" analysis of alternative well field designs and pumping rates from a water quality perspective, or assist in the delineation of wellhead protection zones [*Newsom and Wilson*, 1988; *Environmental Protection Agency*, 1990; *Schafer-Perini and Wilson*, 1991; *Wilson and Linderfelt*, 1991]. They may also be of some help in characterizing past pollution events involving wells, aquifers, and streams or other surface water bodies, and in designing aquifer remediation schemes.

The models are presented in the form of dimensionless curves, describing the conditions under which induced infiltration occurs and giving the amount of induced infiltration as a percentage of well discharge. Under ambient conditions the stream is assumed to be gaining, supplied by ambient aquifer flow. Under pumping the well captures a combination of induced stream water infiltration and ambient aquifer flow from both natural vertical recharge and lateral inflows. The aquifer is assumed to be homogeneous and isotropic. The stream and the well are assumed to fully penetrate the aquifer; the flow is essentially horizontal. The stream channel is assumed to have a negligible gradient so that the ambient flow is essentially perpendicular to the stream. The stream is assumed to be hydraulically connected to the aquifer, and the "skin effect" caused by a possible clogging layer of low conductivity lining the stream channel is ignored. With negligible channel gradient and skin, the stream can be represented as a constant head boundary. In a phreatic aquifer the drawdown is assumed to be small compared to saturated thickness, leading to the Dupuit approximation. Temperature variation and its effect on aquifer hydraulic conductivity are also ignored. Equilibrium (steady state) conditions for both flow and water quality are assumed; the approach is most applicable to average long-term conditions at continuously used water supply wells. Well tests, such as that described by *Rorabaugh* [1956] or *Norris* [1983], are usually too short in duration for equilibrium to occur.

The equations for induced infiltration in a semi-infinite aquifer with ambient flow are developed first. This review introduces the approach, concepts, and notation for a simple case. More sophisticated cases are then presented, with combinations of barrier and stream boundaries, and sources of recharge.

WELL IN A SEMI-INFINITE AQUIFER

Consider a homogeneous semi-infinite aquifer bounded on one side by a fully penetrating stream. The aquifer can be confined or phreatic; Figure 1 illustrates the phreatic case. A uniform ambient flow, $q_a[L^2/T]$, discharges toward the stream, which acts as a constant head boundary. The well, located distance d from the stream, pumps at rate $Q_w[L^3/T]$. Under steady state conditions this situation is described by the LaPlace equation, $\nabla^2\Phi = 0$, where there is a sink of strength of Q_w at $x = 0$, $y = d$. The state variable $\Phi[L^3/T]$ takes on different definitions in confined and phreatic aquifers

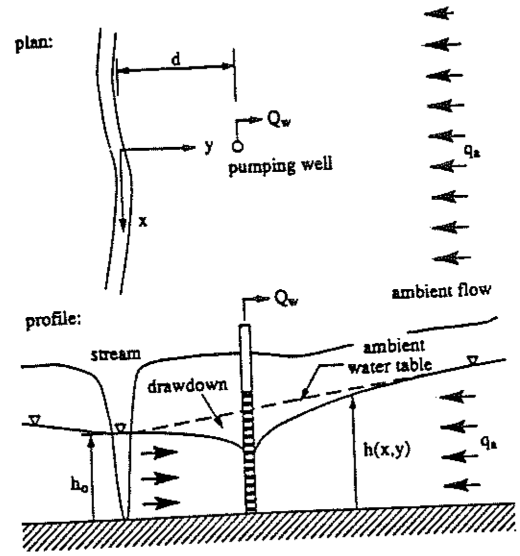

Fig. 1. Schematic of a pumping well in the vicinity of a stream in the presence of ambient aquifer flow in a semi-infinite aquifer.

$$\Phi = Th \qquad \text{confined or linearized phreatic aquifer,}$$
$$\Phi = \frac{Kh^2}{2} \qquad \text{Dupuit type phreatic aquifer,} \tag{1}$$

where $h[L]$ is depth averaged head (also water table elevation in the phreatic aquifer case), $K[L/T]$ is horizontal hydraulic conductivity, and $T = [L^2/T]$ is transmissivity. As the note indicates, the former definition in (1) applies when the concept of constant transmissivity is employed in a confined or phreatic aquifer. The latter definition for a phreatic aquifer with a horizontal bottom leads to a transmissivity, Kh, that depends on the saturated thickness in a phreatic aquifer. As will be shown later, both forms of the model provide identical results for induced infiltration, although it can be shown that results for the interior of the aquifer are different, and thus influence capture zones and other interior features. The solution for Φ is obtained by superposition of the ambient flow and the drawdown due to the well. The drawdown is in turn found via image well theory. The result is

$$\Phi(x, y) = \Phi_0 + q_a y - \frac{Q_w}{4\pi} \ln\left[\frac{(y+d)^2 + x^2}{(y-d)^2 + x^2}\right], \tag{2}$$

in which $\Phi_0 = \Phi(h = h_0)$ is evaluated at the stream boundary, where $h = h_0$. The first term in (2) represents the stream surface elevation, the second term is the rising head away from the stream caused by ambient flow, and the third term is the well drawdown. Darcy's law then can be em-

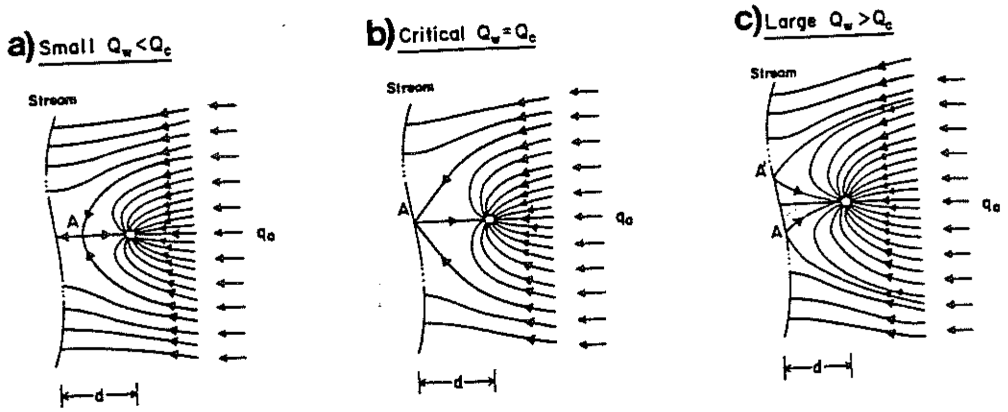

Fig. 2. Flow patterns for a semi-infinite aquifer in the vicinity of the well and the stream for (*a*) a subcritical pumping rate, (*b*) a critical pumping rate, and (*c*) for pumping above the critical rate causing induced infiltration. For the latter case the zone of induced infiltration is located along the stream between the stagnation points A and A'.

ployed to yield the specific discharge integrated over the depth, here called the "discharge per unit width," $q = -\nabla\Phi[L^2/T]$. To compute the rate of induced infiltration examine this discharge along the stream boundary, $y = 0$, or

$$q_0(x) = q(x, 0) = -\left.\frac{\partial\Phi}{\partial y}\right|_{y=0} = -q_a + \frac{Q_w}{\pi}\left[\frac{d}{(d^2+x^2)}\right]. \quad (3)$$

In the absence of pumping the stream is gaining and the discharge to the stream is in equilibrium with the ambient inflow: $q_0 = -q_a$ if $Q_w = 0$.

For small pumping rates the stream continues to gain, as is shown in Figure 2*a*, and the well continues to obtain all of its water from the ambient flow field. A critical situation is reached at a higher pumping rate, pictured in Figure 2*b*, for which the well just begins to draw from the stream. This pumping rate is called the critical pumping rate, Q_c. Mathematically, the critical pumping rate occurs when the stagnation point downgradient of the well (point A in Figure 2*a*) moves onto the stream (Figure 2*b*), so that $q_0 = 0$ at the origin ($x = y = 0$). Setting (3) to zero at $x = 0$ gives the critical pumping rate $Q_c = \pi d q_a$, which is directly proportional to the ambient flow rate and the distance between the well and the stream. Pumping at rates above this critical value induces infiltration from the stream, and the stream begins to lose water to the well. For $Q_w > Q_c$ the stagnation point "splits" and moves equidistantly up and down the stream, to the points labeled A and A' in Figure 2*c*, in order to accommodate the zone of induced infiltration. Actually, the stagnation point does not really split; this is just the appearance of a second image stagnation point not visible in the figure when $Q_w \le Q_c$.

The induced infiltration takes place between points A and A' and is calculated by integration. Let the x coordinates of these points be given by $\pm x'$. The coordinates are found using (3) and the property that $q_0 = 0$ at a stagnation point,

$$x'/d = [Q_w/\pi d q_a - 1]^{1/2} = (\beta - 1)^{1/2}, \quad (4)$$

where β is the dimensionless pumping rate,

$$\beta = Q_w/\pi d q_a. \quad (5)$$

Then (3) is integrated between $\pm x'$ to yield the induced infiltration rate, $Q_s[L^3/T]$,

$$Q_s = \int_{-x'}^{+x'} q_0\, dx = -2q_a x' + \frac{2Q_w}{\pi}\tan^{-1}(x'/d). \quad (6)$$

Substituting the stagnation point location from (4) into this yields the final expression for induced infiltration Q_s, here expressed as a proportion of the total pumping rate, Q_w:

$$\frac{Q_s}{Q_w} = \frac{2}{\pi}\left[\frac{-(\beta-1)^{1/2}}{\beta} + \tan^{-1}\{(\beta-1)^{1/2}\}\right]. \quad (7)$$

This dimensionless relation is graphed in Figure 3. The critical dimensionless pumping rate is $\beta = \beta_c = 1$, and (4) and (7) apply only when pumping exceeds this value, that is, when $\beta \ge 1$. The solution of these equations is indifferent to the definition of Φ and to whether the aquifer is assumed to have a constant transmissivity or one that varies with saturated thickness. This is because the saturated thickness at the stream is fixed by the constant head boundary condition.

The graph in Figure 3 shows that the amount of induced infiltration increases with pumping rate, well proximity to the stream, and decreasing ambient flow rate. The pumped water coming from ambient flow is given by $Q_a = Q_w$ when $\beta \le 1$, and $Q_a = Q_w - Q_s$ when $\beta \ge 1$. Although the proportion of pumped water coming from the ambient flow decreases at higher pumping rates, its absolute contribution

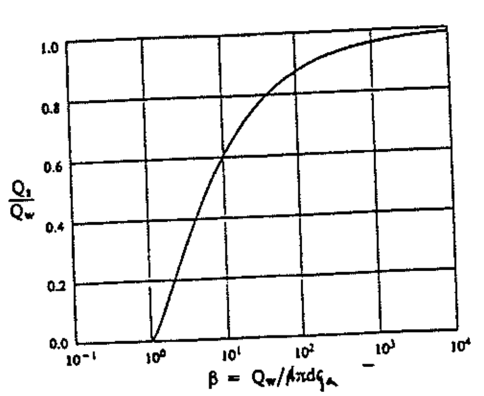

Fig. 3. Induced infiltration as a function of dimensionless pumping rate.

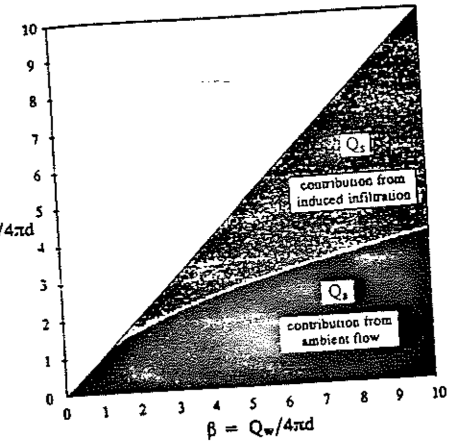

Fig. 4. Contributions of ambient flow and induced infiltration to pumpage.

increases, as is illustrated in Figure 4. This example is a special case of the more general models examined below and has been studied before, usually in a different context. In potential flow theory the typical application concerns an injection production well pair in a confined aquifer [*Jacob*, 1950; *Milne-Thomson*, 1968; *DaCosta and Bennett*, 1960]. It has also been presented in the present context [*Edelman*, 1972; *Wilson*, 1981] for the case of constant transmissivity, including one application with the ambient flow approaching at an angle due to a significant stream channel gradient [*Newsom and Wilson*, 1988].

WELL BETWEEN A STREAM AND A BARRIER

Suppose that beyond the well the aquifer pinches out or is interrupted by a nonconformity. As is depicted in Figure 5, this is represented as a barrier across which some flow may be possible. In the glaciated regions of the United States this barrier typically represents bedrock or glacial till; elsewhere it could be an upthrown fault block of relatively impervious rock. The lateral inflow across the barrier q_L is assumed to be independent of any drawdown in the aquifer and can be estimated through an independent hydrogeological analysis of that source area. A uniform local vertical recharge, $N[L/T]$, is applied across the top of the aquifer. The well draws water from the local recharge and lateral inflow, and for sufficiently strong pumping it induces infiltration from the stream. I hypothesize that the rate of induced infiltration should be greater in this case because of the enhanced drawdown caused by the barrier. The same analysis procedure is employed: first, the head distribution is determined and used to construct the discharge to or from the stream; second, the critical pumping rate is determined by setting the discharge to zero at the origin ($x = y = 0$); and third, for higher pumping rates the discharge is examined for stagnation points, and the induced infiltration rate is computed by integrating the discharge to the stream between these points.

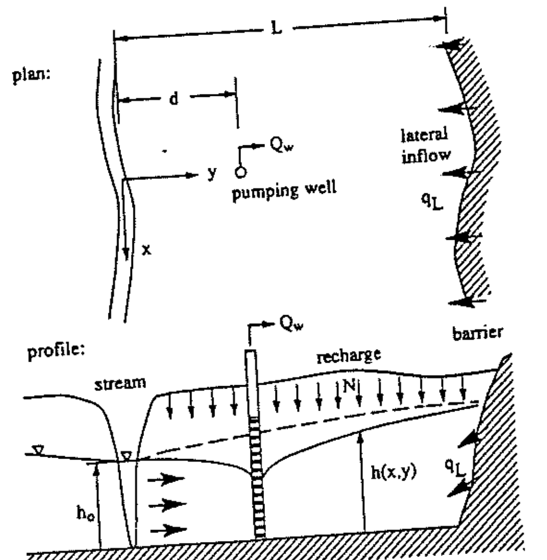

Fig. 5. Schematic of a pumping well located between a stream and a barrier.

The aquifer of Figure 5 is commonly referred to as an infinite strip aquifer and is described by the Poisson equation, $\nabla^2\Phi = -N$, where the same definitions apply. The aquifer can be confined or phreatic. The stream is assumed to be a constant head boundary and the barrier is a prescribed flux boundary. This linear flow problem is decomposed into two parts. In the first part the ambient head Φ_a before pumping is determined by solving the one-dimensional Poisson equation across the aquifer along axis y, for any x. The result is $\Phi_a(x, y) = \Phi_0 + q_L y + Ny(2L - y)/2$. The first two terms are analogous to the first two terms in (2) for the semi-infinite aquifer. The third term represents the effect of local recharge. The second part of the solution addresses the drawdown due to the well. Here the LaPlace equation applies and the barrier boundary is treated as a no-flow boundary. A series solution for this case can be found by image well analysis, but it converges slowly. Conformal mapping provides an exact approach. The Schwarz-Christoffel transform (see, for example, *Milne-Tompson* [1968]) is appropriate, where the transformed space for an infinite strip is the semi-infinite quarter space shown in Figure 6. Representing the strip by the complex coordinate $z = x + iy$ and the transformed space by $\zeta = \xi + i\eta$, the transformation is $\zeta = \exp(\pi z/2L)$, where $i = \sqrt{-1}$. In the transformed domain both the stream and the barrier are simulated by only three image wells, as is illustrated in Figure 6*b*. The real well is located at $\zeta_w = \exp(i\pi d/2L)$.

Subtracting this drawdown from the ambient head Φ_a yields an expression for head and flow anywhere in the aquifer, as influenced by both ambient flow and pumping:

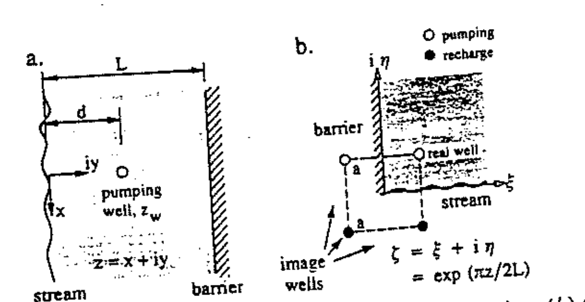

Fig. 6. Transformation of (*a*) the infinite strip aquifer into (*b*) a semi-infinite quarter space aquifer where the boundary conditions can be preserved with just three image wells. ($\zeta = \exp(\pi z/2L)$).

$$\Omega(x, y) = \Phi + i\Psi = \Phi_0 + \left\{\left[\frac{Ny(2L - y)}{2} + q_L y\right] + i[-Nx(L - y) - q_L x]\right\} + \frac{Q_w}{2\pi}\left[\ln\left(\frac{\zeta - \zeta_w}{\zeta - \zeta_w^*}\right) + \ln\left(\frac{\zeta + \zeta_w^*}{\zeta + \zeta_w}\right)\right]. \quad (8)$$

The symbol Ω represents the complex potential, and the superscript asterisk indicates a complex conjugate. The real part of this equation represents the head Φ, whereas the imaginary part represents the stream function Ψ. The first term is the constant head boundary at the stream. The second term is due to the ambient flow caused by local recharge N and lateral inflow q_L. The last term is due to the pumping. The stream function caused by ambient flow is represented by the imaginary part of the second term. It changes with distance from the stream because of the local recharge.

The discharge to or from the stream q_0 is found by differentiating (8) and applying the result at $y = 0$, as is described in the appendix. The result is

$$q_0(x) = q(x, 0) = -\left.\frac{\partial \Phi}{\partial y}\right|_{y=0} = -q_a + \frac{Q_w}{2L \cosh(X)} \cdot \left[\frac{\sin \delta}{(\cos^2 \delta \tanh^2 X + \sin^2 \delta)}\right], \quad (9)$$

where

$$q_a = (q_L + NL), \quad (10a)$$

$$\delta = \pi d/2L, \quad (10b)$$

$$X = \pi x/2L. \quad (10c)$$

The symbol q_a represents the ambient discharge to the stream, and it equals the lateral inflow and local recharge. The other two factors are the scaled dimensionless distance to the well and the scaled x coordinate, respectively. The critical pumping rate is found by setting the discharge in (9) to zero and can be expressed either as a dimensionless function of well location d,

$$\beta_c = \frac{Q_c}{\pi d q_a} = \frac{\sin \delta}{\delta}, \quad (11a)$$

or as a function of aquifer size L,

$$\alpha_c = \frac{Q_c}{2Lq_a} = \sin \delta. \quad (11b)$$

These two functions are plotted in Figure 7.

For pumping greater than the critical value the stagnation points at $\pm x'$ are found by setting (9) to zero and solving for $x' = x$. The results are expressed in terms of the dimensionless pumping rate, $\alpha = \beta\delta = Q_w/2Lq_a$, as a function of the dimensionless stagnation point location $X' = \pi x'/2L$:

$$\alpha = \frac{Q_w}{2Lq_a} = \beta\delta = \frac{\cosh X'}{\sin \delta}(\sin^2 \delta + \cos^2 \delta \tanh^2 X'). \quad (12)$$

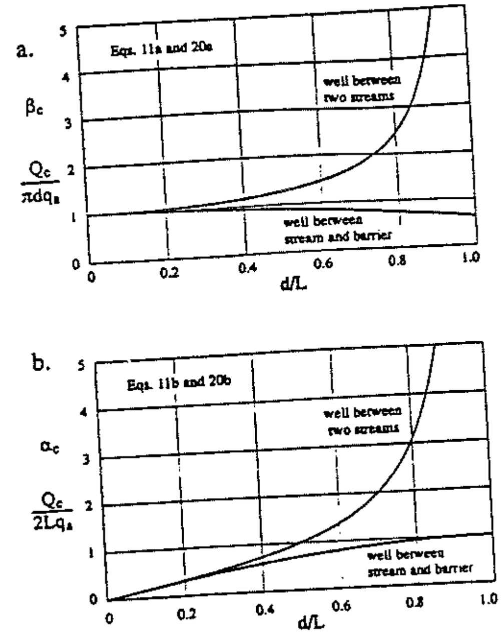

Fig. 7. Critical dimensionless pumping rate necessary to induce infiltration as a function of well location d/L. Scaled by (a) distance from the stream d and (b) distance between barrier and stream L.

The rate of induced infiltration Q_s is found by integrating the discharge (9) between these limits.

$$Q_s = -2q_a x' + \frac{2Q_w}{\pi}\sin \delta \cdot \int_0^{X'} \frac{dX}{(\sin^2 \delta + \cos^2 \delta \tanh^2 X)\cosh X} \quad (13)$$

using symmetry about the y axis. The integral in the last term, represented below by the symbol I, is evaluated by a change of variables, $w = \sin^{-1}(\tanh X)$, so that it becomes

$$I = \int_0^{w'} \frac{dw}{(\sin^2 \delta + \cos^2 \delta \sin^2 w)} = \frac{1}{\sin \delta}\tan^{-1}\left(\frac{\tan w'}{\sin \delta}\right), \quad (14)$$

where w' is evaluated at X'. By definition $\tan w' = \sinh X'$. The final dimensionless form of the induced infiltration equation for a well between a stream and a barrier is

$$\frac{Q_s}{Q_w} = \frac{2}{\pi}\left[\frac{-X'}{\alpha} + \tan^{-1}\left(\frac{\sinh X'}{\sin \delta}\right)\right] = \frac{-2x' q_a}{Q_w} + \frac{2}{\pi}\tan^{-1}\left(\frac{\sinh \pi x'/2L}{\sin \pi d/2L}\right). \quad (15)$$

The rate of infiltration for a given pumping rate is found by substituting in the stagnation point solution from (12). The results are graphed in Figure 8. These results are also indifferent to whether the aquifer is assumed to have a constant transmissivity or one that varies with saturated thickness. Perhaps more curiously the results depend only on the magnitude of the ambient discharge q_a, and not its source. Thus for a fixed ambient discharge, the amount of

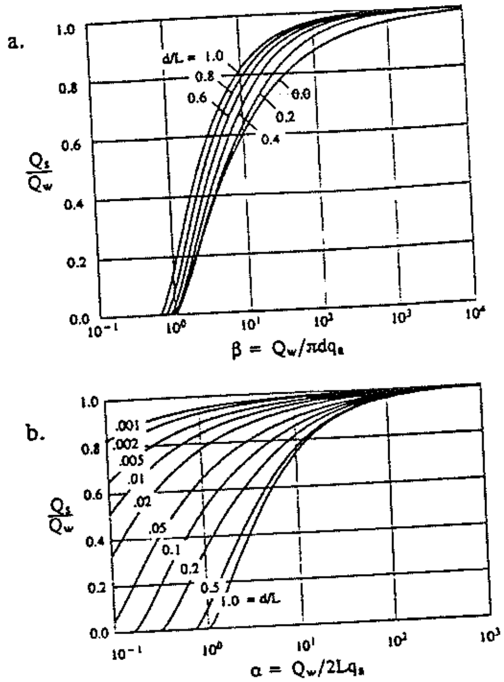

Fig. 8. Induced infiltration from a well located between a stream and a parallel barrier as a function of dimensionless pumping rate and ambient discharge to the stream ($q_a = NL + q_L$). Scaled by (*a*) distance from the stream *d* and (*b*) distance between the stream and the barrier *L*.

induced infiltration in an aquifer with vertical recharge and a no-flow barrier is the same as in an aquifer with no vertical recharge and lateral inflow across the barrier. Apparently, it is the head and ambient flow rate at the stream that determines the induced infiltration rate and not conditions around the well.

Figures 7*b* and 8*b* describe what happens for an aquifer of a fixed width *L* as a well is moved to different positions *d* within the aquifer. No matter where it is located within the aquifer, the well can be pumped hard enough to induce infiltration after it has used up the available water from local recharge and lateral inflow. Even a well located along the barrier requires only a moderate pumping level ($\alpha_c \rightarrow 1$ as $d/L \rightarrow 1$; Figure 7*b*). For example, if local vertical recharge *N* is the only source of ambient flow then the critical pumping rate is equivalent to the local recharge taken over an area $2L^2$, equivalent to a portion of the aquifer twice as long as it is wide. If the well is moved closer to the stream it takes even less pumping to induce infiltration ($\alpha_c \rightarrow 0$ as $d/L \rightarrow 0$). When pumping at rates above the critical value, the rate of infiltration increases with higher pumping rates, less local recharge and lateral inflow, and decreasing distance to the stream (Figure 8*b*). For negligible local recharge and lateral inflow ($\alpha > 100$), or wells located very near the stream (e.g., $d/L < 10^{-4}$ for $\alpha > 0.1$), almost all of the pumped water is induced infiltration.

If instead the well is located a fixed distance *d* from the stream, but in aquifers of different widths, the description is contained in Figures 7*a* and 8*a*. The rate of pumping necessary to induce infiltration increases in larger aquifers (Figure 7*a*) because the well has more aquifer from which to draw its recharge and depends less on induced infiltration. When the aquifer is 5 or more times wider than the distance from well to stream, the critical pumping rate approaches the asymptotic value found for semi-infinite aquifers ($\beta_c \rightarrow 1$, Figure 7*a*). For pumping rates significantly above the critical value the rate of induced infiltration is higher in finite width aquifers, as described by the fairly compact envelop of curves in Figure 8*a*. The lower curve Figure 8 represents the semi-infinite case, $d/L = 0$. Comparing this case to $d/L = 0.2$ suggests that the critical pumping rate is essentially the same, but when pumping at $\beta = 100$ the finite aquifer has almost 5% more induced infiltration. As pumping increases the well has a greater propensity to "feel" the presence of the barrier boundary and thus a greater potential to induce infiltration. For fixed *d* in small aquifers ($d/L \rightarrow 1$) the barrier is closer to the well than is the stream. When the barrier is adjacent to the well the amount of pumping necessary to induce infiltration is only slightly less than that required in a semi-infinite aquifer ($\beta_c = 2/\pi \approx 0.64$ compared to 1.0; Figure 7*a*). The results in both Figures 7*a* and 8*a* are somewhat surprising in that aquifer size seems to count for so little. This misleading conclusion ignores the role of ambient discharge to the stream, a normalizing factor in the curves, which would typically be smaller in smaller aquifers.

In summary, the presence of the barrier boundary increases the propensity for, and rate of, induced infiltration because the well has less aquifer to draw from other sources of recharge. Induced infiltration is independent of the mix of lateral inflow and local recharge and does not depend on whether the aquifer transmissivity is constant or a function of saturated thickness.

WELL BETWEEN TWO STREAMS

Let us now look at the case of a well located between two streams, as is depicted in Figure 9. Although highly idealized, this situation is typical for many watersheds. It also could be used to conceptualize a well pumping between

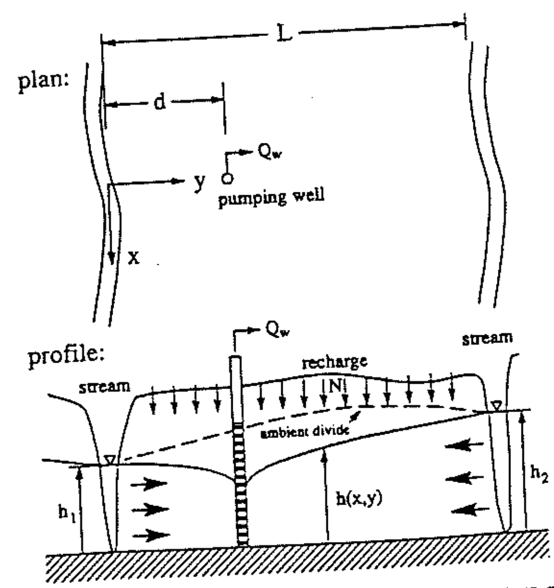

Fig. 9. Schematic of a pumping well located between two parallel streams.

irrigation and drainage canals. The streams can have the same or different elevations, h_1 and h_2, and there is local recharge N between them. The well draws water from the local recharge, and for sufficiently strong pumping induces infiltration from one or both streams. The well always draws some water from the stream with the higher elevation when that elevation is high enough to be losing under ambient conditions.

This is another confined or phreatic strip aquifer with the flow described by the Poisson equation, $\nabla^2\Phi = -N$. Each stream is treated as a constant head boundary. The ambient head Φ_a is found by solving the one-dimensional Poisson equation across the aquifer and is described by $\Phi_a(x, y) = \Phi_1 + (\Phi_2 - \Phi_1)y/L + Ny(L - y)/2$. The first two terms represent the effects of stream elevation. The third term represents the mounding in between the streams caused by local recharge. The well drawdown is again calculated using a Schwarz-Christoffel transform. The transformed space for an infinite strip aquifer bounded by two streams is a semi-infinite half-space with a constant head boundary on the side. In this decomposed problem both streams are assigned the same constant head ($\Phi = 0$) and are represented through a single-image recharge well. The new transformation is $\zeta = \exp(\pi z/L)$. Alternatively, one could use the previous transform by exchanging the sign of the two image wells that are labeled "a" in Figure 6. Either way the determined drawdown is subtracted from the ambient head Φ_a to yield the expression for head and flow, represented by the complex potential:

$$\Omega(x, y) = \Phi + i\Psi = \left[\frac{Ny(L-y)}{2} + \frac{(\Phi_2 - \Phi_1)}{L}\,y + \Phi_1\right] + i\left[\frac{-Nx(L-2y)}{2} - \frac{(\Phi_2 - \Phi_1)}{L}\,x\right] + \frac{Q_w}{2\pi}\left[\ln\left(\frac{\zeta - \zeta_w}{\zeta - \zeta_w^*}\right)\right] \tag{16}$$

The discharge to or from the streams is easily found by differentiation, as is shown in the appendix, and is given for the stream located along the x axis by

$$q_0(x) = q(x, 0) = -\left.\frac{\partial\Phi}{\partial y}\right|_{y=0} = -q_a + \frac{Q_w}{2L}\left[\frac{\sin(2\delta)}{\cosh(2X) - \cos(2\delta)}\right]. \tag{17}$$

The ambient discharge to the stream is

$$q_a = \frac{NL}{2} + \frac{\Phi_2 - \Phi_1}{L}, \tag{18}$$

while $\delta = \pi d/2L$ and $X = \pi x/2L$ are the same dimensionless parameters used for the stream barrier case. The discharge to or from the stream at $x = L$ is given by a similar expression. In fact, (17) applies to either stream by reorienting the coordinate system so that y and d are measured from the stream of interest. Please note that no assumptions have yet been made about the relative magnitude of Φ_1 and Φ_2.

The rate of local recharge N plays a significant role in determining sources of pumped water. If the rate is sufficiently large that a groundwater divide forms between the streams, as is illustrated in Figure 9, then both streams are gaining. Induced infiltration for this case is given below. If the local recharge rate is sufficiently small and the streams are of unequal elevation, then there is no divide. Under ambient conditions the critical recharge rate below which this occurs is given by

$$N_c = 2\,\frac{|\Phi_2 - \Phi_1|}{L^2}, \tag{19}$$

which is found by setting (18) to zero. The higher or upper stream loses water to the aquifer, while the lower stream gains the discharge. In this case there is no need for pumping to induce infiltration from the upper stream; it loses water naturally ($q_a < 0$). A well pumping from this aquifer will always sample both the local vertical recharge and this natural throughflow from losing stream to gaining stream, whatever the pumping rate. It is necessary to actually model spatial capture zones to determine how much of the pumped water comes from the upper stream and how much comes from local recharge [*Wilson and Linderfelt*, 1991].

The critical pumping rate necessary to induce infiltration from a gaining stream is found by setting the discharge in (17) to zero, yielding

$$\beta_c = Q_c/\pi d q_a = \tan\delta/\delta \tag{20a}$$

$$\alpha_c = Q_c/2Lq_a = \tan\delta \tag{20b}$$

where $\alpha = \beta\delta$. These two functions are plotted in Figure 7 for positive values of ambient discharge to the stream. For pumping greater than the critical value the stagnation points $\pm x'$ are found by setting (17) to zero and solving for

$$\alpha = \frac{Q_w}{2Lq_a} = \beta\delta = \frac{\cosh(2X') - \cos(2\delta)}{\sin(2\delta)}. \tag{21}$$

as a function of the dimensionless distance $X' = \pi x'/2L$. Induced infiltration is found by integrating the discharge (17) between these limits:

$$Q_s = -2q_a x' + \frac{2Q_w}{\pi}\sin 2\delta \int_0^{X'} \frac{dX}{\cosh 2X - \cos 2\delta}. \tag{22}$$

The integral in the last term is evaluated by using formula 2.443.3 in the work by *Gradshteyn and Ryzhik* [1980], leading to the final dimensionless form of the induced infiltration equation for a well between a two parallel streams:

$$\frac{Q_s}{Q_w} = \frac{2}{\pi}\left[\frac{-X'}{\alpha} + \frac{1}{2}\cos^{-1}\left[\frac{1 - \cosh(2X')\cos(2\delta)}{\cosh(2X') - \cos(2\delta)}\right]\right] = \frac{-2x'q_a}{Q_w} + \frac{1}{\pi}\cos^{-1}\left[\frac{1 - \cosh(\pi x'/L)\cos(\pi d/L)}{\cosh(\pi x'/L) - \cos(\pi d/L)}\right] \tag{23}$$

The rate of infiltration for a given pumping rate is found by substituting in the stagnation point solution from (21). The results are graphed in Figure 10. These results are indifferent to whether the aquifer is assumed to have a constant transmissivity or one that varies with saturated thickness.

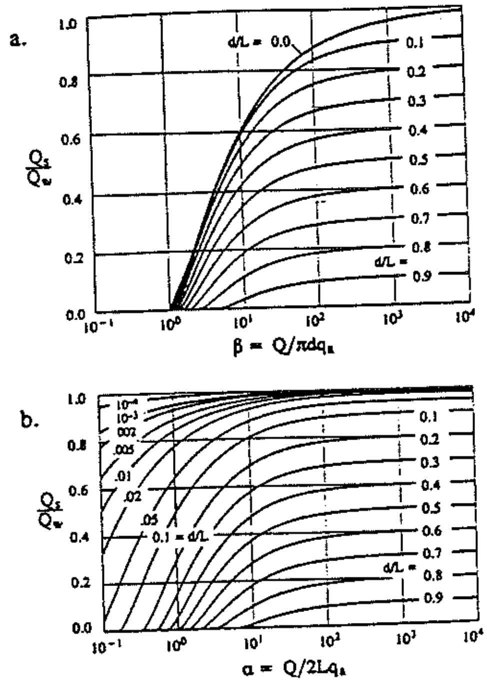

Fig. 10. Induced infiltration to a well between two parallel streams as a function of dimensionless pumping rate and ambient discharge to the stream of interest q_a. Scaled by (*a*) distance from the stream of interest *d* and (*b*) distance between the two streams *L*.

Also, note that as long as the stream gains water under ambient conditions, induced infiltration is independent of source of the ambient discharge.

Figures 7*b* and 10*b* describe what happens to an aquifer of a fixed width *L* as a well is moved to different locations between the streams. If instead the well is located a fixed distance from one of the streams, but in aquifers of different widths, the description is contained in Figures 7*a* and 10*a*. The amount of pumping necessary to induce infiltration from a stream depends on the proximity of the well to the stream (Figure 7*b*). By symmetry arguments a well that is located midway between two equal elevation streams will induce infiltration from both streams at the same pumping rate ($\alpha_c = 1$). A well located farther from one stream than the other finds it much easier to induce infiltration from the nearer stream. For example, a well 3 times farther from one stream than another will induce infiltration from the closer stream at a pumping rate far smaller than one third of the pumping rate it takes to induce infiltration from the farther ($\alpha_c = 0.41$ at $d/L = 0.25$ versus $\alpha_c = 2.41$ at $d/L = 0.75$ in Figure 7*b*). When a well is located very close to one stream and far from the other, then it is difficult to induce infiltration from the far stream unless it is significantly higher in elevation. In this case the critical pumping rate for induced infiltration from the near stream approaches that for the semi-infinite aquifer ($\beta_c \rightarrow 0$ as $d/L \rightarrow 0$; Figure 7*a*).

Once the critical pumping rate is exceeded the rate of induced infiltration from a stream increases with higher pumping rates, less ambient discharge to the stream, and decreasing distance between the stream and the well (Figure 10*b*). For a sufficiently high pumping rate ($\alpha \gtrsim 200$) the amount of induced infiltration from a stream is inversely proportional to its position within the aquifer. Thus the well that is located 3 times farther from one stream than another ultimately draws 3 times more water from the nearer stream than the farther. Wells located much nearer one stream than another behave as if they were in a semi-infinite aquifer (Figure 10*a*).

Figure 11 illustrates what happens for a well located one fifth of the distance across the aquifer ($d/L = 0.2$ from the near stream and $d/L = 0.8$ from the far stream). At a low pumping rate all of the water comes from local recharge, and the well's capture zone does not extend to either stream. At a slightly higher pumping rate ($\alpha_c = 0.32$) the well begins to induce infiltration from the near stream. Increased pumping induces infiltration from this stream and increases the size of the well's capture zone within the aquifer. Not until the pumping rate reaches a substantially higher rate ($\alpha_c = 3.08$) does the capture zone actually extend far enough to induce infiltration from the far stream. When the pumping rate increases two orders of magnitude again ($\alpha \gtrsim 200$), almost all the pumped water comes from induced infiltration, in inverse proportion to the proximity of the well to each stream. The size of the capture zone and the amount of local recharge withdrawn grow with each increase of pumping rate, although it becomes less important compared to the induced infiltration.

The results for the stream-stream strip aquifer and the stream-barrier aquifer are quite similar for wells that are sufficiently close to the gaining stream. Compare Figures 8*b* and 10*b* for $d/L \leq 0.05$. This suggests that a simple semi-infinite model is appropriate for wells that are located within a distance from the stream of less than 5% of the width of the aquifer.

In summary, the presence of the second stream boundary decreases the propensity for and the rate of induced infiltration from the first stream. The second stream offers an additional source of recharge. Once again, the induced infiltration rate does not depend on whether the aquifer transmissivity is constant or a function of saturated thickness, or on the source of the ambient flow, as long as the considered stream is a gaining stream.

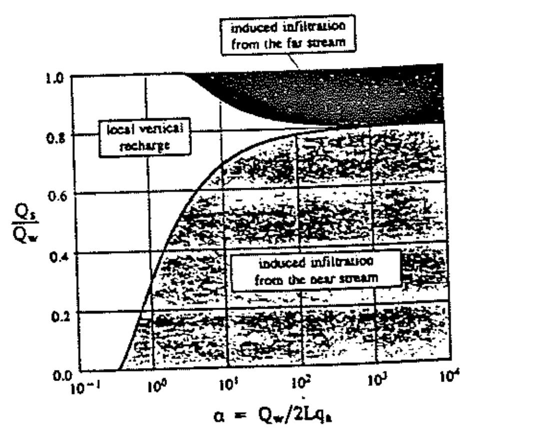

Fig. 11. Induced infiltration to a well from each of the two parallel streams (darker greys) as a function of the dimensionless pumping rate scaled by the distance between the two streams *L*. The well is located at a distance of $0.2L$ from the near stream and $0.8L$ from the far stream.

SUMMARY AND CONCLUSIONS

Induced infiltration causes a gaining stream to become, at least locally, a losing stream. Although in this paper I have used the term "stream" to describe the surface water body, the issues and results also apply to rivers, ponds, lakes, and wetlands. There are two induced infiltration problems. Where water rights are at issue, the problem is one of streamflow depletion. Where water quality is the issue, the problem is identifying the actual sources of the water, each with its own chemical fingerprint. The streamflow depletion problem has been studied for years; the water quality problem has not. In this paper I have presented several simple models that address the water quality problem for well pumping near gaining streams. The models improve the understanding of induced infiltration phenomena and provide a "first cut" analysis of alternative well field designs and pumping rates from a water quality perspective, or assist in the delineation of wellhead protection zones. They may also be of some help in characterizing past pollution events involving wells, aquifers, and streams or other surface water bodies.

For a gaining stream it takes a minimum or critical pumping rate to induce water to leave the stream, enter the aquifer, and make its way to the well. Pumping at rates greater than this minimum induce infiltration and lead to a mixture of water of different origins and quality in the well bore. The propensity for and rate of induced infiltration increases with pumping rate, decreasing distance between the well and the stream, and lower ambient discharge to the stream. If the aquifer is finite in size and there is a nearby parallel barrier boundary, induced infiltration is enhanced. The cone of depression of the well is reflected off the boundary, increasing the hydraulic gradient from the stream to the aquifer. The closer the barrier boundary to the stream and well, the greater the induced infiltration. If a finite aquifer is bounded by two parallel streams, then the induced infiltration from either one is reduced by the presence of the other, which presents an additional source of recharge. If the well is sufficiently close to a stream, say, within a distance of less than 5% of the width of the aquifer, then aquifer geometry plays almost no role and the semi-infinite induced infiltration model suffices.

Induced infiltration to wells located near gaining streams is essentially independent of the source of ambient discharge to the stream, whether its composed of local recharge, lateral inflow, or some combination of the two. Infiltration also appears to be indifferent to the whether the aquifer transmissivity is assumed to be a constant or allowed to vary with the saturated thickness. Both of these findings suggest that induced infiltration is most sensitive to the stream and other lateral boundary conditions, rather than to conditions within the aquifer itself. *Larkin and Sharp* [1992] recently examined data for 24 alluvial stream and river systems, including aspects such as stream penetration, stream channel sinuosity, and channel gradient, which controls the angle between the channel and the ambient flow. My assumptions regarding these boundary condition issues were violated for a significant number of their systems and should be further examined. For the angle between the channel and the ambient flow, the results in *Newsom and Wilson* [1988] suggest that the angle has to exceed roughly 30°–45° in order for this effect to be significant. Perhaps the most important neglected issue is stream penetration and the three-dimensional flow effects that allow the capture zone to extend under the stream to sources of water on the other side [*Morrisey*, 1987; *Wilson and Linderfelt*, 1991]. With these additional sources, partial penetration would presumably decrease the propensity for induced infiltration. A streambed clogging layer, which would further reduce the induced infiltration, should be included in three-dimensional modeling studies. Finally, these results assume steady state conditions. This idealized condition is seldom obtained in the field, either for pumping or ambient flow. All of these issues suggest additional analyses and field studies.

APPENDIX

The discharge to or from the stream q_0 is found by differentiating the complex potential, (8) or (16), and evaluating the resulting expression for $-\partial\Phi/\partial y$ along the x axis, $y = 0$. The differentiation is based on the condition [e.g., *Milne-Thomson*, 1968]

$$\frac{d\Omega}{dz} = \frac{\partial \Phi}{\partial x} + i\frac{\partial \Psi}{\partial x} = \frac{\partial \Psi}{\partial y} - i\frac{\partial \Phi}{\partial y} = -q_x + iq_y \quad (24)$$

which yields the velocity (discharge per width) field for the model ($q_x = -\partial\Phi/\partial x$, $q_y = -\partial\Phi/\partial y$). The imaginary part of this expression is needed for the induced infiltration calculation.

For the case of a well between a stream and barrier the complex potential is given by (8), and its derivative is given by

$$\frac{d\Omega}{dz} = i[-N(L-y) - q_L] + \frac{Q_w}{2L}\left[\frac{1}{\dfrac{\zeta}{\zeta_w} - \dfrac{\zeta_w}{\zeta}} - \frac{1}{\dfrac{\zeta}{\zeta_w^*} - \dfrac{\zeta_w^*}{\zeta}}\right], \quad (25)$$

where $\partial/\partial z = (\pi\zeta/2L)\partial/\partial\zeta$ has been used. To evaluate this expression substitute the transform $\zeta = \exp(\pi z/2L) = \exp(\pi x/2L)[\cos(\pi y/2L) + i\sin(\pi y/2L)]$ and expand, using the definitions of $\sinh x = [e^x - e^{-x}]/2$ and $\cosh = [e^x + e^{-x}]/2$. The result is

$$\begin{aligned} d\Omega/dz = {}& i[-N(L-y) - q_L] + [2\sinh(X - X_w) \\ & \cdot \cos(Y - Y_w) + i2\cosh(X - X_w) \\ & \cdot \sin(Y - Y_w)]^{-1} - [2\sinh(X - X_w)\cos(Y + Y_w) \\ & + i2\cosh(X - X_w)\sin(Y + Y_w)]^{-1} \end{aligned} \quad (26)$$

where dimensionless coordinates $X = \pi x/2L$ and $Y = \pi y/2L$ have been introduced. The subscript w represents the well location. This expression can be resolved into real and imaginary parts to yield the velocity field with x and y components

$$\begin{aligned} q_x = -\text{Real}\left[\frac{d\Omega}{dz}\right] = -\frac{\partial\Phi}{\partial x} = {}& \frac{Q_w}{4L\cosh(X - X_w)} \\ & \cdot \{[\cos(Y - Y_w)\tanh(X - X_w)] \\ & \cdot [\cos^2(Y - Y_w)\tanh^2(X - X_w) + \sin^2(Y - Y_w)]^{-1} \\ & - [\cos(Y + Y_w)\tanh(X - X_w)] \\ & \cdot [\cos^2(Y + Y_w)\tanh^2(X - X_w) + \sin^2(Y + Y_w)]^{-1}\} \end{aligned} \quad (27a)$$

$$q_y = \mathrm{Img}\left[\frac{d\Omega}{dz}\right] = -\frac{\partial \Phi}{\partial y} = -[N(L-y) + q_L]$$
$$+ \frac{Q_w}{4L \cosh (X - X_w)} [[\sin (Y - Y_w)]$$
$$\cdot [\cos^2 (Y - Y_w) \tanh^2 (X - X_w) + \sin^2 (Y - Y_w)]^{-1}$$
$$- [\sin (Y + Y_w)][\cos^2 (Y + Y_w) \tanh^2 (X - X_w)$$
$$+ \sin^2 (Y + Y_w)]^{-1}]. \quad (27b)$$

For the well location as defined in Figure 5, $X_w = 0$ and $Y_w = \delta = \pi d/2L$, and along the stream $Y = 0$. With these substitutions (27*b*) reduces to (9), yielding the flow to or from the stream. Incidentally, the velocities in (27*a*) and (27*b*) can also be used to define capture zones for the well [*Schafer-Perini and Wilson*, 1991; *Wilson and Linderfelt*, 1991].

For a well between two parallel streams the complex potential is given by (16), and its derivative is

$$\frac{d\Omega}{dz} = i\left[\frac{-N(L-2y)}{2} - \frac{\Phi_2 - \Phi_1}{L}\right] + \frac{Q_w}{2L}\left[\frac{1}{1 - \dfrac{\zeta_w}{\zeta}} - \frac{1}{1 - \dfrac{\zeta_w^*}{\zeta}}\right], \quad (28)$$

where $\partial/\partial z = (\pi\zeta/L)\partial/\partial\zeta$ has been used. The x and y components of the velocity field are found by substituting in the transform $\zeta = \exp(\pi z/L)$ and expanding:

$$q_x = -\mathrm{Real}\left[\frac{d\Omega}{dz}\right] = -\frac{\partial \Phi}{\partial x}$$
$$= +\frac{Q_w}{4L}\left[\frac{\exp - (2X_w - 2X) - \cos (2Y_w - 2Y)}{\cosh (2X_w - 2X) - \cos (2Y_w - 2Y)}\right.$$
$$\left. + \frac{\exp - (2X_w - 2X) - \cos (2Y_w + 2Y)}{\cosh (2X_w - 2X) - \cos (2Y_w + 2Y)}\right] \quad (29a)$$

$$q_y = \mathrm{Img}\left[\frac{d\Omega}{dz}\right] = -\frac{\partial \Phi}{\partial y} = -\frac{N(L-2y)}{2} - \frac{\Phi_2 - \Phi_1}{L}$$
$$+ \frac{Q_w}{4L}\left[\frac{\sin (2Y_w - 2Y)}{\cosh (2X_w - 2X) - \cos (2Y_w - 2Y)}\right.$$
$$\left. + \frac{\sin (2Y_w + 2Y)}{\cosh (2X_w - 2X) - \cos (2Y_w + 2Y)}\right], \quad (29b)$$

where the same dimensionless parameters X and Y are used. Finally, for the well location in Figure 9 the flow to or from the stream is found by setting $X_w = 0$, $Y_w = \delta$, and $Y = 0$ in (29*b*). The result is given in the text as (17).

Acknowledgments. The author acknowledges the assistance of Peter J. Riordan, and the reviews of Robert Terberg, William Linderfelt, and the anonymous journal reviewers. This work was funded by U.S. Geological Survey grant 14-08-0001-G1632 and the New Mexico Water Resources Research Institute projects 1345682 and 1423620. The Delaware River Basin Commission provided additional assistance through Camp, Dresser and McKee in Cambridge, Massachusetts.

REFERENCES

Bear, J., *Groundwater Hydraulics*, McGraw-Hill, New York, 1979.

DaCosta, J. A., and R. R. Bennett, The pattern of flow in the vicinity of a recharging and discharging pair of wells in an aquifer having a real parallel flow, Proceedings IUGG General Assembly of Helsinki, *Publ. 52*, pp. 524–536, Int. Assoc. Sci. Hydrol., Gentbrugge, Belgium, 1960.

Edelman, J. H., Groundwater hydraulics of extensive aquifers, *Bull. 13*, Int. Inst. for Land Reclam. and Improve., Wageningen, Netherlands, 1972.

Environmental Protection Agency, WHPA, An integrated semi-analytical model for the delineation of wellhead protection areas, report, Off. of Ground-water Protect., Washington, D. C., 1990.

Ferris, J. G., D. B. Knowles, R. H. Brown, and R. W. Stallman, Theory of aquifer tests, *U.S. Geol. Surv. Water Supply Pap., 1536-E*, 1962.

Glover, R. E., and G. G. Balmer, River depletion resulting from pumping a well near a river, *Eos Trans. AGU*, *35*(3), 468–470, 1954.

Gradshteyn, I. S., and I. M. Ryzhik, *Table of Integrals, Series and Products*, Academic, San Diego, Calif., 1980.

Hantush, M. S., Analysis of data from pumping wells near a river, *J. Geophys. Res.*, *64*(11), 1921–1932, 1959.

Hantush, M. S., Wells near streams with semipervious beds, *J. Geophys. Res.*, *70*(12), 2829–2838, 1965.

Jacob, C. E., Flow of groundwater, in *Engineering Hydraulics*, chap. 5, John Wiley, New York, 1950.

Jenkins, C. T., Techniques for computing rate and volume of stream depletion by wells, *Ground Water*, *6*(2), 37–46, 1968.

Kazman, R. B., Notes on determining the effective distance to a line of recharge, *Eos Trans. AGU*, *27*(6), 854–859, 1946.

Kazman, R. B., Induced infiltration of river water of wells. *Eos Trans. AGU*, *29*(1), 85–92, 1948.

Larkin, R. G., and J. M. Sharp, On the relationship between river-basin geomorphology, aquifer hydraulics, and ground-water flow direction in alluvial aquifers, *Geol. Soc. Am. Bull.*, *104*, 1608–1620, 1992.

Milne-Thomson, L. M., *Theoretical Hydrodynamics*, 5th ed., MacMillan, New York, 1968.

Morrisey, D. J., Estimation of the recharge area contributing water to a pumped well in a glacial-drift, River Valley aquifer, *U.S. Geol. Surv. Open File Rep., 86-543*, 1987.

Newsom, J. M., and J. L. Wilson, Flow of groundwater to a well near a stream: Effect of ambient groundwater flow direction, *Ground Water*, *26*(6), 703–711, 1988.

Norris, S. E., Aquifer tests and well field performance, Scioto River Valley, Ohio, I, *Ground Water*, *21*(3), 287–282, 1983.

Rorabaugh, M. I., Groundwater in Northeastern Louisville, Kentucky with reference to induced infiltration, *U.S. Geol. Surv. Water Supply Pap., 1360-B*, 1956.

Schafer-Perini, A. L., and J. L. Wilson, Efficient and accurate front tracking for two-dimensional groundwater flow models, *Water Resour. Res.*, *27*(7), 1471–1485, 1991.

Theis, C. V., The effect of a well on the flow of a nearby stream, *Eos Trans. AGU*, *22*, 734–738, 1941.

Walton, W. C., *Groundwater Resource Evaluation*, McGraw-Hill, New York, 1970.

Wilson, J. L., Analytical methods in groundwater hydrology, in *Groundwater Hydrology*, Boston Society of Civil Engineers, Boston, Mass., 1981.

Wilson, J. L., and W. L. Linderfelt, Groundwater quality in pumping wells located near surface water bodies, *Tech. Completion Rep. 261*, N. M. Water Resour. Res. Inst., Las Cruces, 1991.

J. L. Wilson, Department of Geoscience, New Mexico Institute of Mining and Technology, Socorro, NM 87801.

(Received June 10, 1991;
revised May 10, 1993;
accepted May 20, 1993.)

Appendix B
MODflow Input and Results

INPUT SUMMARY

Layer Number	Bottom Elevation (ngvd)	Aquifer Thickness (feet)	Desired Kh (feet/day)	Desired Kv (feet/day)	Calculated VCOND	Calculated Trans
1	675	10	250	62.5		2500
					6.94	
2	667	8	250	62.5		2000
					9.62	
3	662	5	250	62.5		1250
					12.50	
4	657	5	250	62.5		1250
					12.50	
5	652	5	250	62.5		1250
					12.50	
6	647	5	250	62.5		1250
					9.62	
7	639	8	250	62.5		2000
					6.94	
8	629	10	250	62.5		2500
				4:1		14000
				AR		

NO FIXED BOUND

RECHARGE = 6 in/year

300 GPM = 57746.291 FT³/DAY
DW-1 635-665' NGVD
∴ LAYERS 2-7
6 @ 9624.4 FT³/DAY
row 8, col 81

Steady state

DW-1 PUMP TEST

$$\frac{CH_{IN}\,(\text{PUMP}) - CH_{IN}\,(\text{NO PUMP})}{\text{PUMPING DW-1}} = \frac{48195 - 20.134}{57746}\left[\frac{FT^3}{DAY}\right] = 83.4\% \pm 5.5\%$$

FROM MASS BALANCE

NO - PUMPING LAYER 1

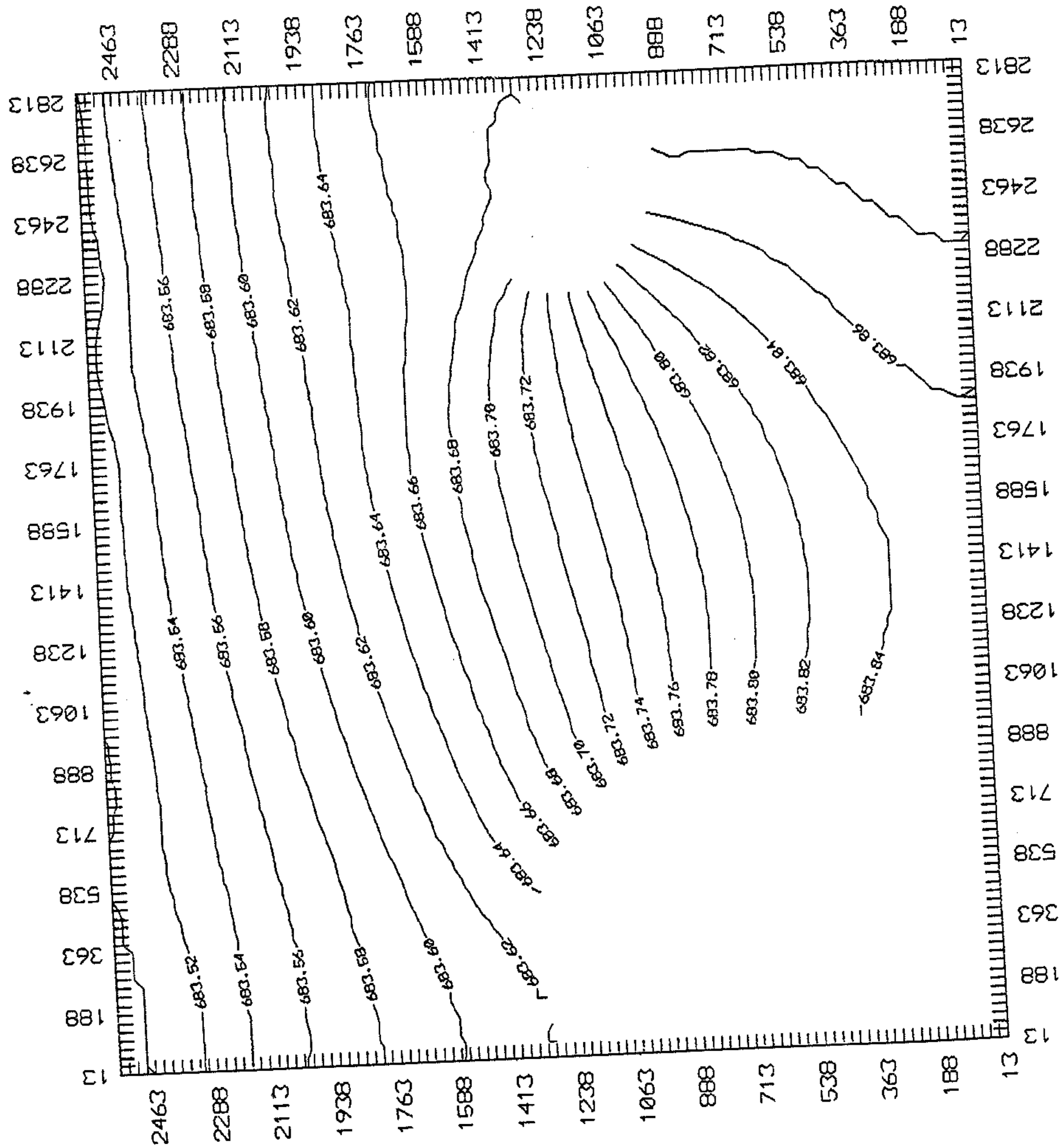

DW-1
Pumping
Heads
Layer 1

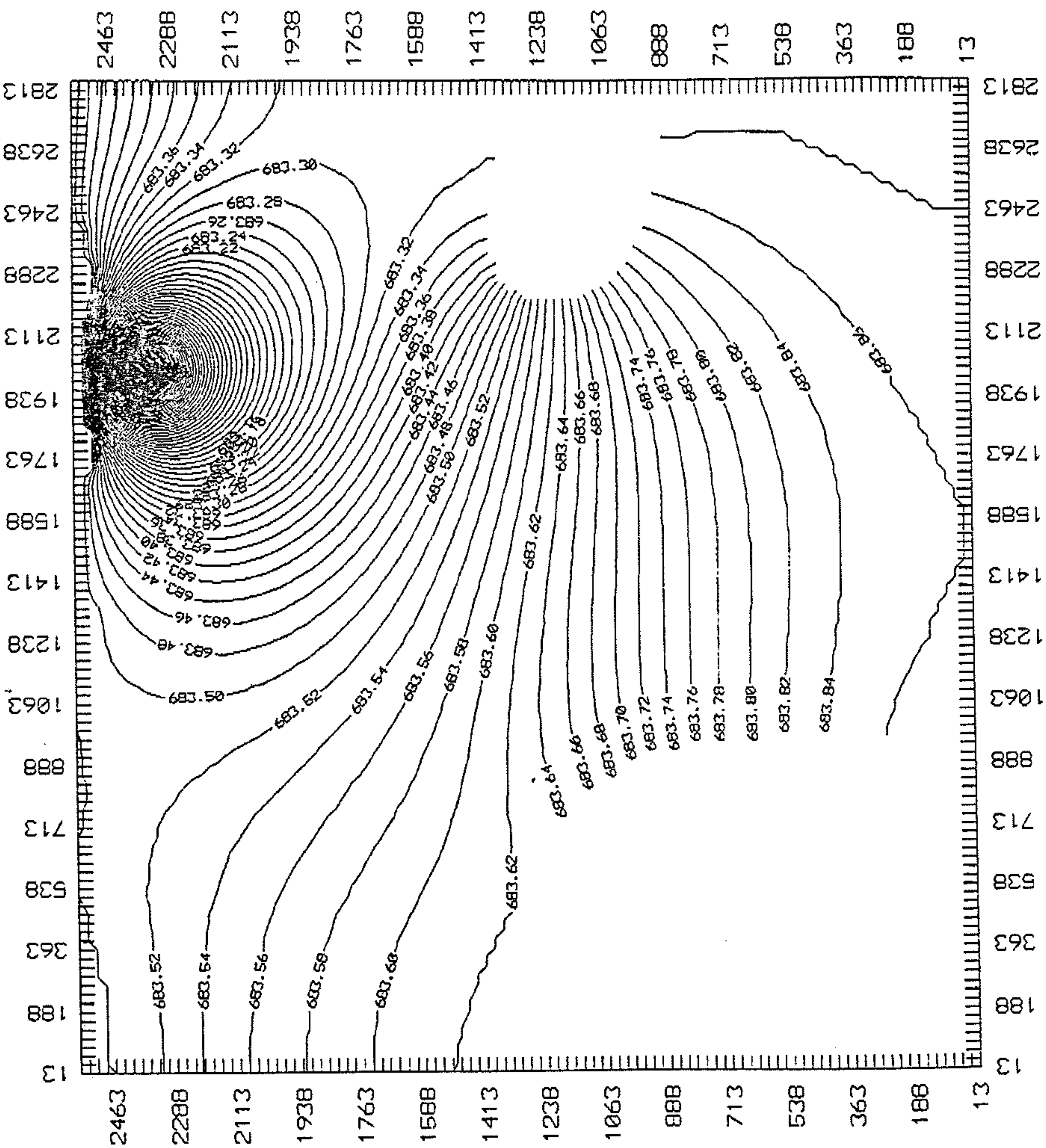

DW-1
DRAWDOWN
LAYER 1